

AD-A209 856

SECURITY CLASSIFICATION OF THIS PAGE

(2)

REPORT DOCUMENTATION PAGE				Form Approved OMB No. 0704-0188	
1a. REPORT SECURITY CLASSIFICATION UNCLASSIFIED		1b. RESTRICTIVE MARKINGS OTIC FILE COPY			
2a. SECURITY CLASSIFICATION AUTHORITY UNCLASSIFIED		3. DISTRIBUTION / AVAILABILITY OF REPORT DISTRIBUTION UNLIMITED			
2b. DECLASSIFICATION / DOWNGRADING SCHEDULE 1 JUL 95 1989					
4. PERFORMING ORGANIZATION REPORT NUMBER(S) AFOSR - 85-0234-1		5. MONITORING ORGANIZATION REPORT NUMBER(S) AFOSR-TR- 89 - 0321			
6a. NAME OF PERFORMING ORGANIZATION AIR FORCE		6b. OFFICE SYMBOL (If applicable) NE		7a. NAME OF MONITORING ORGANIZATION AFOSR/NE	
6c. ADDRESS (City, State, and ZIP Code) CITY COLLEGE OF NEW YORK NEW YORK, NY 10031		7b. ADDRESS (City, State, and ZIP Code) BUILDING 410 BOLLING AFB, DC 20332-16448			
8a. NAME OF FUNDING / SPONSORING ORGANIZATION AIR FORCE OFFICE OF SCIENTIFIC RESEARCH		8b. OFFICE SYMBOL (If applicable) NE		9. PROCUREMENT INSTRUMENT IDENTIFICATION NUMBER AFOSR-85-0234	
8c. ADDRESS (City, State, and ZIP Code) Bolling Air Force Base Washington, D. C. 20322		10. SOURCE OF FUNDING NUMBERS PROGRAM ELEMENT NO. 61102F		PROJECT NO. 2305	TASK NO. B3
				WORK UNIT ACCESSION NO.	
11. TITLE (Include Security Classification) COMMUNICATIONS USING CHANNELS FORMED BY METEOR BURSTS					
12. PERSONAL AUTHOR(S) Donald L. Schilling, Eliphaz Hibshoosh					
13a. TYPE OF REPORT Final Annual Tech. Report		13b. TIME COVERED FROM 7/1/85 TO 11/30/88		14. DATE OF REPORT (Year, Month, Day) 88-11-30	
				15. PAGE COUNT 114	
16. SUPPLEMENTARY NOTATION					
17. COSATI CODES FIELD GROUP SUB-GROUP			18. SUBJECT TERMS (Continue on reverse if necessary and identify by block number) METEOR BURSTS, COMMUNICATION, CHANNEL.		
19. ABSTRACT (Continue on reverse if necessary and identify by block number) <p>We propose to study the use of the meteor burst channel in communication systems by investigating the following important aspects:</p> <p>1) The development and enhancement of an accurate and reliable channel model based on recently available empirical data. Analysis of this model results in analytical expressions for communication parameters such as channel duration and throughput to be used as design and analysis tools.</p> <p>2) The optimization of throughput for fixed transmission rate under the constraint of a given maximum bit error rate. This will demonstrate the room for improvement in existing systems using constant transmission rate.</p> <p>3) The feasibility of efficiently communicating over the MBC using variable bit rate and employing a feedback protocol to monitor the channel. This approach will dramatically improve the throughput in comparison with constant</p>					
20. DISTRIBUTION / AVAILABILITY OF ABSTRACT <input checked="" type="checkbox"/> UNCLASSIFIED/UNLIMITED <input type="checkbox"/> SAME AS RPT. <input type="checkbox"/> OTIC USERS				21. ABSTRACT SECURITY CLASSIFICATION UNCLASSIFIED	
22a. NAME OF RESPONSIBLE INDIVIDUAL Dr. Donald L. Schilling				22b. TELEPHONE (Include Area Code) 212-696-6621 (202) 767-4931	
				22c. OFFICE SYMBOL NE	

DD Form 1473, JUN 86

Previous editions are obsolete.

SECURITY CLASSIFICATION OF THIS PAGE

DISTRIBUTION STATEMENT A

Approved for public release

89 6 29 118

COMMUNICATIONS USING CHANNELS FORMED BY METEOR BURSTS

FINAL TECHNICAL REPORT - 85-0234-1

JULY 1, 1985 - NOVEMBER 30, 1988

GRANT AFOSR - 85-0234-1

AIR FORCE OFFICE OF SCIENTIFIC RESEARCH

BOLLING AIR FORCE BASE

WASHINGTON, D. C. 20322

DONALD L. SCHILLING - H.J.Kayser Professor of Electrical Engineering

ELIPHAZ HIBSHOOSH - ASSISTANT PROFESSOR

PRINCIPAL INVESTIGATORS

COMMUNICATIONS SYSTEMS LABORATORY

ELECTRICAL ENGINEERING DEPARTMENT



THE CITY COLLEGE OF
THE CITY UNIVERSITY of NEW YORK

COMMUNICATION USING CHANNELS FORMED BY METEORS BURSTS

FINAL TECHNICAL REPORT - 85-0234-1

July 1, 1985 - November 30, 1988

GRANT AFOSR - 85-0234

Air Force Office Of Scientific Research

Bolling Air Force Base

Washington, D.C. 20322

Donald L. Schilling
H. J. Kayser Professor of Electrical Engineering
Principal Investigator

COMMUNICATION SYSTEMS LABORATORY

ELECTRICAL ENGINEERING DEPARTMENT

C.C.N.Y.

Table of Contents

1 STATEMENT OF THE PROBLEM	1
1.1 Introduction	1
1.2 Identification of the Problem	2
1.3 Significance of the Problem	3
1.4 Physical Properties of Meteor Trails	3
1.4.1 Meteoric Particles	4
1.4.2 Meteor Trails	6
1.4.3 Reflections Properties of Trails	8
1.4.4 Other Aspects	8
1.5 System Considerations	10
1.5.1 Point to Point Mode	10
1.5.2 Low Probability of Intercept (LPI) and Antijam (AJ) Consideration	11
1.5.3 System Performance	13
1.6 Past Systems	13
2 MATHEMATICAL MODEL AND CONCEPTUAL FRAMEWORK	15
2.1 Power Received and Related Parameters	15
2.1.1 Power Received from an Underdense Trail	15
2.1.2 Electron Line Density Statistics Underdense Case	17
2.1.3 Decay Time Constant Statistics - Underdense Case	18
2.1.4 Joint PDF of q and B -Underdense Case	18
2.1.5 Power received from Overdense Trails	18
2.1.6 Electron Line Density Statistics - Overdense Case	20
2.2 Link Geometry	20
2.3 Trail Arrival	21
2.4 Power Spectral Density of the Received Noise	22
2.5 Modulation and Bit Error Rate	23
3 ANALYSIS AND RESULTS	24
3.1 Introduction and Approach	24
3.1.1 Protocol	25
3.2 Improvements	26
3.3 Sample System	27
3.4 Constant Bit Rate and Constrained BER System	28
3.4.1 Channel Duration	28
3.4.1.1 Burst Duration Statistics for Con- stant Bit Rate -- Underdense	28
3.4.1.2 Burst Duration Statistics for Con- stant Bit Rate -- Overdense	31
3.4.2 Bits per Given Burst	34
3.4.3 Throughput for Constant Bit Rate	37
3.4.3.1 Optimal Average Throughput for Constant Bit Rate System -- Underdense.	38
3.4.3.2 Optimal Average Throughput for Constant Bit Rate System -- Overdense.	41
3.4.3.3 Total Average Throughput for Con- stant Bit Rate System.	45
3.5 Variable Bit Rate and Constant BER System	46
3.5.1 Channel Duration	46

3.5.1.1 Transmission Duration for	Variable	
Bit Rate -- Underdense	-	47
3.5.2 Throughput for Variable Bit Rate System		
Underdense	-	48
3.5.3 Throughput for Variable Bit Rate System		
Overdense	-	51
3.5.4 Comparison of Throughput for Constant and		
Variable Bit Rate Systems		53
4 DERIVATIONS		57
4.1 Link Geometry		57
4.2 Derivation of Average Burst Duration,	Constant Bit	
Rate		58
4.3 Burst Duration Constant Bit Rate - Overdense		58
4.4 Optimal Average throughput for	constant bit rate -	
Underdense		61
4.5 Transmission Duration & Throughput	for Variable Bit	
Rate System		62
5 AUTOAMATIC-REPEAT-REQUEST (ARQ) TRANSMISSION over MBC		65
5.1 Performance Measures		65
5.1.1 Throughput Rate		65
5.1.2 Waiting Time		71
5.1.3 Duty Cycle		72
5.2 Meteor Burst Communication System		73
5.2.1 Uncoded Transmission		75
5.2.1.1 Transmission over Underdense Trails		75
5.2.1.2 Transmission over Overdense Trails		76
5.2.2 Coded Transmission		76
5.2.2.1 Transmission over Underdense Trails		79
5.2.2.2 Transmission over Overdense Trails		79
6 CONCLUSION AND IDENTIFICATION OF FUTURE WORK		80
7 TABLES		84
8 FIGURES		86
9 REFERENCES		111

Table of Figures

1. Space Density Of Meteors- Seasonal Variation	86
2. Diurnal Variation In Meteor Activity	87
3. Correlation Patterns Near Mb Receiver	88
4. Geometry Of Meteor Burst-1	89
5. Geometry Of Meteor Burst-2	90
6. Geometry Of Meteor Burst-3	91
7. Idealized Time Variations - Underdense And Overdense.	92
8. Power Received- Underdense	93
9. Pdf And Cdf Of Tb- Underdense (Case 1)	94
10. Pdf And Cdf Of Tb- Underdense (Case 2)	95
11. Burst Duration- Underdense	96
12. Burst Duration- Overdense	97
13. Bits Per Given Burst	98
14. Average Burst Duration - Underdense	99
15. PDF of underdense burst duration	100
16. Throughput Vs. Fixed Rate - Underdense	101
17. Throughput Vs. Wavelength- Fixed and Adaptive Rate	102
18. Throughput Vs. Fixed Rate - Overdense	103
19. Optimal Constant Bit Rate Vs. Wave Length- Underdense	104
20. Optimal Constant Bit rate Vs. Link Distance -Underdense	105
21. Max. (Avg.) Throughput Vs. Wave Length-Underdense	106
22. Max. (Avg.) Throughput Vs. Link Distance -Underdense	107
23. Throughput Rate, Stop & Wait Strategy.	108
24. Waiting Time, Stop & Wait Strategy.	109
25. Throughput Rate, Selective Repeat Strategy.	110

Table of Tables

Estimates of the Properties of Sporadic Meteors	84
Average Interval Between Bursts for the Comet System	85

ABSTRACT

We propose to study the use of the meteor burst channel in communication systems by investigating the following important aspects:

- 1) The development and enhancement of an accurate and reliable channel model based on recently available empirical data. Analysis of this model results in analytical expressions for communication parameters such as channel duration and throughput to be used as design and analysis tools.
- 2) The optimization of throughput for fixed transmission rate under the constraint of a given maximum bit error rate. This will demonstrate the room for improvement in existing systems using constant transmission rate.
- 3) The feasibility of efficiently communicating over the MBC using variable bit rate and employing a feedback protocol to monitor the channel. This approach will dramatically improve the throughput in comparison with constant transmission rate systems.
- 4) Analysis of Automatic-Repeat-Request (ARQ) Transmission over MBC by studying performance measures such as duty cycle, throughput and waiting time as a function of packet length, coding, data rate and modulation technique.

1 STATEMENT OF THE PROBLEM

1.1 Introduction

There is currently an urgent need for alternate channels for communication. The large variety and quantity of users throughout the world have caused all of the existing channels to become extremely congested. A world wide search for such alternate channels is now being conducted for both present day and future communication systems through the use of different types of channels such as optical, laser, cable, satellite, etc. [14, 15, 17]

The particular application of Beyond-Line-of-Sight (BLOS) communications, which uses the High Frequency (HF) spectral band from 3 to 30 MHz, is very important to many current and potential users. However, HF is very sensitive to solar disturbances such as sunspot activity, solar storms and other galactic phenomena, as well as multipath returns from both ground and atmosphere, weather related attenuation, and other degrading factors [18,19]. Because of these factors a channel for communication is needed which has low congestion, is robust and relatively indestructible, has very little outside interference and does not compete for bandwidth with existing communication systems. The research proposed herein represents such an alternative mode for communication.

Meteors are small aggregates of matter which upon entering the Earth's atmosphere burn up and form long columns or trails of ionized particles in the upper atmosphere at altitudes of 80 to 120 km. The ionized columns diffuse within seconds yet are able to support radio communication over a range of distance up to 2000 km by reflecting a radio signal and thus provide us with the so-called meteor burst channel (MBC). The frequency range used is from 30 to 100 MHz. The lower limit is dictated by the need to be above the HF range and avoid ionospherically reflected signals. The upper limit is set primarily by equipment sensitivity limitations since reflections at the higher frequencies are weaker than those at lower frequencies.

Excluding showers (annual Pleiades shower) the occurrence of a meteor burst appears in time to be random with a Poisson arrival and an average interval time on the order of several seconds to minutes depending upon time of day, season, and global location, and communication system parameters.

Two types of trails are described in the literature: Underdense trails which are more frequent and have an electron line density below 10^{14} e/m; and overdense trails which are less frequent and have electron line densities of more than 10^{14} e/m. The power received from an underdense trail is approximated as an exponential time function whose initial amplitude is proportional to the square of the electron line density and the exponential decay time constant

varies randomly from one trail to the next. The power received from an overdense trail is modeled by a complex time function whose shape for a given set of communication system parameters is determined by the value of the electron line density.

In the late fifties and early sixties, a considerable amount of research was conducted on the use of meteor burst communications for beyond line-of-sight (BLOS) transmission of digital data. In recent years, interest in meteor burst has been renewed because of several factors. The development of microprocessors (enabling inexpensive implementation of sophisticated system control procedures) and inexpensive solid-state memories (for the buffering required to interface a burst transmission scheme to constant data sources and sinks) is partly responsible. In addition, the nuclear survivability of the meteor burst medium is superior to other BLOS media such as satellite and HF skywave, resulting in considerable interest in the military community.

1.2 Identification of the Problem

The research proposed herein represents such an alternative mode for BLOS communication. It relates a novel approach for BLOS communication. The approach is aimed at efficaciously using a previously under utilized and inefficiently used method of communication, namely, the Meteor Burst Channel (MBC) [1, 9]. This medium possesses all of the qualities mentioned above for a new communications channel. The channel operates in the relatively unused lower portion of the Very High Frequency (VHF) band ranging from 30 to 100 MHz. It avoids the degradations exhibited by HF on the low end and ionospheric phenomena at the high end. This region of the spectrum provides a sufficiently large bandwidth for efficient data communication. It is not easily destroyed. It has a privacy feature inherent in its structure [1,9] and by virtue of its "newness" does not interfere with existing systems. For MBC, the antennas have a high elevation angle and rarely interfere with present use of the frequency band when such is present.

This study seeks to define systematically and analytically the limits of transmission of digital information over the meteor burst channel by using an improved model to develop the mathematical relationships among link geometry, communication circuitry parameters, physical meteor characteristics, modulation technique and a given communication protocol. Furthermore, the research will be aimed at the determination of optimal average throughput for both constant and variable transmission rates under the employment of an information feedback scheme for reliable channel monitoring.

These results will serve as a vital design and analysis tool for the communication system engineer using the MBC. Furthermore, they will demonstrate the viability and potential improvement over past and currently implemented systems. Finally, they will identify the necessary and challenging areas for future research.

1.3 Significance of the Problem

Meteor Burst communications has wide ranging effects for modern society. It offers simple and reliable communications and can operate in the simplex, half-duplex and full-duplex mode over distances of 200 to 1200 miles. [9,22]. Efficient use of this channel will result in increased data throughput for applications such as facsimile transmission (FAX), TELEX, transmission of computer data, radio amateur usage, voice burst transmission using phonemes (i.e., transmission in which the voice is digitally encoded using rates of 50 to 250 bits per second) and military communication systems. These types of communications and data transmission facilities involve transactions of banks, universities and medical centers, corporate business concerns such as online systems, and government agencies. In addition, recreational and pleasure or leisure activities could make use of this mode of communication.

If shown to be feasible and commercially cost effective business as well as home users could provide a potentially large market. The advent of the microprocessor will reduce the cost of such systems thus enabling inexpensive implementation of the control requirements to be met [9,22,23]. This potential for low cost will open up the home and business market which has already invested millions of dollars in personal computers and modems. Furthermore, the number of these types of users is increasing daily.

Some of the government agencies interested in alternate communications means are the Department of Agriculture, the Department of Energy (DOE), the National Oceanic and Atmospheric Administration (NOAA), the Department of Defense (DOD), the National Aeronautics and Space Administration (NASA) and the Defense Communications Agency-(DCA) [9,22].

1.4 Physical Properties of Meteor Trails

Nearly all of the present knowledge regarding the physical properties of meteors has been obtained from visual, optical, and radio observations of the trails formed by the meteoric particles as they enter the atmosphere of the earth. In this section the properties of the meteoric particles themselves and the trails which they form will be reviewed. The mathematical model and conceptual

framework reflecting physical and radio properties of the trail will be presented in chapter 2. The review of meteoric particles and the trails they form in sections 1.4.1-1.4.4 is taken directly from Sugar's [1] 1964 review paper.

1.4.1 Meteoric Particles

For the purposes of this discussion the term "Meteors" will be used to apply to those particles entering the earth's atmosphere that are burned by frictional heating. This definition includes the very small particles, the micrometeorites, that slowly settle through the atmosphere without being destroyed. It also includes the large meteors which manifest themselves as fireballs or the even larger ones which reach the earth's surface as meteorites. The micrometeorites are not of concern because even though they are the most numerous of the various types, they enter the atmosphere too slowly to produce any significant ionization. The large meteoroids, although they produce substantial ionization, are of little concern here because their rate of occurrence is extremely low.

Some of the properties of meteoric particles are summarized in Table 1 [24], [25]. The particles of interest in meteor propagation are those with masses in the range 10^3 to 10^{-7} g and dimensions in the range 8 cm to 40 microns. Before being trapped by the gravitational field of the earth these particles move in orbits around the sun. Their composition is uncertain; however, they appear to be almost entirely of cometary origin. A substantial fraction of them are not single solid particles but fragile loosely-bound agglomerates, sometimes called "dustballs",

The meteors can be divided into two classes, the shower meteors and the sporadic meteors. The shower meteors are collections of particles all moving at the same velocity in fairly well-defined orbits or streams around the sun. Their orbits intersect the orbit of the earth at a specific time each year and at these times the well-known meteor showers are observed. In the cases where the particles are uniformly distributed around the orbit, the size of the shower varies little from year to year. If, on the other hand, there is a concentration of particles within the orbit, the extent of a shower can vary substantially in successive years. (The Leonid shower of 1833 is an example of an unusual display of meteor activity. During the peak of the shower as many as 20 meteor trails were often seen by a single observer in one second.) The shower meteors, while the most spectacular, account for only a small fraction of all meteors. It is the nonshower or sporadic meteors that comprise nearly all of the meteors of interest in radio propagation. These meteors are those which do not have well-defined streams but rather seem to move in random orbits. Thus, whereas

shower meteors appear to be coming from a specific point in the sky--the radiant point for the shower--sporadic meteors have radiants that appear to be randomly distributed over the sky.

The relation between sporadic and shower meteors is not clear at the present time. It is possible that the sporadic meteors represent the final stages in the decay of meteor streams. On the other hand there is some indication that the sporadic meteors are in fact distributed in a large number of relatively small groups and that the earth is immersed in about 11 such groups at a time. Further work is needed to resolve the origins of the sporadic meteors [1].

Shower meteors are most easily recognized in terms of their radiants, velocities, and time of occurrence, since these parameters are relatively fixed. The radiants and times of occurrence of sporadic meteors are random. Their radiant points are not, however, uniformly distributed in the sky but are for the most part concentrated toward the ecliptic plane (the plane of the earth's orbit) and move in the same direction around the sun as the earth moves [26]. The orbits are not uniformly distributed along the earth's orbit but are concentrated so as to produce a maximum incidence of meteors at the earth in July and a minimum in February. This variation in the space density of meteors is shown in Fig. 1 which has been adapted from the data of Hawkins [26].

The rate of incidence of sporadic meteors at the earth is further modified by two factors. The first of these--resulting in a regular diurnal variation in meteor rate is illustrated in Fig. 2. On the morning side of the earth, meteors are swept up by the forward motion of the earth in its motion around the sun. On the evening side the only meteors reaching the earth are those which overtake it. This results in a maximum occurrence rate around 6 a.m. and a minimum rate around 6 p.m. The ratio of maximum to minimum depends on the latitude of the observer. A further minor seasonal variation is introduced because of the tilt of the earth's axis relative to the ecliptic plane [27]. This variation, also dependent on the latitude of the observer, can change the expected hourly rates by factors as large as 1.4:1.

The mass distribution of sporadic meteors is such that there are approximately equal total masses of each size of particle. There are, for example, 10 times as many particles of mass 10^{-4} g as there are particles of mass 10^{-3} g. This approximate relation between particle mass and number is given in Table 1. The mass distribution of shower meteors is somewhat similar to that for the sporadic meteors with the important difference that there are more large particles relative to the number of smaller ones than for the sporadic meteors.

The velocities of meteors approaching the earth are in the range 11.3 to 72 km/sec. The lower limit is the escape velocity for a particle leaving the earth and is therefore the lowest velocity that a particle falling toward the earth can have. The upper limit is the sum of two components, a 30 km/sec component associated with the earth in its orbit around the sun, and a 42 km/sec component associated with the meteor itself. This latter velocity is the escape velocity for a particle leaving the solar system. Nearly all observations have indicated that meteor velocities fall in the above range and that the meteors are thus members of the solar system.

1.4.2 Meteor Trails

1) *Formation*: As a meteoric particle enters the earth's atmosphere it collides with air molecules which then become trapped in its surface. The impact energy produces heat which evaporates atoms from the meteor and these move off with a velocity which is substantially equal to that of the meteor. Collisions between these high velocity atoms and the surrounding air result in the production of heat, light, and ionization, distributed in the form of a long, thin, paraboloid of revolution with the particle at the head of it. The electron line density in the trail is proportional to the mass of the particle. In the evaporation process each original impact frees many meteoric atoms and thus the total mass of air molecules striking the meteor is small compared to the meteoric mass itself. As a consequence the velocity of the meteor remains quite constant until the meteor is nearly completely evaporated. (Those meteors that appear to be dustballs rather than solid particles break up or "fragment" upon entering the atmosphere and proceed as a group of smaller particles. For this case the above description appears to be correct if it is applied to the individual particles after fragmentation occurs.)

2) *Heights*: As a meteoric particle approaches the earth no appreciable ionization is formed until the particle enters the relatively dense air at heights below about 120 km. Above that height collisions of the particles with air molecules are not frequent enough to be of significance. As the particle traverses the region below about 120 km it vaporizes rapidly and most particles are completely evaporated before reaching 80 km. The relatively small thickness of the meteor region is a result of the rapid change in air density which occurs over the height range quoted. At 120 km the mean free path is 5.4 m and this decreases in an approximately logarithmic manner so that at 80 km it is only 3.8 mm.

The height distribution of trails varies somewhat with particle characteristics. The higher velocity particles produce trails at the higher heights with the mean trail height increasing to about 10 km as velocity increases from less than 15 km/sec to greater than 60 km/sec [1]. The particles of higher mass produce maximum trail ionization at lower heights. Over the mass range of 10^3 to 10^{-7} g the height variation is around 44 km. There is also a height variation with the zenith angle of the trail orientation, with the larger angles corresponding to greater heights. A variation of about 13 km is associated with nearly the whole range of zenith angles.

3) *Lengths*: The lengths of meteor trails are primarily dependent on particle mass and zenith angle. Typical lengths range up to 50 km with the most probable trail length for sporadic meteors being 15 km. (Several definitions of "length" can be used and the one chosen here uses as end points the points with a threshold value chosen.)

4) *Initial Radius*: Until recently it has been assumed that, at the time of their formation, trails had an initial radius of the order of the mean free path or at most about 14 times this radius. However, photographic and radio measurement have suggested that the initial radius is significantly larger than indicated above and that this increase is probably associated with the dustball and fragmentation hypothesis.

The trail radii indicated by these measurements are in the range 0 to 1.2 m (with a mean value of 0.65 m) for the photographic work, and 0.55 to 4.35 m for the radio work. The 0.55 m was for a height of 81 km where the mean free path is only 5×10^{-4} m. The results at 121 km are more nearly consistent with Manning's hypothesis since the initial radius observed is 4.35 m and the mean free path is 5 m.

5) *Dissipation*: Once the trail is formed it expands by diffusion [21] at a relatively low rate, producing a radial distribution of material that is approximately Gaussian. The quantity $(4Dt + r^2)^{1/2}$ may be taken as the approximate radius of the trail after a time t where D is the diffusion coefficient and r is the initial radius of the trail. D varies from $1 \text{ m}^2/\text{sec}$ at an 85 km height to $140 \text{ m}^2/\text{sec}$ at 115 km. Thus after one second a trail will have a radius in the range 2 to 20 m.

The practical lifetime of a trail is of course dependent on the means for detecting it. Most trails detected by radio means are those resulting from small particles and these last only a fraction of a second. The larger particles produce more densely ionized trails and trails with durations of the order of a minute are observed several times per day. Trails with durations of the order of an hour or more are extremely rare.

The dissipation of trails is further complicated by the presence of winds in the meteor region. At the time of formation trails are quite straight but they are rapidly deformed by these winds which have typical velocities of the order of 25 m/sec and vertical gradients with mean relative maxima of about 100 m/sec/km. A wind shear of this magnitude can rotate part of a trail through an angle of 5° in one second.

1.4.3 Reflections Properties of Trails

The distribution of energy reflected by a meteor trail is a function of many variables. The ionization density distribution across and along the trail, the orientation of the trail, the radio wavelength, the polarization of the incident wave relative to the trail, motion of the trail either as part of the process of formation or due to ionospheric winds, and the straightness of the trail are all significant. In discussing the reflection properties it is convenient to divide the trails into two classes underdense trails and overdense trails and to examine the properties of each class independently. Underdense trails are those wherein the electron density is low enough so that the incident wave passes through the trail and the trail can be considered as an array of independent scatterers. Overdense trails are those wherein the electron density is high enough to prevent complete penetration of the incident wave and to cause reflection of waves in the same sense that the ordinary ionospheric reflections occurs. A rough sorting of trails into these two categories can be done on the basis of trail lifetime or duration. At long wavelengths the underdense trails have durations of less than about one second while the overdense trails have longer durations. At long wavelengths the effective duration of a trail is large compared to the time it takes the trail to form, and the trail may be considered to have a cylindrical shape.

The solutions to be considered here are useful approximations to the physical problems. They will apply quite well to some of the trails observed and rather poorly to others. A complete analysis of the reflections from even a relatively simple trail would be far too complex to be of any practical use or interest.

1.4.4 Other Aspects

In this section some additional practical aspects will be discussed from a qualitative viewpoint. The discussion is directed toward the long wavelength cases since relatively few short wavelength observations have been made and analyzed.

1) *Long Wavelength Reflections during Trail Formation:* The transient state associated with trail formation is of interest since it accounts for some of the observed characteristics of trail reflections. As a trail is being formed, but before the meteor reaches the first Fresnel zone, a weak reflection is obtained from the incomplete trail. This comes primarily from the part of the trail corresponding to the shortest transmission path at the instant; and when, as is usually the case, this is the head of the trail, the reflected signals are shifted in frequency because of the motion of the effective reflecting point. As the meteor approaches the first Fresnel zone for the trail this frequency shift approaches zero, and thus the received frequency decreases with time. The observed frequency will of course depend on trail orientation, meteor velocity and observing wavelength. A maximum shift of the order of 5 kHz is possible for 50 MHz forward-scatter observations over a 1000 km path.

2) *Trail Drift and Distortion:* The effects of ionospheric winds are appreciable for trails which last for the order of a second or more. A Doppler shift of the received frequency will be associated with the average wind velocity of the trail. For a velocity of 25 m/sec this "body Doppler" can be as large as 18 Hz for backscatter observations at 50 MHz and will be somewhat less for forward-scatter observations.

The trail distortion resulting from wind shears can lead to the formation of several local first Fresnel zones for the trail since a distorted trail can have several points where the transmission path length has a local minimum. These local minima, or "glints" as they have been called [41], are strong scatters and the received signal is a composite of their contributions. Since they are moving at different velocities the signals from each have different Doppler shifts and the resultant composite signal fades in an irregular manner [24]. (At 50 MHz the fading rate observed for forward scatter are of the order of 1-10 Hz.) In addition to producing the fading observed for long-enduring trails the wind shears can rotate a trail sufficiently to produce reflections when the initial orientation has not been suitable. Thus these trails lose their aspect sensitivity as time goes on, and if their life is of the order of 10 seconds they will scatter in all directions.

3) *Polarization Effects:* Thus far the only indication that the polarization of the incident wave can be of significance was the inclusion of the $\sin^2(\alpha)$ term in each of the transmission equations for the forward-scatter cases. This term accounts for the foreshortening of the electric vector of the incident wave which occurs when it is viewed from the receiver. In addition to this, a kind of electron resonance can occur which increases the reflection coefficient for the trail. This is associated with the restoring force that the electrons

experience as the incident electric field displaces them from their equilibrium positions in a direction normal to the trail. This resonance can occur only for underdense trails and only then for trail diameters much less than the wavelength. This resonance at most doubles the reflection coefficient and thus can increase the received power by a factor of 4.

4) *Diversity Effects*: Underdense trails act as small coherent sources, and therefore CW signals scattered by them exhibit good space and frequency correlation. Correspondingly, very little pulse broadcasting is observed when pulse signals are used. The limited available data, suggest that for a forward-scatter path about 1000 km in length, operating near 50 MHz the correlation coefficient observed for single underdense trails will fall to 0.5 for antenna spacings of the order of 150 km along the path, for antenna spacings of the order of 30 km across the path, and for frequency separations greater than 5 MHz. Three micro-sec pulses show no appreciable broadening under these conditions.

Overdense trails, in contrast to the underdense trails, tend to act like relatively large sources and therefore exhibit much poorer space and frequency correlation properties. Again, as in the underdense case, specific data on these properties are not available. Present results suggest that the correlation observed for single overdense trails will fall to 0.5 for antenna spacings of the order of 50 [41]. Measurements using short pulses over a 1000-km path indicate that the received composite signal can have a total time spread as large as 10 micro- sec [44].

1.5 System Considerations

There are three potential modes of operation for a meteor burst system: point-to-point, netted, and broadcast. While a meteor burst system could be operated in any or all of these modes, all known meteor burst systems that have currently been implemented have been designed for point-to-point applications. In this section, we discuss some of the possibilities for configuring meteor burst systems in point to point mode. The general discussion in the following sections 1.5.1-1.5.3 is taken directly from Oetting's [9] 1980 review paper.

1.5.1 Point to Point Mode

The point-to-point mode is, of course, straightforwardly implemented. The only requisite for effective system control is the ability of the transmitting terminal to discern, as accurately as possible, the beginning and end of a useful burst. If transmission begins too late or ends too soon, valuable burst time will be wasted. If the transmission extends past the useful portion of the burst, a high error rate will result.

In all point-to-point systems, we assume that a feedback path is available. In the half-duplex case, the forward and return links share the same frequency, while in the full-duplex case, they use two different frequencies. For achieving data transmission between point A and point B, perhaps the simplest strategy is to assign a different frequency to each transmitter and to continuously transmit a probe signal from the master station (say, point A). When point B detects the probe, he transmits a preamble followed by his information. Point A uses the preamble to synchronize his receiver and is subsequently able to receive data. It is usually required that A acknowledge the reception of the message or block of data.

Several variations of this basic point-to-point approach have been developed. Early meteor burst systems used a signal amplitude threshold to determine if the probe signal were being received. The JANET system [1]-[13] improved upon this procedure by substituting a signal-to-noise ratio measurement for the fixed threshold test, thereby reducing the false alarm rate. After extensive testing of the JANET B system, the SHAPE Technical Centre concluded that, even with the SNR approach, a suitable compromise between efficient use of the channel and low error rate was not achievable. Thus, they developed their own approach using ARQ with one teletype character per seven-bit block. This approach is referred to as the COMET system [5] and [9].

The possibilities for netted meteor burst systems have not been well explored to date. The only known system capable of netted operation is the Western Union hardware currently being installed for the Department of Agriculture [28]. This system will consist of 511 remote sites that communicate with two master stations. Although the Department of Agriculture application involves one-way transmission of data from the remote to the master stations, the system can be configured to provide two-way data transmission. A network could then be achieved by having a master station operate in a store-and-forward mode.

1.5.2 Low Probability of Intercept (LPI) and Antijam (AJ) Consideration

One of the primary attractions of meteor burst communications is its inherent privacy resulting from the restricted footprint of reflections from meteor trails. This property has received considerable attention in the meteor burst literature and has prompted a large number of industry proposals to provide LPI meteor burst systems for numerous Department of Defense (DoD) and non-DoD agencies.

Signals propagating between a specific transmitter and receiver can normally be detected by an eavesdropping receiver only if the latter is located in an elliptically bounded "footprint" in the vicinity of the primary receiver. By reciprocity, interfering signals from a remote transmitter will propagate to a meteor burst receiver only if the interfering transmitter is within the footprint of the desired transmitter. Measurements indicate that the major and minor axes of the footprint are on the order of 2000 and 25 mi, respectively. Clearly, the footprint is not a well-defined boundary within which the signal is always received and beyond which it is never received. Instead, the situation is better depicted by Fig. 3 which shows theoretical and experimental results for the correlation between the signals detected by two different receivers as a function of the distance between them. When the unintended receiver is moved in a direction perpendicular to the transmission path, the correlation falls off more rapidly than when the unintended receiver is moved along the propagation path. [9]

While the theoretical along-the-path correlation falls off at an alarmingly slow rate, the experimental results illustrate two key points: the theoretical performance is difficult to achieve in practice, and the correlation decreases at higher operating frequencies. In addition, it has been shown [29] that fading reflections are responsible for a significant part of the correlation at large separations (trails that have been distorted by winds exhibit broader reradiation patterns than newly formed trails). By communicating only during the nonfading portion of each burst, the size of a footprint can be kept to a minimum.

LPI is best achieved by operating in a burst mode with a low duty cycle. While interception by a beyond-the-horizon transmitter is then governed by the probabilities shown in Fig. 3, a meteor burst system is vulnerable to line-of-sight interception unless spread spectrum techniques are employed.

As for AJ considerations, line-of-sight jamming can be easily accomplished in view of the losses incurred by the desired signal in the course of being reflected from a meteor trail. In the case of beyond-the-horizon jamming, the jammer can disrupt only a small fraction of the traffic if he relies on reflections from meteor trails to propagate his jamming signals. A much better strategy is to use extremely high power (perhaps in a pulsed model) and rely on ionosscatter propagation. This approach can be defeated by operating at the higher meteor burst frequencies, since ionosscatter falls off much faster with increasing frequency than does meteor trails reflections. Finally, a jammer can attempt to spoof the system by transmitting a simulated probe signal, but spoofing can be defeated by judicious system design.

1.5.3 System Performance

The performance parameters of greatest interest in commercial applications are the average throughput (in bit per second), the average waiting time (to transmit a message of specific length), and the probability of error. These parameters will be influenced to varying degrees by the environmental variables: background noise level, external interference, geographic location, season, and time of day. The system designer, on the other hand, can exert control over system performance by manipulating his design variables - transmitted power, RF frequency, instantaneous data rate, modulation technique and antenna gain.

The throughput of a meteor burst system depends on factors such as transmitted power, operating frequency, communications range, received noise and instantaneous data rate. The increase in throughput that can ultimately be attained is limited by intersymbol interference due to multipath effects, practical bit synchronization problems, and, of course, the available transmitter power and antenna gains.

In addition to the factors under the control of the system designer, the throughput also depends on such environmental variables as time of day and season of the year. These variations typically involve a factor of five diurnally and three seasonally.

1.6 Past Systems

A landmark meteor trail communication system was operational in the 1950s--the Canadian JANET system. It was used for teletype communications between Toronto and Port Arthur, a distance of approximately 1000 km [1],[4]. A double sideband AM duplex channel was used to transmit and receive cosine-squared shaped pulses in pulse position modulation (ppm) at a rate of 650 bits per second (bps). Punched paper tape, magnetic tape, and a toroidal magnetic matrix storage core were used as storage media to compress messages in time for transmission and to store and expand the messages at the receiving station. Despite its relative antiquity, the JANET system embodied many of the features of today's systems: stored digital data which is transmitted/received in bursts after carrier detection, duplex operation at VHF frequencies around 50 MHz, and low effective duty cycles (about 0.1 for the JANET system). Other links, such as a one way Bozeman, MONTANA-Stanford, California meteor burst link were also operational during the 1950s, but the JANET system represents the first mature, complete, practical hardware implementation of a meteor burst system.

Subsequent experimental tests were conducted during the 1960s and 1970s. Notable among these efforts is the experimental work summarized by Sugar [4] and the implementation of the COMET (COMMunication by METeor Trails) system which has operated between the Netherlands and Southern France. COMET made use of frequency diversity and Automatic Repeat for reQuest (ARQ) which allowed for signal repetition in the event of no radio path. The COMET system used a 2000 baud signaling rate and FSK with a 6 KHz deviation. The storage devices were similar to those of the JANET system. COMET demonstrated the practicality of meteor burst communications under a variety of conditions. Typical results indicated successful transmission of a 50 baud (average) message, 150 characters long with a delay of about a minute. Worst case delays of 3 or 4 minutes were typical [5]. Studies of COMET-type systems have continued into the 1980s [5][9].

2 MATHEMATICAL MODEL AND CONCEPTUAL FRAMEWORK

In this chapter the basic equations that model the meteor burst channel are presented. In addition, basic assumptions, constraints and empirical factors are stated.

2.1 Power Received and Related Parameters

The power received from the trail model used here is from the classic paper by Eshelman and Manning [6] and Hines and Forsyth [16].

2.1.1 Power Received from an Underdense Trail

Meteor trails with fewer than 10^{14} electrons per meter of length are referred to as underdense. Eshelman has shown that a simple Fresnel description of the process is normally sufficient. The scattering then is specular for the majority of received signals that is the incident and scattered rays make equal angles δ with the axis of the trail and the received signal comes, in effect, from the principal Fresnel zone alone. See Fig. 4

The principal Fresnel zone is centered on a point P in the trail at a distance R_T and R_R from the transmitter T and receiver R respectively such that $R_T + R_R$ is a minimum for the trail in question. The received power rises rapidly in the fraction of a second taken by the meteor to traverse the principal zone and reaches a peak volume at time $t=0$.

Although the meteor trail is formed as a narrow column, a few centimeters in diameter, it immediately begins to expand by diffusion. As the diameter increases, the scattered signal suffers increasingly from a destructive interference of the fields scattered by individual electrons. In ideal circumstances, neglecting Fresnel ripples and initial diameter, the received power decays exponentially in time, see fig. 7. The above is summarized in the next equation.

$$P(t) = \frac{P_T G_T G_R r_e^2 \sin^2(\alpha) \lambda^3 \exp\left(-\frac{8\pi^2 r_0^2}{\lambda^2 \sec^2 \phi}\right)}{16\pi^2 R_T R_R (R_T + R_R) (1 - \cos^2 \beta \sin^2 \phi)} q^2 \exp\left(-\frac{32\pi^2 D}{\lambda^2 \sec^2 \phi} \cdot t\right)$$

'where,'

(2.1.1-1)

P_T Transmitter power.

G_T, G_R Transmitter and receiver antenna gains, respectively.

r_e Classical radius of an electron ($2.82 \cdot 10^{-15}$ m).

- α Angle between the electron field vector E and R_R .
 q Electron line density of the trail.
 λ Carrier wavelength.
 r_0 Initial radius of the trail (.65 m.).
 ϕ Angle of incidence/reflection of the transmitted plane wave.
 R_T Distance from transmitter to trail.
 R_R Distance from receiver to trail.
 D Diffusion coefficient of the atmosphere.
 β Angle between the trail and the propagation plane formed by R_T and R_R .

Figures 4, 5, and 6 depict the geometrical parameters.

A minimal set of assumptions is applied in the literature [7,11,21] for analysis:

- 1.) The trail occurs at midpoint between receiver and transmitter i.e. $R_T = R_R$
- 2.) The burst occurs at an altitude of 100 km.
- 3.) The trail is travelling at a plane perpendicular to the plane formed by R_T and R_R i.e. $\beta = \pi/2$. In addition, we set $\alpha = \pi/2$

Under these assumptions and after substituting for the physical constants we rearrange the above equation to arrive at the power received equation for the underdense case.

$$P(t) = C_U q^2 e^{-t/\bar{B}} \quad (2.1.1-2)$$

where,

$$C_U = 2.5179581 \cdot 10^{-32} \cdot \frac{P_T G_T G_R \lambda^3 \exp\left(-\frac{33.359}{\lambda^2 \sec^2 \phi}\right)}{R_T^3}$$

$$\bar{B} = 3.166 \cdot 10^{-3} \cdot \frac{\lambda^2 \sec^2 \phi}{D}$$

It should be emphasized that:

- 1.) $P(0)$, the maximum power from the underdense trail is proportional to q^2 ; for a specific trail q is fixed. (The random character of q is discussed later).
- 2.) C_U , the constant of proportionality, incorporates the effects of link geometry, transmitter power, antenna gains and carrier wavelength. For a given communication system C_U is constant since link distance, transmitter power, antenna gains and carrier frequency are set.

3.) The decay time constant B given above is found to be randomly varying from trail to trail. The expression in the classic model corresponding to a decay time constant is taken as the average decay time constant in accordance with observations. To date, however, researchers have assumed all underdense trails to share the same decay time constant to facilitate their analysis. It is in this added complexity to the model that our treatment deviates from published analysis and enhances its accuracy.

4.) The decay time constant B and the electron line density q are functionally independent [1] [7] and hence statistically independent.

5.) For a given communication system (i.e. C_U fixed) knowledge of the electron line density q , and decay time constant B , completely specify the underdense trail behavior in time.

2.1.2 Electron Line Density Statistics - Underdense Case

Based on recent empirical data [33] the pdf for q is:

$$f_q(q) = Qq^{-p} \quad q_{\min} \leq q \leq q_u = 10^{14} \text{ e/m} \quad (2.1.2-2)$$

where,

$$Q = (p-1)q_{\min}^{p-1} \cdot \frac{1}{1 - \left(\frac{q_{\min}}{q_u}\right)^{p-1}}$$

$$p = 1.6$$

q_{\min} = Minimum q as explained below.

q_{\min} is the minimum electron line density q a trail must possess to be 'seen' by the communication system i.e. $C_U q_{\min}^2$ is the minimum power level P_{\min} detected by the communication system. In the context of constant transmission rate systems (as discussed later) P_{\min} is the power level that corresponds to the maximum allowed bit error rate. See fig. 8

2.1.3 Decay Time Constant Statistics - Underdense Case

We start by stating that the expected value of the decay time constant B is well approximated by:

$$E(B) = \bar{B} = 3.16610^{-3} \cdot \frac{\lambda^2 \sec^2 \phi}{D} \quad \text{sec} \quad (2.1.3-1)$$

as defined in section 2.1.1

The random decay time constant B is assumed to be exponential or Rayleigh. Both assumptions have been shown to be consistent with recent experimental observation [33]. In general the Rayleigh distribution will be used since for very small B (extremely fast decay) the probability is very near zero. This is appealing from a physical viewpoint and consistent with observation. It should also be noted that even if such exceedingly fast decaying trails occur they are of no utility for communication.

Exponential:

$$f_s(b) = \frac{1}{\bar{B}} e^{-b/\bar{B}} \quad (2.1.3-2)$$

where \bar{B} is defined above.

Rayleigh:

$$f_s(b) = \frac{b}{\alpha^2} e^{-b^2/2\alpha^2} \quad (2.1.3-3)$$

where,

$$\alpha = \sqrt{\frac{2}{\pi}} \bar{B}$$

2.1.4 Joint PDF of q and B -Underdense Case

Since the electron line density and the decay time constant are statistically independent the joint pdf is given by their product i.e.

$$f_{q,s}(q,b) = f_q(q) \cdot f_s(b) \quad (2.1.4-1)$$

where the individual densities are given in the previous sections.

2.1.5 Power received from Overdense Trails

Trails with more 10^{14} electrons per meter are often termed "overdense." When treating them, it is no longer satisfactory to think of the incident wave as penetrating the trail without serious modification. Instead, coupling between

individual electrons plays a prominent part, and the whole of the scattering process is conceived more simply in terms of reflections from a cylindrical surface.

The surface in question surrounds the axis of the trail at a radius r , where the electron volume density has the critical value normally associated with reflection of the incident wave (cf. reflection from the ionosphere). The volume density within the trail exceeds the critical value, and cannot support propagation in the usual sense at the pertinent frequency. As the electrons diffuse outwards, r increases from an initially small value, passes through a maximum, and falls to zero as the volume density at the axis of the trail decreases below the critical value. In the very latest stages the scattering reverts to the underdense type, but only after some time, and so only when the underdense scattering is extremely small.

The scattering process is again specular, the angles of incidence and reflection being equal. The received power variation is given by:

$$P(t) = C'_0 \sqrt{\frac{r_0^2 + 4Dt}{\sec^2 \phi}} \ln \left(\frac{r_0 \lambda^2 \sec^2 \phi}{\pi^2 (r_0^2 + 4Dt)} \cdot q \right) \quad (2.1.5-1)$$

where,

$$C'_0 = \frac{P_T G_T G_R \sin^2(\alpha) \lambda^2}{32 \pi^2 R_T R_R (R_T + R_R) (1 - \cos^2 \beta \sin^2 \phi)}$$

and all other parameters are as defined for the underdense burst.

Using the same assumptions as for underdense case ($\alpha = \beta = \pi/2$ and $R_T = R_R$) and some algebra we rewrite the above as:

$$P(t) = C_0 \sqrt{(k+t) \cdot \ln \left(\frac{\alpha \cdot q}{k+t} \right)} \quad t \leq \alpha q - k \quad (2.1.5-2)$$

where,

$$C_0 = 3.166286 \cdot 10^{-3} \sqrt{D} \frac{P_T G_T G_R \lambda^2}{R_T^3}$$

$$k = .105625/D$$

$$\alpha = 7.143143 \cdot 10^{-17} \cdot \frac{\lambda^2 \sec^2 \phi}{D}$$

As in the underdense case we have rearranged the classic equation for ease of handling. Note that C_0 contains the transmitted power, antenna gains, diffusion coefficient, carrier frequency and the effects of link distance. Fig. 7

In addition, from eq. (2.1.1-2) we relate C_U and C_O by

$$C_O = 1.257481610^{29} \frac{\sqrt{D}}{\lambda} \cdot e^{\left(\frac{33.359}{\lambda^2 \sec^2 \phi}\right)} \cdot C_U \quad (2.1.5-3)$$

2.1.6 Electron Line Density Statistics

- Overdense Case

Based on recent empirical data [33] the pdf for q is:

$$f_q(q) = Q q^{-p} \quad q_{\min o} \leq q \leq q_{uo} = 10^{16} \text{ e/m} \quad (2.1.6-2)$$

where,

$$Q = (p-1) q_{\min o}^{p-1} \cdot \frac{1}{1 - \left(\frac{q_{uo}}{q_{\min o}}\right)^{p-1}}$$

$$p = 1.5$$

$q_{\min o}$ = Minimum q as explained below.

$q_{\min o}$ is the minimum electron line density q an overdense trail must possess to be 'seen' by the communication system. Note that $q_{\min o} > q_{Lo}$ the (physically) lowest possible electron line density for an overdense trail. $q_{Lo} = 10^{14}$ e/m. We define another constant which we refer to later as:

$$Q' = 1/[1 - (q_{\min o}/q_{Lo})^{p-1}].$$

2.2 Link Geometry

In this section we present the relationship between link distance, L , and station to trail distance, R_T ($=R_R$) and angle of incidence/reflection ϕ See Fig.

6

The station to trail distance is given by

$$R_T = R_R = \sqrt{(h + L^2/8R_s)^2 + L^2/4} \quad (2.2-1)$$

And the incidence/reflection angle ϕ is found thru

$$\sec^2(\phi) = 1 + \frac{L^2}{\left(2h + \frac{L^2}{4R_s}\right)^2} \quad (2.2-2)$$

where,

- h trail altitude (100 km).
- L great circle distance between stations.
- R_T distance from transmitter to trail.
- R_R distance from receiver to trail.
- R_e radius of the earth, 6400 km.

The derivation of the above is done in section. 4.1

Since it is often convenient to express L and the resulting R_R in thousands of kilometers for ease of computation we then have:

$$R_T = R_R = \sqrt{(.1 + (.01953)L^2)^2 + L^2/4} \quad (2.2-3)$$

$$\sec^2(\phi) = 1 + \frac{L^2}{(0.2 + (.039)L^2)^2} \quad (2.2-4)$$

s.t. for $L=1000$ km. we use $L=1$ to quickly yield $R_T=R_R = 514$ km. and $\sec^2 \phi = 18.5$

2.3 Trail Arrival

In this section we are concerned with quantifying the trail arrival process in terms of communication system parameters. Since the arrival is Poisson we need to estimate the average time between bursts or equivalently the number of bursts per second. Oetting, [9] summarized the results of the COMET system showing an average time between bursts of 4 to 20 seconds.

It is often necessary to estimate the number of arrivals of bursts per second with an electron line density of q between some q_1 and q_2 . We let $A'(q)$ be the number of trails/s with an electron line density between q and $q+dq$ e/m. Using Weitzen [10] we write

$$A'(q) = \frac{19.1667 \cdot \phi \sin \phi \cdot (R_e \zeta)^2}{q^2} \quad q_{\min} \leq q \leq q_{\max} = 10^{17} \quad (2.3-1)$$

where ζ is the idealized beamwidth of the antenna and all other parameters have been previously defined. The number of trails/s with q in a given range $[q_1, q_2]$, A , is found by integrating the above density over q yielding the following

$$A = \frac{19.1667 \cdot \phi \sin \phi (R_r \xi)^2}{q_1} \left[1 - \frac{q_1}{q_2} \right] \quad (2.3-2)$$

$$A = \frac{19.1667 \cdot \phi \sin \phi (R_r \xi)^2}{q_1} \left[1 - \frac{q_1}{q_2} \right] \quad (2.3-2)$$

note that for overdense trails ($q_1 > 10^{14}$) we scale the constant 19.1667 in the above Eq. to be 3.

In addition, care must be exercised in setting q_{\min} since this is an empirical relationship. For example, for a 1000 km link with antenna angle of 46° q_{\min} must be above 10^{13} e/m for the formula above to yield reasonable rates.

Finally, we mention again the dependence of the number of bursts/s, A, on other factors such as global location, time of day, and season. These factors should appropriately scale any value of A used for analysis.

2.4 Power Spectral Density of the Received Noise

For signal frequencies appropriate to the MBC the dominant noise sources are galactic and man-made in origin. Consequently, the received noise power spectral density, N_0 , is a function of the galactic noise picked up by the receiver antenna and the receiver thermal noise.

N_0 is modeled as follows:

$$N_0 = kT_0 \left[\frac{104 \left(\frac{\lambda}{15} \right)^{2.3}}{L_r} + F \right] \quad (2.4-1)$$

where,

k = Boltzmann constant, $1.3805 \cdot 10^{-23} J/K$

T_0 = $290^\circ K$

L_r = power loss between the antenna and receiver

F = receiver noise figure

λ = wavelength in meters

We choose typical values for L_r and F as 1.3 and 2.5, respectively to yield the following model for N_0

$$N_0 = 4 \cdot 10^{-21} \left[80 \left(\frac{\lambda}{15} \right)^{2.3} + 2.5 \right] \text{ W/Hz} \quad (2.4-2)$$

2.5 Modulation and Bit Error Rate

The bit error rate, BER, denoted here as P_b , is in general related to the bit energy E_b and power spectral density of the received noise N_0 as

$$P_b(t) = g\left(\frac{E_b(t)}{N_0}\right) \quad (2.5-1)$$

where $g(\cdot)$ is determined by the modulation technique.

Since $E_b(t) = P(t)/R(t)$ where $R(t)$ the bit transmission rate may be time varying or fixed we have from Eq. (2.5-1)

$$P_b(t) = g\left(\frac{P(t)}{N_0 R(t)}\right) \quad (2.5-2)$$

or alternatively, we can solve for the power

$$P(t) = N_0 \cdot R(t) \cdot g^{-1}(P_b(t)) \quad (2.5-3)$$

where

$g^{-1}(\cdot)$ is the inverse of $g(\cdot)$.

For BPSK we have:

$$P_b(t) = \frac{1}{2} \operatorname{erfc}\left(\sqrt{\frac{P(t)}{N_0 R(t)}}\right) \quad (2.5-4)$$

and

$$P(t) = N_0 \cdot R(t) [\operatorname{erfc}^{-1}(2 \cdot P_b(t))]^2 \quad (2.5-5)$$

For BFSK we have:

$$P_b(t) = \frac{1}{2} \exp\left(-\frac{1}{2} \cdot \frac{P(t)}{N_0 R(t)}\right) \quad (2.5-6)$$

and

$$P(t) = N_0 \cdot R(t) \cdot \ln\left(\frac{1}{2P_b(t)}\right) \quad (2.5-7)$$

3 ANALYSIS AND RESULTS

This chapter presents and explain our approach and reasoning to the use and analysis of the MB channel. The significant analytical expression to be used as design and analysis tools are given.

3.1 Introduction and Approach

As stated earlier, our aim in the analysis is to arrive at a set of analytical relationships for important communication parameters such as burst duration and throughput using as accurate a model as possible. These relationships will serve as analysis and design tools where the effects of system parameters and constraints (power, geometry, BER) on throughput can be assessed. Our goal is to estimate the optimal average throughput for a given communication system.

Two types of communication systems are considered:

- 1) A system with a constant transmission rate and a time varying bit error rate which is constrained not to exceed some maximum allowable value.
- 2) A system employing a variable transmission rate which mimics the time varying power in order to maintain a practically constant bit energy and BER for all transmitted bits.

For the constant bit rate system, since the power is time varying, the probability of bit error will be time varying in a fashion dictated by the relevant modulation function. Specifically, for the underdense burst we have an exponentially decaying power in time and consequently the BER is monotonically increasing. Whether underdense or overdense we see the need then to impose a ceiling on the BER. For such systems, where the probability of bit error is time varying, we specify a maximum allowable BER, P_{bmax} , such that all transmitted bits shall have a BER less than or equal to P_{bmax} . This constraint on the probability of bit error for constant transmission rate systems implies the existence of a minimum power level P_{min} such that all transmitted bits have a received power greater than or equal to P_{min} . Such is obvious when remembering that the modulation function relating power to BER is an increasing function for decreasing argument. In short, $P_b(t) = P_{bmax}$ when $P(t) = P_{min}$. The time for which the power received from the meteor burst exceeds a prescribed threshold (P_{min}) is the burst duration t_b (also duty cycle [1]).

Clearly the duration of time for which the received power P is greater than P_{min} varies from one meteor burst to the next. For a constant bit rate system the burst duration is crucial in determining the number of bits transmitted

during a given burst and ultimately in estimating throughput. We shall therefore analyse its relationship to system parameters, derive its statistics and compare it with current dogma.

As we increase our set constant bit rate the corresponding P_{\min} has to be increased resulting in shortening the effective duration of transmission. This clear tradeoff between transmission rate and duration of transmission, t_B , suggests an optimal choice for transmission rate (or equivalently an optimal t_B) so as to maximize the throughput. The link between the number of bits transmitted per burst and throughput is done through the average arrival rate statistics and trail shape statistics (variation in q and/or B). The judicious choice of transmission rate for the given system provides us, therefore, with the optimal throughput.

The second type of communication system considered here is a variable transmission rate system. Under such a system the bit rate mimics the time behavior of the received power (or equivalently stated the bit duration varies in a reciprocal manner to the received power variation) so as to maintain a constant bit energy. The direct outcome of such approach is a constant probability of bit error. More importantly, we note that we are not restricted by the need to operate above a prescribed threshold of received power; for as the power diminishes we simply compensate by increasing the bit duration. This adaptive approach implies, theoretically at least, for the underdense burst an infinitely long time of transmission. This of course, is offset by the practical limitation on bit duration and the need to maintain a fairly constant BER. The assumption here is that the hardware is fast enough to vary the transmission rate (bit duration) from one bit to the next. Since the power in most cases diminishes during the duration of the bit, for long bit duration we deviate from the requirement to maintain a constant bit energy and constant BER. It is therefore necessary to take this fact into account in determining the duration of transmission. This criterion of allowing only a small drop in the assumed constant bit energy imposes a restriction on the maximum bit duration which in turn limits the duration of transmission. As in the previous case we estimate the throughput by averaging over the ensemble of trails and incorporating the effects of trail arrival statistics. Finally, we express the correct packet probability in terms of the modulation function, packet length and communication system parameters.

3.1.1 Protocol

Both stations have receiving and transmitting capabilities. The station which acts as transmitter of data listens continuously for a continuous tone

which is being sent from the receiver. Upon detection of this tone both the presence and the strength of the channel is known to the transmitter which immediately commences transmission. The situation is completely symmetrical with respect to the receiver. Clearly, the beginning of the burst, i.e. availability of the channel, is known to the transmitter within a negligible propagation delay (less than 3.5 msec for a 1000 km link). The continuous tone used for monitoring the channel is at a different frequency than the data for ease of gating and synchronizing. For constant bit rate systems the essential feature of this scheme is the ability of the transmitter to discern the beginning of the burst. For variable bit rate systems the strength of the channel as gauged by the transmitter in addition to the burst's start are important for adaptive bit rate determination.

The above description is the rudimentary layer upon which additions and refinements could be made.

3.2 Improvements

The advantages of the analysis herein stem basically from considering a more complex MBC model than found in the literature. Most researchers [9, 21] while acknowledging the significant contribution to communication of the rare yet robust overdense burst have tended to concentrate on the underdense burst phenomenon because its simpler exponential form is more mathematically tractable. Able [11], however, does analyze the overdense trail by a piecewise linear (first order) approximation resulting in conservative channel duration estimation. We choose a second order approximation to improve the fit of the overdense transcendental power time function. This yields better results for channel duration for the overdense case. For the exponential case, researchers to date have assumed a fixed decay time constant. Hampton [21] in his analysis of an MB broadcast system used a constant decay rate which was the conditional expected time constant given a fixed burst duration. This approach, however, implies that the decay time constant is dependent upon an average of a function of the electron line density whereas it is known that the time constant is independent of the electron line density. To enhance the accuracy of our model we chose to adhere to empirical results and assume the decay time constant to be a random quantity independent of the electron line density.

Some researchers [34] have further simplified the MBC model by assuming a fixed electron line density for all exponential bursts. This is contrary to experimental observation. Here, as in the case of the exponential decay time constant, we incorporate this random parameter into our model.

In analyzing throughput we compare two systems: constant bit rate system and variable bit rate system and derive the average throughput for both. For constant bit rate we derive the expression for the optimal average throughput. This optimal average throughput is achieved by finding the "best" bit rate to be used for the communication system so as to maximize throughput for the underdense burst. This is not to be confused with the optimal bit rate for a given burst that maximizes the number of transmitted bits for the burst under consideration.

In summary we note that the bedrock of a communication system using the MBC is its model. To enhance the analysis we used a model with as few simplifications as possible while maintaining mathematical tractability.

3.3 Sample System

For quantitative appreciation of the results we need to assume some values for a communication system. The set of these assumed parameters values will comprise what will heretofore be referred to as our sample system. This sample communication system represents practical or average values. Chapter 2 contains the definition of the parameters.

L - 1000 km link distance. From section 2.2
we have for the next two parameters:

sec(ϕ) - 18.5 and

$R_T = R_R$ - 514 km.

P_T - 1000 w

G_T - 10 dB.

G_R - 10 dB. And for antenna beamwidth we use

ζ - 45.84° (.8 rad)

λ - 6 m. (50 MHz)

D - 8 m²/s

P_{bmax} - 10⁻⁵ Max. BER for constant bit
rate system.

Using BPSK modulation we get:

$g^{-1}(P_{bmax}) = 9$

$$N_0 = 4 \cdot 10^{-21} \left[80 \left(\frac{\lambda}{15} \right)^{2.3} + 2.5 \right] \text{ W/Hz}$$

See discussion above Eq. (2.4-2).

N_0 = $4.89 \cdot 10^{-20}$ at 50 MHz.

For comparison the BER for variable rate system, P_b ,

is set equal to P_{bmax}

R_{minV} = 1000 b/s (minimum variable rate allowed)

3.4 Constant Bit Rate and Constrained BER System

3.4.1 Channel Duration

Channel duration or burst duration, t_b is the time for which the power received from the burst exceeds a given minimum value P_{min} . It is also the duration of data transmissions for a given burst where all bits possess a probability of error less than some maximum allowable BER, P_{bmax} . P_{min} is determined thru the modulation function by the following parameters: Transmission rate (non-time-varying), power spectral density of the received noise, and the maximum allowable bit error rate. The burst duration t_b is determined by P_{min} and C_u which incorporates system parameters such as transmitter power, link geometry effects, carrier wavelength etc.

3.4.1.1 Burst Duration Statistics for

Constant Bit Rate -- Underdense

The channel duration, t_b , - burst duration - is the time of transmission for a given burst i.e. the usable portion of the burst, assuming a constant transmission rate, R , some given maximum allowed BER, and power spectral density, N_0 , see Fig. 11.

For such conditions for the underdense burst we have:

$$t_b = B \cdot \ln \left(\frac{q}{q_{min}} \right)^2 \quad (3.4.1.1 - 1)$$

where

$$q_{min} = \sqrt{\frac{P_{min}}{C_u}}$$

$$P_{min} = N_0 \cdot R \cdot g^{-1}(P_{bmax})$$

and

$$C_u = 2.517958110^{-32} \cdot \frac{P_T G_T G_R \lambda^3 \exp \left(-\frac{33.359}{\lambda^2 \sec^2 \theta} \right)}{R_T^3}$$

or equivalently

$$t_b = B \cdot \ln \left(\frac{C_U}{N_0 \cdot R \cdot g^{-1}(P_{bmax})} \cdot q^2 \right) \quad (3.4.1.1-2)$$

We now average over the ensemble of underdense bursts (averaging over q and b) to yield the average burst duration:

The Average Burst Duration-- Underdense:

$$\bar{t}_b = \frac{2\bar{B}}{p-1} \cdot \frac{1}{1-x} \cdot [1 - x(1 - \ln x)] \quad (3.4.1.1-3)$$

where

$$x = \left(\frac{q_{min}}{q_U} \right)^{p-1} = \left[\frac{N_0 \cdot R \cdot g^{-1}(P_{bmax})}{C_U q_U^2} \right]^{\frac{p-1}{2}}$$

and

$$\bar{B} = 3.16610^{-3} \cdot \frac{\lambda^2 \sec^2 \phi}{D} \quad q_U = 10^{14} \quad p = 1.6$$

$$R_N = \frac{R}{R_{max}} = \left(\frac{q_{min}}{q_U} \right)^2$$

$$R_{max} = \frac{C_U q_U^2}{N_0 g^{-1}(P_{bmax})}$$

For a given communication system C_U , R , N_0 , P_{bmax} , \bar{B} and $g(\cdot)$ are specified. R_N is the normalized (with respect to the highest possible rate for an underdense burst) bit rate.

Fig. 14 plots the above for our sample system (Sec. 3.3) for various link distance as a function of R_N . ($R_N = R/R_{MAX}$, $R_{MAX} = 86.5$ kb/s)

The variance of t_b is given by:

$$\sigma_{t_b}^2 = \frac{4}{(p-1)^2} \cdot \frac{1}{(1-x)^2} [c_1 \sigma_b^2 + c_2 \bar{B}^2] \quad (3.4.1.1-4)$$

where

$$c_1 = 2 - x(3 + y^2) + x^2(1+y^2)$$

$$c_2 = 1 - x(2 + \ln^2(x)) + x^2$$

$$y = 1 - \ln(x)$$

x from previous equation

and

$$\sigma_{t_s} = \frac{2}{(p-1)(1-x)} \sqrt{kc_1 + c_2 \cdot \bar{B}} \quad (3.4.1.1-5)$$

For B Rayleigh $k = \frac{4}{\pi} - 1$. For B exponential $k = 1$

The n^{th} moment of t_B is given by:

$$\bar{t}_B^n = \frac{2^n \bar{B}^n}{(p-1)^n} \cdot \frac{n!}{1-x} \cdot \left\{ 1 - x \sum_{i=0}^n (-1)^i \frac{\ln^i(x)}{i!} \right\}$$

The PDF and CDF of t_B are:

$$f_{t_s}(t_1) = p' Q' \int_{b_{\min}}^{\infty} \frac{1}{b} \exp\left(-\frac{p' t_1}{b}\right) f_B(b) db \quad (3.4.1.1-6)$$

$$F_{t_s}(t_1) = Q' \left\{ 1 - x F_B(b_{\min}) - \int_{b_{\min}}^{\infty} \exp\left(-\frac{p' t_1}{b}\right) f_B(b) db \right\} \quad (3.4.1.1-7)$$

where

x and p are from above eq. (3.4.1.1-3)

$$p' = (p-1)/2$$

$$b_{\min} = t_1 / \left[(1/p') \ln(1/x) \right]$$

$$Q' = 1/(1-x)$$

See Fig. 15 for a plot of Eq. (3.4.1.1-6) (where B is assumed Rayleigh), and an exponentially distributed burst duration is drawn for comparison.

For the case of $x \ll 1$ i.e. $P_{\min} \ll C_U q_U^2$, essentially ignoring P_{\max} (considering all physical trails) we have for the solution of the above integrals ($b_{\min} = 0$):

B assumed exponential:

$$f_{t_1}(t_1) = 2 \frac{P'}{B} \cdot K_0(z) \quad (3.4.1.1-8)$$

and

$$F_{t_1}(t_1) = 1 - z K_1(z) \quad t_1 \geq 0 \quad (3.4.1.1-9)$$

$$\text{where } z = \sqrt{4 \frac{P'}{B} \cdot t_1}$$

where, K_0 and K_1 are the modified Hankel functions of order 0 and 1 respectively.

B assumed Rayleigh:

$$F_{t_1}(t_1) = 1 - 2 \int_0^\infty b \exp(-b^2 - t_1/b) db \quad (3.4.1.1-10)$$

$$= 1 - 2 f_1(t_1)$$

where $f_1(t_1)$ is a tabulated function [35]. See Fig. 9.

3.4.1.2 Burst Duration Statistics for Constant Bit Rate -- Overdense

An exact solution to the roots of the power received equation - overdense - is not known. The difference between these time instances yields the duration of the channel. We can approximate the power function in a piecewise linear fashion (comprised of two straight lines) or alternatively use a second order approximation. The second order approximation used here improves the accuracy of the results.

The results are stated without the lengthy derivation. For derivation see section 4.3

$$t_s = .95 a q \sqrt{1 - \frac{q_T}{q}} \quad q_{\min} \leq q \leq q_{uo} = 10^{16} \text{ e/m} \quad (3.4.1.2-1)$$

where

a and C_0 are from Eq (2.1.5-2)

$$q_T = (e/a) (P_{\min}/C_0)^2 = q_{uo} R_{NO}^2$$

$R_{NO} = R/R_{\max}$, normalized bit rate.

$$R_{\max} = C_0 [a q_{uo}/e]^{.5} / N_0 g^{-1}(P_{b\max})$$

maximum possible bit rate for any overdense burst.

$$q_{\min} = \max \{q_T, q_{LO}\} \quad q_{LO} = 10^{14} \quad q_{uo} = 10^{16} \text{ e/m.}$$

e is the natural logarithm base.

Note that q_{LO} is the minimum (physical) electron line density that can support an overdense burst. q_T is specified by our choice of system parameters and bit rate and may not correspond to a real level of overdense electron line density. See discussion following Eq. (3.4.1.2-3). See Fig. 12. but note that in the figure $q_T < q_{LO}$.

We can also relate q_T to q_{\min} recalling the definition of $P_{\min} = C_U q_{\min}^2$;

$$q_T = \frac{e}{a} \left(\frac{C_U}{C_0} \right)^2 q_{\min}^4 \quad (3.4.1.2-2)$$

where the parameters C_U , C_0 , a and q_{\min} are defined in Eqs. (2.1.1-2) and (2.1.5-2) and (3.4.1-1) respectively.

Average Burst Duration - Overdense:

The average burst duration for the overdense case is found by averaging over the ensemble of bursts, yielding

$$\bar{t}_s = 1.9 a Q \sqrt{q_T} \left\{ \sqrt{\frac{q_{uo}}{q_T}} - 1 - \sqrt{\frac{q_{\min}}{q_T}} + \cos^{-1} \left(\sqrt{\frac{q_T}{q_{\min}}} \right) - \cos^{-1} \left(\sqrt{\frac{q_T}{q_{uo}}} \right) \right\} \quad (3.4.1.2-3)$$

where,

$$q_{\min} = \max\{q_T, q_{LO}\}$$

$$q_T = q_{UO} \cdot R_{NO}^2$$

$$R_{NO} = \frac{R}{R_{\max}}$$

$$R_{\max} = \frac{C_0 \sqrt{\alpha \cdot q_{UO}}}{\sqrt{e \cdot N_0} \cdot g^{-1}(P_{\max})}$$

R_{NO} is the normalized bit rate with respect to the maximum rate possible for any overdense burst, R_{\max} . Note that the above can be expressed as two functions one for $q_T < q_{LO}$ (or equivalently $R_{NO} < .1$) where $q_{\min} = q_{LO}$ and the other for $q_T > q_{LO}$ (or equivalently $R_{NO} > .1$) where $q_{\min} = q_T$. In addition, the value of Q varies with the domain as well since Q is a function of q_{\min} - see Eq. (2.1.6-2). For the case where $R_{NO} > .1$ ($q_T > q_{LO}$) we have

$$Q = .5(q_{UO})^{.5} R_{NO} / (1 - R_{NO})$$

For the case where $R_{NO} < .1$ ($q_T < q_{LO}$) we have

$$Q = .5(q_{LO})^{.5} / .9$$

For many practical systems we generally have

$q_T \ll q_{LO} \ll q_{UO}$ i.e. $q_{\min} = q_{LO}$, $Q = (q_{LO})^{1/2} / 2$
resulting in:

$$\bar{i}_B = .95 \alpha \cdot \sqrt{q_{UO} q_{LO}} \quad (3.4.1.2-4)$$

and for $q_T < .01 q_{UO}$ we have for the burst duration variance:

$$\sigma_{i_B}^2 = .95 \frac{\alpha^2}{3} \sqrt{q_{LO} q_{UO}^3} = .95 \frac{\alpha^2}{3} 10^{31} \quad (3.4.1.2-5)$$

For our sample system defined in Sec. 3.3 the standard deviation of $t_B = 11$ sec.

Burst Duration pdf and cdf - Overdense:

CDF of t_B :

$$F_{t_B}(t_1) = \begin{cases} 0 & t_1 \leq t_{1\min} \\ Q \cdot \left[1 - \left(\frac{2}{q_T} \frac{q_{\min}}{1 + \sqrt{1 + (t_1/\tau)^2}} \right)^{p-1} \right] & t_{1\min} \leq t_1 \leq t_{1\max} \end{cases} \quad (3.4.1.2-6)$$

where

$p=1.5$ and

$$t_{1\min} = .95 \alpha q_{\min} \sqrt{1 - \frac{q_T}{q_{\min}}} \quad q_{\min} = \max\{q_T, q_{L0}\}$$

$$t_{1\max} = .95 \alpha q_{L0} \sqrt{1 - \frac{q_T}{q_{L0}}}$$

$$\tau = .95 \frac{\alpha q_T}{2} = .95 \frac{e}{2} \left(\frac{P_{\min}}{C_0} \right)^2$$

PDF of t_B :

$$f_{t_B}(t_1) = (p-1) \frac{Q}{\tau^2} \left(\frac{2q_{\min}}{q_T} \right)^{p-1} \left[(1+z)^{-p} \cdot \frac{t_1}{z} \right] \quad t_{1\min} \leq t_1 \leq t_{1\max} \quad (3.4.1.2-7)$$

where

$$z = \sqrt{1 + \left(\frac{t_1}{\tau} \right)^2}$$

and all other parameters are defined by previous equations.

3.4.2 Bits per Given Burst

Bits per given burst under constant bit rate and constrained BER is the number of bits transmitted for the burst whose q and/or B are known. Since the bit rate, R , is assumed constant the number of bits, N_B , is simply the product of R times the burst duration t_B as defined in previous sections. Clearly, the level of power P_{\min} which reciprocally affects t_B is dictated by the modulation function and in general increases with increasing bit rate R . As a result we see the trade-off between the bit rate, R , and transmission duration, t_B , such that increasing one decreases the other. This suggests the existence of an optimal bit rate, R_B^* , (or equivalently, optimal transmission duration) that maximizes the number of bits transmitted during the given burst. Clearly, using any bit rate other than the optimal R_B^* will result in under-utilization of the

burst. Alternatively stated, given a bit rate one should transmit only for as long as the optimal burst duration dictates. The optimal bit rate for the given burst is then used to calculate the maximum number of bits, N_b^* , that can be transmitted during this burst. A ratio is then obtained for the same burst between the number of bits transmitted using variable bit rate (BER constant = P_{bmax}) and the N_b^* using constant bit rate. This ratio has been shown by Abel [11] to be around 2.5. Using the "best" (highest q) burst for overdense and underdense trails bounds can be found for the maximum possible N_b^* (constant rate system) and maximum transmitted bits using variable rate.

Two points however, must be kept in focus:

- 1) Since R^* varies from trail to trail and a priori knowledge of the trail behavior is impossible to obtain, the optimal (constant) bit rate for the system, i.e. for all possible bursts, is still unknown. Paranthetically, we note that attempting to find the burst's shape from knowledge of its beginning is both wasteful of valuable transmission time and unreliable since many bursts deviate from ideal behavior. As will be shown, the important parameter for throughput determination is not N_b -- the number of bits for a given burst -- but rather the number of bits per burst averaged over the ensemble of all bursts since the latter is directly proportional to the average throughput.
- 2) While it is true that more bits can be transmitted using variable bit rate during the burst rather than employing constant bit rate, the situation is somewhat analogous to an apples/oranges comparison. For the underdense burst and constant bit rate all bits except the last one will possess a BER smaller than P_{bmax} -- the worst BER, whereas for variable bit rate all bits will possess the same BER = P_{bmax} . Consequently, the probability of having an error-free packet of data is higher for constant bit rate than for variable bit rate.

We present the analysis for the given underdense burst by first considering constant bit rate with constrained BER and then considering variable bit rate system with constant BER.

Constant Bit rate system

Given an underdense burst - q and B are assumed known. P_{bmax} is specified for the system and R is the constant bit rate. Let N_b be the number of bits transmitted on this burst. All bits have $BER < P_{bmax}$. All bits have power $P > P_{min}$. From the discussion on burst duration and the above definition of N_b we have:

$$N_b = R \cdot t_b \quad (3.4.2-1)$$

Using eq. (3.4.1.1-2) for t_b we rewrite the above as

$$N_s = R \cdot B \cdot \ln(R_0/R) \quad (3.4.2-2)$$

$$\text{where } R_0 = C_u q^2 / N_0 g^{-1}(P_{bmax})$$

Note that R_0 is a constant set by the choice of system parameters and physical characteristics (1) of the given burst. From the above it is clear that for a given burst a different choice of bit rate R yields different number of transmitted bits, N_s . To find the bit rate R_s that maximizes N_s we simply set its derivative with respect to R to zero and solve

$$\frac{dN_s}{dR} = 0 = \ln(R_0/R) - 1 \quad (3.4.2-3)$$

or $R_s^* = R_0/e$ where e is the natural logarithm base. Using the last result in eq (3.4.2-2) yield N_s^* the maximum number of bits for this burst.

$$N_s^* = \frac{R_0 \cdot B}{e} \quad (3.4.2-4)$$

$$\text{where } R_0 = C_u q^2 / N_0 g^{-1}(P_{bmax})$$

From the above we see that P_{min}^* the minimum power corresponding to R_s^* is equal to $P(0)/e$. This implies that the burst duration (transmission time) i.e. the time it takes to drop to P_{min}^* from $P(0)$ is equal to one decay time constant B . Equivalently, then, the above analysis states that for a given bit rate R the optimal time of transmission T_s^* must be set to B to yield the above maximum transmitted bit N_s^* . This result has been demonstrated by Ables' work [11] as well.

Variable Bit Rate System

For the given underdense burst we have $P_b(t) = P_{bmax}$ for all bits. Under such conditions the variable bit rate $R(t)$ is given by

$$R(t) = R_0 e^{-t/B} \quad ((3.4.2-5))$$

$$\text{where } R_0 = C_u q^2 / g^{-1}(P_{bmax})$$

Note that the power to transmission rate ratio which specifies the bit energy is constant and hence the BER is maintained constant.

Since the burst is assumed to be known a-priori we can compute the bit duration (inverse of bit rate) for each bit exactly such that the integral of power received over the individual bit duration i.e. the bit energy is the

same for all transmitted bits. See Fig. 13.

The number of bits for variable rate is given by

$$N_{BV} = \int_0^{\infty} R(t) dt = R_0 \cdot B \quad (3.4.2-6)$$

Comparison of the Two Systems

We now compare constant bit rate system using the optimal R (with $\text{BER} < P_{b\max}$) for the particular burst versus variable bit rate which mimics the bursts power behavior (such that all bits possess the same BER , $P_{b\max}$). For each of the above we found the number of bits transmitted N_B^* and N_{BV} respectively. Taking the ratio:

$$N_{BV}/N_B^* = e$$

We see an improvement of 2.7 for the utilization of variable bit rate over constant bit rate. We stress however that the necessary priori knowledge (or estimation) of burst characteristics is unreliable. In addition, although variable bit rate results in a higher number of transmitted bits for a given burst versus constant bit rate there is a price; all bits have a $\text{BER} = P_{b\max}$ for variable bit rate system whereas for the constant bit rate system $P_{b\max}$ is a worst case (last bit BER). This fact portends worse probability of correct packet transmission for variable rate system than constant rate system under the above conditions.

3.4.3 Throughput for Constant Bit Rate

We are given a communication system with a specified maximum allowed BER $P_{b\max}$, constant transmission rate R , received noise power spectral density N_0 and general system parameters (link distance, frequency, etc.) as defined by C_U or C_0 .

To express the throughput T of the system we introduce N_{bi} as the number of bits transmitted on the i^{th} burst and M_i as the number of bursts occurring in the period of τ seconds. Since the bursts are independent of each other, and assuming no overlap of bursts, we have:

$$T = \lim_{\tau \rightarrow \infty} \frac{1}{\tau} \sum_{i=1}^{M_i} N_{bi} \quad (3.4.3-1)$$

$$= A \cdot \bar{N}_b$$

where A is the average number of bursts/s and \bar{N}_b is the expected number of bits per burst as averaged over the ensemble of all bursts' profiles. (The subscripts U or O are added to distinguish between underdense and overdense cases.)

For underdense:

$$\bar{N}_{bu} = \int \int N_b(q, B) f_q(q) f_B(b) dq db \quad (3.4.3-2)$$

where $f_x()$ is the pdf of x .

For overdense:

$$\bar{N}_{bo} = \int N_b(q) f_q(q) dq \quad (3.4.3-3)$$

Note that the above three equations are dependent on the choice of bit rate R .

3.4.3.1 Optimal Average Throughput for Constant Bit Rate System -- Underdense.

In this section the optimal average system throughput for the underdense burst is given. This is the maximum average number of bits per unit time for the 'best' transmission rate R (and other system constants) assuming only underdense bursts are present.

This optimal throughput is found by first deriving the dependence of the average throughput (Eq. 3.4.3-1) on the bit rate R , and solving for the optimal bit rate R^* that would yield the desired optimal throughput T^* . The solution is done with respect to the normalized bit rate, R_N , which yields a result independent of a particular choice of system values.

For the given system P_{\max} , N_0 , R and C_U are specified. We have defined R_N the normalized bit rate as:

$$R_N = \frac{R}{R_{\max}} = \left(\frac{q_{\min}}{q_U} \right)^2$$

where

$$R_{\max} = \frac{C_U q_U^2}{N_0 g^{-1}(P_{\max})} \quad (3.4.3.1-1)$$

the maximum bit rate achievable in a given system using underdense bursts.

Omitting the cumbersome derivation we present the following results: (for the relevant derivation see Sec. 4.2)

The average number of bits per underdense burst $\bar{N}_{BU} = R \cdot \bar{T}_B$ can be expressed in terms of the normalized bit rate using Eq. (3.4.1.1-3) as:

$$\bar{N}_{BU} = \frac{2\bar{B}}{p-1} R_{\max} \frac{1}{1 - R_N^{p'}} [R_N - R_N^{p'+1} + R_N^{p'+1} \ln(R_N^{p'})] \quad (3.4.3.1-2)$$

where

$p' = (p - 1)/2$, $p = 1.6$ and R_{\max} is defined above.

Note that in the above expression the bursts considered were those with an electron line density q between q_{\min} (as defined by P_{\min}) and q_U (the physical limit). The arrival rate for such condition is given by Eq. (2.3-2) where q_1 is set to q_{\min} and q_2 is q_U . Together with Eq. (3.4.3.1-1) we have for the arrival rate of underdense bursts:

$$A_U = A' \cdot \left[\frac{1}{\sqrt{R_N}} - 1 \right] \quad (3.4.3.1-3)$$

where,

$$A' = \frac{19.1667 \cdot \phi \sin \phi (R_R \zeta)^2}{q_U}$$

$$q_U = 10^{14}$$

The expression for throughput using underdense bursts is given by the product of the last two Eqs. as specified by Eq. (3.4.3-1). The result is a function

of the normalized bit rate which is just a scaled bit rate. In the product we substitute for R_{\max} from Eq. (3.4.3.1-1) and for C_U and \bar{B} from Eq. (2.1.1-2). For a given set of system parameters we thus have the throughput (using underdense bursts) for any choice of (normalized) bit rate as:

$$T_U = 3.056 \cdot 10^{-19} \cdot \frac{P_T G_T G_R \zeta^2 \phi \sec^2 \phi \exp\left(-\frac{33.359}{\lambda^2 \sec^2 \phi}\right) \cdot \lambda^3}{(p-1)N_0 \cdot g^{-1}(P_{b\max}) \cdot D \cdot R_T} \cdot \frac{\sqrt{R_N - R_N^p}}{1 - R_N^p} [1 - R_N^{p'} + p' R_N^{p'} \cdot \ln(R_N)]$$

(3.4.2.1-3)

where

- p is an empirical constant, $p' = (p-1)/2$
 (taken here as 1.6, Section 2.1.2)
- ζ idealized antenna beamwidth.
- R_T and ϕ geometric parameters determined
 by link distance (from section 2.2)
- P_T transmitter power.
- G_T, G_R transmitter and receiver antenna gains.
- λ carrier wavelength.
- D diffusion coefficient of the atmosphere.
- N_0 power spectral density of the noise.
 (Sec. 2.4)
- $g^{-1}(P_{b\max})$ ratio of minimum bit energy to N_0 .

Note that the equation is written in two parts; the first incorporates all the parameters of the particular system and the second part reflects the variation in throughput with choice of bit rate. The above throughput (normalized with respect to its maximum) for our sample system (defined in Sec. 3.3) is plotted in Fig. 16.

We would like to find from the above equation the optimal normalized bit rate R_N^* which yields the maximum throughput T_U^* . This optimal normalized bit rate for any given system is found numerically to be (see Fig. 16):

$$R_M^* = .07$$

or equivalently the optimal bit rate,

$$R^* = .07 R_{\max} \quad (3.4.3.1-5)$$

See Figs. 19 and 20 for plots of the above.
resulting in

$$T_U^* = 3.433 \cdot 10^{-20} \cdot \frac{P_T G_T G_R \zeta^2 \phi \sin(\phi) \sec^2(\phi) \exp\left(-\frac{33.359}{\lambda^2 \sec^2 \phi}\right) \lambda^5}{R_T N_0 g^{-1}(P_{b\max}) D} \quad (3.4.3.1-6)$$

where all the parameters are defined above.

The above expression for the maximum throughput T_U^* allows us to quantify the affects of various system parameters and constraints on the best throughput using a constant bit rate. As an example we plotted the variation of T_U^* as a function of wavelength for our sample system (Sec 3.3). See Fig. 17 bottom curve. Using our sample system with a wavelength of 6 m. (50 MHz) we get $R_{\max} = 86.5$ kb/s, $R^* = 6.055$ kb/s and $T_U^* = 214$ b/s. Additional plots are given by Figs 21 and 22.

3.4.3.2 Optimal Average Throughput for Constant Bit Rate System -- Overdense.

In this section the optimal average system throughput for the underdense burst is given. This is the maximum average number of bits per unit time for the 'best' transmission rate R (and other system constants) assuming only overdense bursts are present.

This optimal throughput is found by first deriving the dependence of the average throughput (Eq. 3.4.3-1) on the bit rate R , and solving for the optimal bit rate R^* that would yield the desired optimal throughput T_U^* . The solution is done with respect to the normalized bit rate, R_{NO} , which yields a result independent of a particular choice of system values.

For the given system P_{bmax} , N_0 , R , a and C_0 are specified. With a reference to Eq. (3.4.1.2-3) and the accompanying discussion we rewrite R_{NO} -- the bit rate normalized with respect to R_{maxo} , the maximum bit rate achievable for the given system using overdense bursts -- and related parameters:

$$q_T = q_{UO} \cdot R_{NO}^2$$

$$R_{NO} = \frac{R}{R_{maxo}}$$

$$R_{maxo} = \frac{C_0 \sqrt{a \cdot q_{UO}}}{\sqrt{e \cdot N_0 \cdot g^{-1}(P_{bmax})}}$$

$$q_{minO} = \max\{q_T, q_{LO}\}$$

(3.4.3.2-1)

where, $q_{UO} = 10^{16}$ and $q_{LO} = 10^{14}$
 a and C_0 are defined in Eq. (2.1.5-2).
 N_0 is defined in Sec. 2.4

We note from the above that for $q_T < q_{LO}$ (or equivalently $R_{NO} < .1$) where $q_{minO} = q_{LO}$ and the other for $q_T > q_{LO}$ (or equivalently $R_{NO} > .1$) where $q_{minO} = q_T$. In addition, the value of Q (Eq. (3.4.1.2-3)) varies with the R_{NO} as well since Q is a function of q_{minO} - see Eq. (2.1.6-2). For the case where $R_{NO} > .1$ ($q_T > q_{LO}$) we have

$$Q = .5(q_{UO})^{.5} R_{NO} / (1 - R_{NO})$$

For the case where $R_{NO} < .1$ ($q_T < q_{LO}$) we have

$$Q = .5(q_{LO})^{.5} / .9$$

Using the above relationships in Eq. (3.4.1.2-3) to express the average overdense burst duration as a function of R_{NO} we get:

For $R_{NO} \leq 0.1$:

$$\bar{i}_s = \sqrt{q_{LO} q_{UO}} a \cdot R_{NO} \left\{ \sqrt{\frac{1}{R_{NO}^2} - 1} - \sqrt{\frac{0.01}{R_{NO}^2} - 1} + \cos^{-1}(10 R_{NO}) - \cos^{-1}(R_{NO}) \right\}$$

(3.4.3.2-2)

For $R_{NO} > 0.1$:

$$\bar{i}_s = .95 \sqrt{q_{LO} q_{UO}} a \cdot R_{NO} \left\{ \sqrt{\frac{1}{R_{NO}^2} - 1} - \cos^{-1}(R_{NO}) \right\}$$

The average number of bits per overdense burst is by definition

$$\bar{N}_{BO} = R \cdot \bar{t}_B \quad (3.4.3.2-3)$$

and can be expressed in terms of the normalized bit rate using Eq. (3.4.3.2-1) for R as a function of R_{NO} and Eq. (3.4.3.2-2) for the average overdense burst duration.

Since the throughput T_0 according to Eq. (3.4.3-1) is the product of the arrival rate and the last equation i.e.

$$T_0 = A_0 \cdot \bar{N}_{BO} \quad (3.4.3.2-4)$$

we need to express the arrival rate of overdense bursts A_0 as a function of R_{NO} . We start by employing Eq. (2.3-2) with q_1 set to q_{\min} (the lowest overdense q as determined from the choice of P_{\min} i.e. bit rate) and q_2 set to q_{uo} (the physical maximum). The dependence of q_{\min} on R_{NO} is then used (discussed above after Eq. (3.4.3.2-1)) yielding the following arrival rate:

$$A_0 = \begin{cases} .99 \cdot A' & R_{NO} \leq .1 \\ .01 \cdot A' \left[\frac{1}{R_{NO}^2} \right] & R_{NO} > .1 \end{cases} \quad (3.4.3.2-5)$$

where,

$$A' = \frac{3 \cdot \phi \sin \phi (R_{\text{ex}} \xi)^2}{q_{LO}}$$

$$q_{\text{uo}} = 10^{16} \quad \text{and} \quad q_{LO} = 10^{14}$$

By direct substitutions from the above equations we express the throughput using overdense bursts as a function of normalized bit rate and system parameters as:

$$T_0 = .33 \cdot 10^{-18} \cdot \frac{P_T G_T G_R \xi^2 \phi \sin \phi \sec^3 \phi \cdot \lambda^3}{N_0 \cdot g^{-1}(P_{\text{bmax}}) \cdot D \cdot R_T} \cdot \left\{ \begin{aligned} & 11 R_{NO}^2 \left\{ \sqrt{\frac{1}{R_{NO}^2} - 1} - \sqrt{\frac{0.01}{R_{NO}^2} - 1} + \cos^{-1}(10 R_{NO}) - \cos^{-1}(R_{NO}) \right\} & R_{NO} \leq .1 \\ & \frac{R_{NO} - R_{NO}^3}{1 - R_{NO}} \left\{ \sqrt{\frac{1}{R_{NO}^2} - 1} - \cos^{-1}(R_{NO}) \right\} & R_{NO} > .1 \end{aligned} \right\} \quad (3.4.3.2-6)$$

where,

ξ idealized antenna beamwidth.
 R_T and ϕ geometric parameters determined
 by link distance (from section 2.2)
 P_T transmitter power.
 G_T, G_R transmitter and receiver antenna gains.
 λ carrier wavelength.
 D diffusion coefficient of the atmosphere.
 N_0 power spectral density of the noise.
 (Sec. 2.4)
 $g^{-1}(P_{bmax})$ minimum of bit energy to N_0 ratio.

Note that the equation is written in two parts; the first incorporates all the parameters of the particular system and the second part reflects the variation in throughput with choice of bit rate. The above throughput (multiplied by 2.55) for our sample system (Sec 3.3) is plotted in Fig. 18.

We would like to find from the above equation the optimal normalized bit rate R_{NO}^* which yields the maximum throughput T_0^* . This optimal normalized bit rate for any given system is found numerically to be (see Fig. 18):

$$R_{NO}^* = .1$$

or equivalently the optimal bit rate,

$$R^* = .1 R_{maxo} \quad (3.4.3.1-7)$$

The result is intuitively obvious since $R_{NO} = .1$ is the maximum bit rate that still includes all overdense trails i.e maximum arrival rate. For a higher bit rate we have a smaller arrival rate that reduces the throughput. A smaller bit rate will not change the overdense arrival rate but will diminish the throughput.

Using the optimal bit rate for overdense bursts we get the maximum overdense throughput T_0^* by substituting Eq.(3.4.3.2-7) into Eq. (3.4.3.2-6) yielding:

$$T_0^* = .3078 \cdot 10^{-18} \cdot \frac{P_T G_T G_R \xi^2 \phi \sin \phi \sec^3 \phi \cdot \lambda^5}{N_0 \cdot g^{-1}(P_{bmax}) \cdot D \cdot R_T} \quad (3.4.3.2-8)$$

where all the parameters are defined above.

The above expression for the maximum throughput T_0^* allows us to quantify the affects of various system parameters and constraints (wavelength, power, link distance, maximum bit error rate etc.) on the best throughput using a constant bit rate. Using our sample system (Sec 3.3) with a wavelength of 6 m. (50 MHz) we get $R^* = 252$ kb/s and $T_0^* = 8688$ b/s.

3.4.3.3 Total Average Throughput for Constant Bit Rate System.

In this section we combine the result of the last two sections to present the total throughput and optimal throughput. Since we used differently normalized variables for underdense and overdense we shall now employ a single normalized variable; the one corresponding to the overdense case.

Recalling previous definitions:

For underdense we used

$$R_N = \frac{R}{R_{max}} = \left(\frac{q_{min}}{q_U} \right)^2$$

where

$$R_{max} = \frac{C_U q_U^2}{N_0 g^{-1}(P_{bmax})} \quad (3.4.3.3-1)$$

the maximum bit rate achievable in a given system using underdense bursts. C_U and N_0 are defined in Eq. (2.11-2) and Eq. (2.4-2), respectively.

For overdense we used

$$R_{NO} = \frac{R}{R_{maxo}}$$

where

$$R_{maxo} = \frac{C_O \sqrt{a \cdot q_{UO}}}{\sqrt{e} \cdot N_0 \cdot g^{-1}(P_{bmax})} \quad (3.4.3.3-2)$$

where, $q_{UO} = 10^{16}$ and $q_{LO} = 10^{14}$

a and C_O are defined in Eq. (2.1.5-2).

N_0 is defined in Sec. 2.4

From the above we can write

$$\frac{R_{max}}{R_{max}} = s = 6.446 \cdot e^{(33.359/\lambda^2 \sec^2 \phi)} \cdot \sec \phi \quad (3.4.3.3-3)$$

and

$$R_N = s \cdot R_{NO} \quad (3.4.3.3-4)$$

Note that $R_N=1$, the maximum underdense bit rate, corresponds to $R_{NO} = 1/s$.

Using Eq. (3.4.3.1-4) for the underdense throughput, with R_N expressed by the last equation, and Eq. (3.4.3.2-6) for the overdense throughput we get for the total throughput T:

$$T = .509 \cdot 10^{-18} \cdot \frac{P_T G_T G_R \zeta^2 \phi \sin \phi \sec^2 \phi \cdot \lambda^5}{N_0 \cdot g^{-1}(P_{dmax}) \cdot D \cdot R_T} \cdot \{T_U + T_{O1} + T_{O2}\} \quad (3.4.3.3-5)$$

where

$$T_U = \exp\left(-\frac{33.359}{\lambda^2 \sec^2 \phi}\right) \frac{\sqrt{s R_{NO}} - s R_{NO}}{1 - (s R_{NO})^p} \{1 - (s R_{NO})^p + p' (s R_{NO})^p \cdot \ln(s R_{NO})\} \cdot U\left(\frac{1}{s} - R_{NO}\right)$$

$$T_{O1} = \frac{\sec \phi R_{NO}^2}{.1401} \left[\sqrt{\frac{1}{R_{NO}^2} - 1} - \sqrt{\frac{0.01}{R_{NO}^2} - 1} + \cos^{-1}(10 R_{NO}) - \cos^{-1}(R_{NO}) \right] \cdot U(.1 - R_{NO})$$

$$T_{O2} = .649 \cdot \sec \phi \cdot \frac{R_{NO} - R_{NO}^3}{1 - R_{NO}} \left[\sqrt{\frac{1}{R_{NO}^2} - 1} - \cos^{-1}(R_{NO}) \right] \cdot U(R_{NO} - .1)$$

$$s = 6.446 \cdot e^{(33.359/\lambda^2 \sec^2 \phi)} \cdot \sec \phi$$

and

$$U(x) = \begin{cases} 1 & \text{for } x \geq 0 \\ 0 & \text{for } x < 0 \end{cases}$$

is the unit step function.

All other parameters are defined in previous sections.

3.5 Variable Bit Rate and Constant BER System

3.5.1 Channel Duration

For a variable bit rate system the bit rate is changed so as to maintain a reasonably constant energy per bit. Clearly it implies a constant BER, P_b , for all transmitted bits. Considering for example the underdense burst, if apriori knowledge of the burst were available, we could divide the received power

curve into equal energy portions and compute the resulting individual bit durations before we transmit. Under such conditions all bits will possess exactly the same energy and hence the same BER. The total number of bits transmitted for that burst will simply be proportional to the total area under the received power -versus- time curve. Since we don't have an apriori knowledge of the burst but rather an instantaneous (within a negligible delay) indication of channel strength we can only evaluate the necessary duration for the current bit and transmit it as such. During the duration of the transmitted bit the power received drops. If the bit duration is small the resulting drop in bit energy is negligible and our assumption of constant bit energy is not violated. As time progresses, however, the bit duration increases (power received decays) and the drop in bit energy relative to the assumed constant bit energy becomes appreciable and finally intolerable. This fact limits the maximum bit duration which in turn restricts the duration of transmission or, equivalently, channel duration.

3.5.1.1 Transmission Duration for Variable Bit Rate -- Underdense

We start by imposing our fidelity constant, k , for the normalized bit energy -- the ratio of the real bit energy to the desired one. For our derivation we will assume $k > .9$ i.e. no more than 10% drop in bit energy shall be tolerated. We further define:

P_b	Assumed constant BER for all transmitted bits.
T_{bi}	Duration of the i^{th} bit
$R(t)$	Instantaneous bit rate
T_0	Duration of the first bit, $1/R_0$
N	Last bit
$T(m)$	Total duration of the first m bits; also starting time of the $(m+1)^{\text{th}}$ bit:

$$\sum_{i=1}^m T_{bi}$$

T_t	Duration of transmission (burst duration) - $T(N)$
c	Max (T_{bN}/B) for a given k .

In order to maintain a constant BER, P_b , we have for the variable bit rate

$$R(t) = \frac{C_U q^2}{N_0 g^{-1}(P_b)} e^{-t/T_0} = R_0 \cdot e^{-t/T_0} \quad (3.5.1.1-1)$$

and the n^{th} bit duration is given by

$$T_{bn} = T_0 e^{\frac{T(N-1)}{B}} \quad (3.5.1.1-2)$$

where

$$T_0 = 1/R_0 = N_0 g^{-1}(P_b)/C_U q^2$$

For $k > .9$ we have for the last bit, N :

$$T_{bN} \leq [1.5 - \sqrt{2.25 - 6(1-k)}] \cdot B = c \cdot B \quad (3.5.1.1-3)$$

Combining with eq (3.5.1.1-2) we have

$$\frac{T_{bN}}{B} = \frac{T_0}{B} \cdot e^{\frac{T(N-1)}{B}} \leq c \quad (3.5.1.1-4)$$

Since the transmission duration is given by

$$T_t = T(N-1) + T_{bN} \quad \text{we have from the last 3 eqns.}$$

$$T_t \leq B \cdot [c + \ln\left(\frac{c \cdot B}{T_0}\right)] \quad (3.5.1.1-5)$$

for $k = .9$, $c = .2$ we have from the above $T_t/B = .2 + \ln(R_0 B/5)$.

For all practical systems we can safely use

$$T_t = B \cdot \ln\left(\frac{R_0 \cdot B}{5}\right) \quad (3.5.1.1-6)$$

where R_0 is defined in Eq. (3.5.1.1-1)

3.5.2 Throughput for Variable Bit Rate System

- Underdense

Using the results from the previous section on transmission duration we can find the approximate number of transmitted bits by integrating $R(t)$ from time 0 to time T_t :

$$N_{BU} = R_0 B = C_U B q^2 / g^{-1}(P_b) N_0 \quad (3.5.2-1)$$

where R_0 is the variable bit rate at time 0.

and since B and q are independent the average of N_{BU} over the joint space of q and B yields:

$$\bar{N}_{UV} = \frac{C_U \bar{B} q^2}{g^{-1}(P_b) \cdot N_0} \quad (3.5.2-2)$$

The derivation of the above equations is in section 4.5

We shall assume that the bit rate shall vary between $R_{\min V}$ and $R_{\max V}$. Bearing in mind that for a given bit rate R we have a corresponding q such that

$$C_U q^2 = N_0 \cdot g^{-1}(P_b) \cdot R \quad q_L < q < q_U \quad (3.5.2-3)$$

As a result we have

$$q_{\min V} = \sqrt{\frac{N_0 \cdot g^{-1}(P_b)}{C_U}} \cdot \sqrt{R_{\min V}} \quad (3.5.2-4)$$

$$q_{\max V} = \sqrt{\frac{N_0 \cdot g^{-1}(P_b)}{C_U}} \cdot \sqrt{R_{\max V}} \quad (3.5.2-5)$$

$R_{\min V}$ must be chosen such that $q_{\min V} > q_L$, the physical minimum.

$R_{\max V}$ must be chosen such that $q_{\max V} < q_U$, the physical maximum.

Note that because our empirical arrival rate relationship (Sec. 2.3) is valid for $q > 10^{13}$ we shall set $R_{\min V}$ such that $q_{\min V} > 10^{13}$.

To get the most throughput out of our system we set $R_{\max V}$ to its maximum value i.e. corresponding to $q = q_U$. We thus have set $q_{\max V} = q_U$ and using it in the last two equations we have

$$\frac{q_{\min V}}{q_{\max V}} = \frac{q_{\min V}}{q_U} = \sqrt{\frac{R_{\min V}}{R_{\max V}}} = \sqrt{R_{NV}} \quad (3.5.2-6)$$

where $R_{\max V}$ is given by Eq.(3.5.2-5) as

$$R_{\max V} = \frac{C_U q_U^2}{N_0 g^{-1}(P_b)} \quad (3.5.2-7)$$

where, C_U is from Eq.(2.1.1-2), N_0 is from (2.4-2) resulting in Eq.(3.5.2-13).

Note that $R_{\max V} = R_{\max}$ the maximum underdense for constant bit rate system if we set $P_b = P_{b\max}$, a direct result from Eq. (3.4.3.1-1)

Evaluating $E(q^2)$ for Eq. (3.5.2-2) in the range of q_{\min} , q_U is done using eq (2.12-2)

$$\overline{q^2} = \frac{(p-1)}{(3-p)} q_{\min}^{p-1} q_U^{3-p} \frac{(1-y^{3-p})}{(1-y^{p-1})} \quad (3.5.2-8)$$

where $p=1.6$ and (with Eq. (3.5.2-6))

$$y = \frac{q_{\min}}{q_U} = \sqrt{R_{NV}}$$

Rewriting we get for the last equation

$$\overline{q^2} = \frac{.6}{1.4} q_U^2 \frac{(R_{NV}^3 - R_{NV})}{(1 - R_{NV}^3)} \quad (3.5.2-9)$$

Substituting into Eq. (3.5.2-2) we get

$$\overline{N}_{UV} = \frac{C_U \overline{B}}{g^{-1}(P_b) \cdot N_0} \cdot \frac{.6}{1.4} q_U^2 \frac{(R_{NV}^3 - R_{NV})}{(1 - R_{NV}^3)} \quad (3.5.2-10)$$

For throughput expression we need to have the arrival, A_V , expressed as a function of our variable R_{NV} . From Eq. (2.3-2) we have

$$A_V = \frac{A'_V}{q_{\min}} \left(1 - \frac{q_{\min}}{q_U} \right) = \frac{A'_V}{q_U} \left(\frac{1}{\sqrt{R_{NV}}} - 1 \right) \quad (3.5.2-11)$$

where

$$A'_V = 19.1667 \cdot \phi \sin \phi (R_R \zeta)^2$$

The expression for the throughput, T_{UV} is dictated by Eq. (3.4.3-1) and is arrived at by the product of Eq. (3.5.2-11) and Eq. (3.5.2-10) above. Using the definitions of Eq. (2.1.1-2) and Eq. (3.5.2-7) we get

$$T_{UV} = 6.54821 \cdot 10^{-20} \cdot \frac{P_T G_T G_R \zeta^2 \phi \sin(\phi) \sec^2(\phi) \exp\left(-\frac{33.359}{\lambda^2 \sec^2 \phi}\right) \lambda^5}{R_T N_0 g^{-1}(P_b) D} \cdot \left(\frac{1}{\sqrt{R_{NV}}} - 1 \right) \frac{(R_{NV}^3 - R_{NV})}{(1 - R_{NV}^3)} \quad (3.5.2-12)$$

where, (Eq. (3.5.2-7) , Eq. (2.1.1-2) and (2.4-2))

$$R_{\max V} = 2.518 \cdot 10^{16} \cdot \frac{P_T G_T G_R \lambda^3 \exp\left(-\frac{33.339}{\lambda^2 \sec^2 \phi}\right)}{(.063 \lambda^{2.3} + 1) \cdot g^{-1}(P_b) \cdot R_T^2} \quad (3.5.2-13)$$

R_{NV} $R_{\min V}/R_{\max V}$; $R_{\max V}$ defined in Eq. (3.5.2-7)
 $R_{\min V}$ is arbitrary yet if resulting R_{NV} is small system complexity and cost increases.
 ξ idealized antenna beamwidth.
 R_T and ϕ geometric parameters determined by link distance (from section 2.2)
 P_T transmitter power.
 G_T, G_R transmitter and receiver antenna gains.
 λ carrier wavelength.
 D diffusion coefficient of the atmosphere.
 N_0 power spectral density of the noise.
 (Sec. 2.4)
 $g^{-1}(P_{b\max})$ minimum of bit energy to N_0 ratio.

For our sample system (Sec. 3.3) we chose $R_{\min V} = 1000$ b/s i.e $q_{\min V} = 1.1 \cdot 10^{13}$.
 $g^{-1}(P_b) = 9$ we get $R_{NV} = .011558$ and T_{UV} about 1150 b/s.

If we assume the constant bit energy of the variable rate system to be the same as the minimum bit energy of the constant rate system then for our sample system (underdense only) we improved the throughput from 214 (Sec. 3.4.3.1) to 1150 - a ratio of 5.3.

3.5.3 Throughput for Variable Bit Rate System

- Overdense

The maximum power point of an overdense burst P_{\max} is well approximated by (Eq. (2.1.5-2) neglecting k)

$$P_{\max} = C_0 \sqrt{\frac{\alpha \cdot q}{e}} \quad (3.5.3-1)$$

We recall that for our variable rate system the rate varies as the power scaled by the bit energy $N_0 g^{-1}(P_b)$

This variation in time can be approximated as a triangle whose base lies on time axis from the origin to the point given by aq and whose top vertex is at

$$P_{\max}/N_0 g^{-1}(P_b).$$

Since the number of bits sustained by this overdense burst, N_{bv} , is theoretically equal to the area underneath the rate time function we have

$$N_{bv} = \frac{1}{2} \frac{P_{\max}}{N_0 g^{-1}(P_b)} \cdot a \cdot q = \frac{1}{2\sqrt{e}} \frac{C_0 \alpha^{3/2}}{N_0 g^{-1}(P_b)} \cdot q^{3/2} \quad (3.5.3-2)$$

Averaging over the ensemble of overdense bursts using Eq. (2.1.6-2) with $q_{\min} = q_{LO} = 10^{14}$ ($q_{LO}/q_{VO} = .01$) we get

$$\overline{q^{3/2}} = \frac{1}{2} q_{VO} \sqrt{q_{LO}} \left(1 + \sqrt{\frac{q_{LO}}{q_{VO}}} \right) \quad (3.5.3-3)$$

which yields for average number of bits

$$\overline{N}_{ov} = \frac{1}{4\sqrt{e}} \frac{C_0 \alpha^{3/2}}{N_0 g^{-1}(P_b)} \cdot q_{VO} \sqrt{q_{LO}} \left(1 + \sqrt{\frac{q_{LO}}{q_{VO}}} \right) \quad (3.5.3-4)$$

and the arrival rate is given by Eq. (2.3-2)

$$A_v = \frac{3 \cdot \phi \sin \phi (R_k \zeta)^2}{q_{LO}} \left(1 - \frac{q_{LO}}{q_{VO}} \right) \quad (3.5.3-5)$$

Combining all of the above for the throughput expression (variable rate and overdense bursts) we get

$$T_{ov} = 94.686 \cdot 10^{-20} \frac{P_T G_T G_R \zeta^2 \phi \sin \phi \sec^3 \phi \cdot \lambda^5}{N_0 \cdot g^{-1}(P_b) \cdot D \cdot R_T} \quad (3.5.3-7)$$

For our sample system (Sec. 3.3) we get a throughput of 26.7 kb/s.

If we assume the constant bit energy of the variable rate system to be the same as the minimum bit energy of the constant rate system then for our sample system (Sec 3.3) (assuming overdense only) we improved the throughput from 8688 b/s (Sec. 3.4.3.2) to 26.7 kb/s - an improvement ratio of 3.

3.5.4 Comparison of Throughput for Constant and Variable Bit Rate Systems

In this section we shall apply the derived relationships in the previous sections to a practical system. The various parameters of interest are computed. The throughput of the system for the optimal constant bit rate is computed and compared with that of throughput of the system using variable bit rate. This comparison will demonstrate the improvement in throughput for variable bit rate. We start by copying the parameters of the system from Sec. 3.3:

L - 1000 km link distance. From section 2.2
 we have for the next two parameters:
 sec(ϕ) - 18.5 and
 $R_T = R_R$ - 514 km.
 P_T - 1000 w
 G_T - 10 dB.
 G_R - 10 dB. And for antenna beamwidth we use
 ζ - 45.84° (.8 rad)

λ - 6 m. (50 MHz)
 D - 8 m²/s
 P_{bmax} - 10⁻⁵ Max. BER for constant bit
 rate system.

Using BPSK modulation we get:

$$g^{-1}(P_{bmax}) = 9$$

$$N_0 = 4 \cdot 10^{-21} \left[80 \left(\frac{\lambda}{15} \right)^{2.3} + 2.5 \right] \text{ W/Hz}$$

See discussion above Eq. (2.4-2).

N_0 - 4.89 10⁻²⁰ at 50 MHz.

For comparison the BER for variable rate system, P_b ,
 is set equal to P_{bmax}

R_{minv} - 1000 b/s (minimum variable rate allowed)

Underdense Comparison

The improvement we get for underdense bursts is arrived at under the assumption that the optimal rate is used for the constant bit rate system and for the variable bit rate system some R_{minv} is assumed. In addition, we assume that the $P_b = P_{bmax}$ i.e. the constant bit energy (variable rate) is assumed equal to the

minimum allowed bit energy (constant rate system). We thus divide the relevant equations: Eq. (3.5.2-12) and Eq. (3.4.3.1-6) resulting in the improvement I_U

$$I_U = 1.9 \cdot \left(\frac{1}{\sqrt{R_{NV}}} - 1 \right) \frac{(R_{NV}^3 - R_{NV})}{(1 - R_{NV}^3)}$$

where,

$$R_{NV} = \frac{R_{minV}}{R_{maxV}}$$

$$R_{maxV} = 2.518 \cdot 10^{16} \cdot \frac{P_T G_T G_R \lambda^3 \exp\left(-\frac{33.359}{\lambda^2 \sec^2 \phi}\right)}{(.063 \lambda^{2.3} + 1) \cdot g^{-1}(P_b) \cdot R_T^3} \quad (3.5.2-13)$$

The above is evaluated using the values of our sample system where

$$R_{NV} = R_{minV}/R_{max} = 1000/86500 = .01156$$

resulting in

$$I_U = 5.38 \text{ or about } 7 \text{ dB}$$

Overdense Comparison

The relevant equations to be used for comparison of throughputs are Eq. (3.5.3-7) and Eq. (3.4.3.2-8) resulting in an improvement of

$$I_O = T_{OV}/T_O = 3$$

Discussion

We shall compare now the improvement in throughput of adaptive rate relative to fixed rate systems for underdense in terms of its components; the arrival rate and the average number of bits transmitted per burst. For fixed rate (underdense bursts) we have the following results:

Fixed Rate:

$$R_{max} = 86.5 \text{ kb/s}$$

Since the normalized optimal bit rate is $\approx .07$ we have

$$R^* = .07 R_{\max} = 6.05 \text{ kb/s}$$

For our system we also have

$$\bar{B} = .264 \text{ sec}$$

$$C_v = 3.8 \cdot 10^{-42}$$

From eq 2.4-2 we have:

$$N_0 = 4.89 \cdot 10^{-20}$$

For this rate we can compute some parameters for general interest:

the average number of bits per underdense burst is (from Eq. (3.4.3.1-2)) 1.846 kb/s per burst

$$q_{\min} = .26457 \cdot 10^{14} \text{ e/m (from eq. 3.4.1.1-1 set } R \text{ to } R^*)$$

Which yields an arrival rate of

.116 bursts per sec or equivalently an average inter-arrival time = 8.6 s.

The product of the last two results yield a throughput of 214 b/s

Variable Rate

In general the ratio of the bursts' arrival rates of variable bit rate to fixed bit rate system is given by

$$A_v/A^* = .36 \{ (R_{\max}/R_{\min V})^{.5} - 1 \} \quad (\text{Eq. (3.4.3.1-3) and Eq. (3.5.2-11)})$$

which in our example yields 2.9.

The average number of bits per burst using variable rate is from Eq. (3.5.2-10)

3.328 kb/s per burst.

The ratio of improvement for the average number of bits per burst is

$$3.328/1.846 = 1.8$$

whereas the improvement in arrival rate is

2.9 yielding a total improvement of 5.3

It is interesting to note that the larger improvement is due to the arrival rate.

The arbitrary set $R_{\min V}$, the minimum rate allowed in adaptive rate system, sets a lower threshold of electron line density, $q_{\min V}$, which utilizes bursts that are

precluded for the fixed rate system with its higher electron line density threshold q_{min} . It should be noted that however that system hardware complexity increases with lower R_{minV} .

4 DERIVATIONS

This chapter supplements the derivations outlined in the previous chapter for the results that have thus far been presented.

4.1 Link Geometry

With reference to fig. 6 and the definitions in section 2.2 we have the following relationships:

$$\psi = L/4R_e \quad (4.1-1)$$

$$\gamma = \frac{\pi}{2} + \psi \quad (4.1-2)$$

$$x = 2R_e \sin^2(\psi) \quad (4.1-3)$$

$$y = x \sin(\psi) = 2R_e \sin^3(\psi) \quad (4.1-4)$$

Since it's always true ($L < 2000$ km) that $(L/4R_e)^2 \ll 1$ we have

$$\sin^2(\psi) = \psi^2 = \frac{L^2}{16R_e^2} \quad (4.1-5)$$

By the Law of Cosine we have:

$$h^2 + x^2 - 2xh \cos(\gamma) = R_e^2 - R_r^2 \quad (4.1-6)$$

We substitute for x and y and $\sin^2(\psi)$ from eqns. (4.1-3), (4.1-2), (4.1-5) respectively in eqn. (4.1-6) and arrive at the stated result in section 2.2 after some trivial algebra.

$$R_r = R_e = \sqrt{(h + L^2/8R_e)^2 + L^2/4} \quad (2.2-1)$$

From the figure we also have:

$$\sec^2(\phi) = \frac{R_e^2}{(h+y)^2}$$

which when combined with eqs. (4.1-4), (4.1-5) and (2.2-1) yields:

$$\sec^2(\phi) = 1 + \frac{L^2}{\left(2h + \frac{L^2}{4R_e}\right)^2} \quad (2.2-2)$$

and thus completing the derivation.

4.2 Derivation of Average Burst Duration.

Constant Bit Rate

This derivation is for the underdense case. We start with equation (3.4.1.1-1) as the expression for t_b . Since we want to average over the joint space of q and B which are statistically independent. The joint pdf is given by the product of the individual pdfs. Because B acts as a coefficient in the expression for t_b the two integrals are separable. (The individual pdfs for q and B are from equations (2.1.2-2) and (2.1.3-2,3) respectively.

$$\bar{t}_b^2 = 2^n \bar{B}^n \cdot Q \int_{q_{min}}^{q_n} (\ln(q/q_{min}))^n \cdot q^{-p} dq \quad (4.2-1)$$

The above integral can be solved by employing the following substitutions:

$$z = (p-1) \ln(q/q_{min})$$

$$q = q_{min} e^{z/(p-1)}$$

$$dq = [q_{min} / (p-1)] e^{z/(p-1)} dz$$

$$\ln^n(q/q_{min}) = [z/(p-1)]^n$$

Reduces the above to a single integral of the form

$$\bar{t}_b^2 = \frac{2^n \bar{B}^n}{(p-1)^n} \cdot \frac{1}{1-x} \cdot \int_0^{\ln(1/x)} z^n e^{-z} dz \quad (4.2-2)$$

where

$$x = \left(\frac{q_{min}}{q_u} \right)^{p-1} = \left[\frac{N_0 \cdot R \cdot g^{-1}(P_{bmax})}{C_u q_u^2} \right]^{\frac{p-1}{2}}$$

which can be solved recursively by parts, yielding

$$\bar{t}_b^2 = \frac{2^n \bar{B}^n}{(p-1)^n} \cdot \frac{n!}{1-x} \left\{ 1 - x \sum_{i=0}^n (-1)^i \frac{\ln^i(x)}{i!} \right\}$$

Setting $n=1$ and $n=2$ in the above yields the necessary equations for the expected value and variance of t_b although some wading through algebra is necessary for the derivation of the variance.

4.3 Burst Duration Constant Bit Rate - Overdense

Since the roots of the overdense power received equation cannot be solved for directly we use a second order approximation. In fact each side of the overdense 'mountain' is fit with a parabola. The parabolas are expanded about the maximum power point. For the left parabola (which approximate the left side) we use the smaller root and subtract it from the larger root of the right parabola

(which approximates the right side of the power equation). This difference is the burst duration for the overdense trail. We start by copying eq. (2.1.5-2)

$$P(t) = C_0 \sqrt{(k+t) \cdot \ln\left(\frac{a \cdot q}{k+t}\right)} \quad t \leq aq - k \quad (2.1.5-2)$$

where,

$$C_0 = 3.16628610^{-3} \sqrt{D \frac{P_T G_T G_R \lambda^2}{R_T^3}}$$

$$k = .105625/D$$

$$a = 7.14314310^{-17} \cdot \frac{\lambda^2 \sec^2 \phi}{D}$$

We need to solve for the roots t_2, t_1 of the above eq. when P is set to P_{\min} since their difference is our transmission interval - burst duration. To do so we first modify the above eq. as:

$$P_N = \sqrt{r \cdot \ln\left(\frac{1}{r}\right)} \quad k/aq \leq r \leq 1 \quad (4.3-2)$$

or equivalently

$$r \ln(r) + P_N^2 = 0 \quad (4.3-4)$$

where

$$P_N = P / C_0 (aq)^{1/2}$$

$$r = (k+t)/aq$$

The above will yield the roots r_2, r_1 for $P = P_{\min}$

Note that the burst duration is defined as

$$t_B = t_2 - t_1 = aq(r_2 - r_1) \quad (4.3-4)$$

We are now ready to approximate $r_2 - r_1$ where r_1 is the 'left' root and r_2 the 'right' root. Note that the above eq. has a maximum P_N of $1/(e)^{1/2}$ at $r = 1/e$.

To approximate r_1 we expand $\ln(r)$ about $r = 1/e$ and substitute the first two terms for $\ln(r)$ in the last eq resulting in: $r^2 - (2/e)r + (1/e)P_N^2 = 0$

Solving and using the smaller root we thus approximate r_1 as:

$$r_1 = \frac{1}{e} \cdot (1 - \sqrt{1 - 3P_N^2}) \quad (4.3-5)$$

To approximate r_2 we expand $r \ln(r)$ about $r = 1/e$ and substitute the first three terms in eq (4.3-3) and solve for the larger root.

$$r_2 = \frac{1}{e} \cdot (1 + \sqrt{2(1 - eP_N^2)}) \quad (4.3-6)$$

$$r_2 - r_1 = \frac{(1 + \sqrt{2})}{e} \cdot \sqrt{1 - eP_N^2} = 0.88 \sqrt{1 - eP_N^2} \quad (4.3-7)$$

A comparison of the above with an iterative solution of the real (without approximation) roots of the eq (4.3-3) and their difference allows us to replace the .88 constant in the last eq. with .95

$$r_2 - r_1 = .95 \text{ root } [1 - e P_{\text{sub } N \text{ super } 2}]$$

Since the power for which we want to find the roots is P_{min} from eqs. (4.3-3) and (4.3-4) we have the desired approximation for t_B

$$t_B = .95a \cdot q \cdot \sqrt{1 - \frac{eP_{\text{min}}^2}{C_o^2 a} \cdot \frac{1}{q}} \quad (4.3-8)$$

which is the result stated in (3.4.1.2-1).

Note that $q > q_{\text{mino}} = \max(q_T, q_{L0})$. If q_T (which is set by P_{min} and system parameters reflected in C_o and a) is less than q_{L0} than the minimum overdense electron line density, q_{mino} , is set to the physical minimum overdense electron line density q_{L0} . On the other hand if q_T is bigger than q_{L0} than the overdense trails with electron line density between q_{L0} and q_T have zero burst duration and are not "seen" by our system.

For most practical systems which utilize underdense bursts P_{min} is such that:

$q_T \ll q_{L0}$ i.e. $q_{\text{mino}} = q_{L0}$ and t_B is approximated as aq , ($q > q_{L0}$) and

$$E(t_B) = .95a E(q) = a(q_{uo} q_{L0})^{1/2} = a 10^{15}.$$

Derivation of CDF and PDF:

From eq. (3.4.1.2-1) we note that t_B is monotonically increasing with q such that for any $t_B < t_1$ we have correspondingly a $q < q_1$. For $t_B = t_1$ we have from eq. (3.4.1.2-1) :

$$q_1 = \frac{q_T}{2} \cdot \left(1 + \sqrt{1 + \left(\frac{t_1}{\tau} \right)^2} \right) \quad (4.3-8)$$

$$\text{where } \tau = a q_T / 2 = (e/2)(P_{\text{min}}/C_o)^2$$

From the above discussion there is a minimum t_1 , $t_{1\text{min}}$ corresponding to q_{mino} and

a maximum t_1 , $t_{1\max}$ corresponding to q_{uo} , the max overdense electron line density. We can now relate the following probability events:

$$\text{Prob}\{t_1 \leq t_1\} = \text{Prob}\{q_{\min} \leq q \leq q_1\} \quad t_{1\min} \leq t_1 \leq t_{1\max} \quad (4.3-9)$$

We get the CDF of q using eq (2.1.2-2) such that the right hand side of the last eq. becomes

$$Q' [1 - (q_{\min} / q_1)^{p-1}]$$

Eq (4.3-9) then becomes

$$F_{t_1}(t_1) = Q' \left\{ 1 - \left(\frac{q_{\min}}{q_1} \right)^{p-1} \right\} \quad t_{1\min} \leq t_1 \leq t_{1\max} \quad (4.3-10)$$

Substituting eq (4.3-8) into the above eq. we get the desired eq. (3.4.1.2 -6).

To get eq. (3.4.1.2-7) we simply take the derivative of eq. (3.4.1.2-7)

4.4 Optimal Average throughput for constant bit rate - Underdense

Our first objective is to derive eq. (3.4.3.1-2) from section 3.4.2 we know the number of bits per given underdense burst for a given R and a set of specified system parameters is given by

$$N_{BU} = R t_B \quad (4.4-1)$$

Averaging N_{BU} over the ensemble of underdense bursts (q and B independent) is given by

$$\bar{N}_{BU} = R \cdot \bar{t}_B \quad (4.4-2)$$

rewriting the result in Eq. (3.4.1.1.-3) which is derived in Sec. 4.2

$$\bar{t}_B = \frac{2\bar{B}}{p-1} \cdot \frac{1}{1-x} \cdot [1 - x(1 - \ln x)] \quad (3.4.1.1-3)$$

where

$$x = \left(\frac{q_{\min}}{q_u} \right)^{p-1} = \left[\frac{N_0 \cdot R \cdot g^{-1}(P_{b\max})}{C_u q_u^2} \right]^{\frac{p-1}{2}}$$

and

$$\bar{B} = 3.16610^{-3} \cdot \frac{\lambda^2 \sec^2 \phi}{D} \quad q_U = 10^{14} \quad p = 1.6$$

$$R_N = \frac{R}{R_{\max}} - \left(\frac{q_{\min}}{q_U} \right)^2$$

$$R_{\max} = \frac{C_U q_U^2}{N_0 g^{-1}(P_{b\max})}$$

we substitute for x and R in terms of their R_N definitions and write

$$(R_N)^{p'} = x \quad p' = (p-1)/2 \quad (p = 1.6)$$

$$R = R_N R_{\max}$$

Substituting these into eq. (4.4-2) yields the desired eq. (3.4.3.1-2)

$$\bar{N}_{BU} = \frac{2\bar{B}}{p-1} R_{\max} \frac{1}{1-R_N^{p'}} [R_N - R_N^{p'+1} + R_N^{p'+1} \ln(R_N^{p'})] \quad (3.4.3.1-2)$$

This eq. specifies for a given choice of R the average number of bits/burst. The rest is in Sec. 3.4.3.1

4.5 Transmission Duration & Throughput for Variable Bit Rate System

With reference to section 3.5.1.1 we define again the following terms:

P_b Assumed constant BER for all transmitted bits.

T_{bi} Duration of the i^{th} bit

$R(t)$ Instantaneous bit rate

T_0 Duration of the first bit, $1/R_0$

N Last bit

$T(m)$ Total duration of the first m bits;
also starting time of the $(m+1)^{\text{th}}$ bit:

$$\sum_{i=1}^m T_{bi}$$

T_t Duration of transmission (burst duration) = $T(N)$

c Max (T_{bN}/B) for a given k .

We wish to maintain the actual bit energy above a certain fraction say 90% of the assumed bit energy. This will insure a relatively constant BER corresponding to the assumed bit energy. Since the last bit, the N^{th} bit, has the longest duration (power is monotonically decreasing) the loss in bit energy relative to the assumed level is the largest. in equation form:

$$E_{b \text{ actual}} > k E_{b \text{ assumed}}$$

i.e.

$$\int_0^{T_{bN}} P(T(N-1)) \cdot e^{-t/B} dt \geq k \cdot P(T(N-1)) \cdot T_{bN}$$

which implies

$$1 - kT'_{bN} > \exp(-T'_{bN}) \quad \text{where } T'_{bN} = T_{bN}/B$$

and assuming $T'_{bN} < 1$ we use the first four terms in the series expansion of the exponential (about 0) and get the root of T'_{bN} yielding

The quadratic equation in T'_{bN} yields

$$T'_{bN} = \frac{T_{bN}}{B} < 1.5 - \sqrt{2.25 - 6(1-k)} = c$$

From the above definitions of the N^{th} bit duration we have

$$T_{bN}/B = [1/R_0 B] \exp(T(N-1)/B) < c$$

yet by definition $T(N-1) = T_t - T_{bN}$

we have then $T_t < B [c + \ln(cR_0B)]$

which is the result stated in eq. (3.5.1.1-5)

We now evaluate the number of bits for a given burst using variable bit rate as

$$N_{BU} = \int_0^{T_{burst}} R(t) dt = R_0 B \left(1 - \exp\left(-\frac{T_t}{B}\right) \right)$$

Using the maximum T_t from eq. (3.5.1.1-4) i.e. letting $N_B = \text{maximum } N_B$ we have

$$N_{BU} = R_0 B + 1 - 1/c$$

For $K=.9$ $c=.2$

For all practical system $R_0 B \gg 4$

such that

$$N_{BU} = R_0 B = c_u B q^2/q^{-1}(P_b) N_0$$

as stated in section 3.5.2 Eq. (3.5.2-1)

The average throughput is proportional to the ensemble average of N_{BU} . Since B and q are statistically independent we have

$$\overline{N_{su}} = \frac{C_u}{g^{-1}(P_0) \cdot N_0} \cdot \overline{B} \cdot \overline{q^2}$$

which is Eq. (3.5.2.-2)

5 AUTOAMATIC-REPEAT-REQUEST (ARQ) TRANSMISSION over MBC

5.1 Performance Measures

Three performance measures were used to characterize a meteor burst channel: duty cycle, throughput, and waiting time. Duty cycle is a function of system parameters only, but throughput and waiting time are strongly dependent on the chosen communication protocol.

5.1.1 Throughput Rate

We will examine two ARQ protocols for point-to-point data transmission over a meteor burst channel, similar to those described in [36]. The main difference is in the channel behavior, since it is not continuous but rather intermittent. When stop-and-wait strategy is used, transmitting terminal has to wait for the receiver response not only because of the processing in the receiver, that is done in the idle time between trails. The main cause of the delay is the fact that a receiver must wait for the next available trail to send back its acknowledgment, after it is done with checking the validity of received packet. In a selective-repeat strategy, the communication is full-duplex only during the burst duration. Forward channel is used for the transmission of new and repeated packets, and along feedback channel goes the information about the numbers of packets that have to be repeated. In the idle time between the trails, communication stops in both channels.

In a stop-and-wait strategy, the transmitting terminal sends one data packet per burst. The opening of a channel (i.e. the beginning of a burst) is indicated either by a probe signal from the receiving terminal at the beginning of a session or, later on, by acknowledgment signals. Data packet is N -bits long, consisting of k information bits and r bits for error detection. After sending a packet the transmitter waits for the receiver response. Upon examining the incoming packet the receiver sends back an s -bit positive (ACK) or negative (NAK) acknowledgment signal during the next available burst. The transmitter repeats the current packet if it received the NAK signal or proceeds to a new packet of data in case of the ACK signal. The repeated or the new packet are sent immediately upon reception of the ACK/NAK signal.

The throughput rate of such a strategy is defined as the ratio of information bits to total number of bits [37]

$$T_{sv} = \frac{N-r}{(N+\tau+s) \cdot E} , \quad (5.1.1-1)$$

where τ denotes the number of idle bit times between the last bit of a data packet transmitted and the first bit of an ACK/NAK signal received. E represents the expected number of transmissions of one packet accumulated to the moment the transmitter proceeds to a new packet of data.

The probability Δ that a given transmission of a packet at the same time happens to be the last one is

$$\Delta = P_c + P_e , \quad (5.1.1-2)$$

where we assumed that ACK/NAK signal is received correctly with probability equal to 1. (In practice, this assumption can be closely achieved by heavy coding of acknowledgment signals. These signals are short and even with long codes they would occupy negligible amount of a burst time. Furthermore, they are sent at the beginning of the burst when bit error probability is at its minimum. If the burst time is critical, the pilot signal itself can carry acknowledgment information.) P_e is the probability that a received packet contains an undetectable error pattern. For an average linear (n,k) code it is bounded by [38]

$$P_e \leq 2^{-(n-k)} (1 - P_c)$$

or, for a double-error-correcting primitive BCH code by

$$P_e \leq 2^{-(n-k)} ,$$

which means that P_e can be neglected as compared to P_c , the probability that a packet is correct, for any practical packet length. The same conclusion is valid for the case when cyclic redundancy check (CRC) polynomials are used for error detection. Thus, we can safely continue the derivation with Eq. (5.1.1-2) reduced to

$$\Delta = P_c . \quad (5.1.1-3)$$

Now, the probability that we need exactly $n - 1$ transmissions of a packet to receive it correctly is

$$P\{n=i\} = \Delta_i \prod_{k=0}^{i-1} (1 - \Delta_k), \quad (5.1.1-4)$$

and the expected number of transmissions becomes

$$\begin{aligned} E &= \sum_{i=1}^{\infty} i \Delta_i \prod_{k=0}^{i-1} (1 - \Delta_k) \\ &= \sum_{i=1}^{\infty} i P_{ci} \prod_{k=0}^{i-1} (1 - P_{ck}). \end{aligned} \quad (5.1.1-5)$$

Averaging E over all possible values for underdense and overdense electron line densities q_1 and q_2 , respectively, and decay constant b , we obtain from Eq. (5.1.1-5)

$$E = \sum_{i=1}^{\infty} i \bar{P}_c (1 - \bar{P}_c)^{i-1}, \quad (5.1.1-6)$$

since the probabilities P_c in different trails are statistically independent and have identical averages. Performing the summation of a geometric series in Eq. (5.1.1-6), the average number of packet transmissions becomes

$$E = \frac{1}{\bar{P}_c}. \quad (5.1.1-7)$$

On the other hand, the probability that a packet is received correctly during a particular try may be calculated as the total probability

$$\begin{aligned} P_c &= P\{C | \text{underdense transmission}\} \times P\{\text{underdense transmission}\} + \\ &+ P\{C | \text{overdense transmission}\} \times P\{\text{overdense transmission}\} \\ &= P_{cu} P_u + P_{co} P_o. \end{aligned} \quad (5.1.1-8)$$

The probability that a packet is transmitted over an underdense trail is the ratio of the expected number of underdense trails to the total expected number of trails (during some observation time T_D .)

$$P_u = \frac{\frac{\tau_d}{t_{1U}}}{\frac{\tau_d}{t_{1U}} + \frac{\tau_d}{t_{1O}}} = \frac{t_1}{t_{1U}}. \quad (S.1.1-9)$$

Similarly, the probability that a packet is transmitted over an overdense trail is

$$P_o = \frac{t_1}{t_{1O}}. \quad (S.1.1-10)$$

The new statistical parameter t_1 is defined in Eq. (5.1.2-3). Averaging P_c from Eq. (5.1.1-8) over q_1 , q_2 , and b ,

$$\bar{P}_c = \bar{P}_{cu} P_u + \bar{P}_{co} P_o.$$

and substituting the result into the Eq. (5.1.1-1), the throughput rate follows as

$$T_{SV} = \frac{N-r}{N+\tau+s} [\bar{P}_{cu} P_u + \bar{P}_{co} P_o]. \quad (S.1.1-11)$$

Dividing the numerator and denominator in Eq. (5.1.1-12) with the bit rate R we obtain

$$T_{SV} = \frac{T_p - T_r}{T_p + T_{idle} + T_s} [\bar{P}_{cu} P_u + \bar{P}_{co} P_o]. \quad (S.1.1-12)$$

where T_p , T_s , and T_r are the durations of a packet, ACK/NAK signal, and parity bits, respectively.

Idle time T_{idle} is a random variable,

$$T_{idle} = x - T_p,$$

with x the time distance between consecutive bursts. With respect to the probability density function for x [39]

$$f(x) = \frac{1}{t_i} e^{-\frac{x}{t_i}}$$

we find the average value for T_{idle} as

$$\bar{T}_{idle} = \int_0^{\infty} (x - T_p) f(x) dx = t_i - T_p. \quad (5.1.1-13)$$

Combining Eqs. (5.1.1-9), (5.1.1-10), (5.1.1-12), and (5.1.1-13), the final expression for throughput rate is

$$T_{sw} = \frac{T_p - T_r}{t_i + T_p} \left[\frac{t_i}{t_{lu}} \bar{P}_{cu} + \frac{t_i}{t_{lo}} \bar{P}_{co} \right]. \quad (5.1.1-14)$$

when stop-and-wait strategy is used.

In a selective-repeat strategy, the transmitter sends as many data packets as the duration of a current burst allows. The transmitter determines the burst duration with the help of a feedback channel, which is continuously used for reception of acknowledgment information. If the receiver buffer is infinite and if we assume no errors in the feedback channel, the throughput is equal to the probability that the packet is received correctly [40],

$$T_{SR} = P_c, \quad (5.1.1-15)$$

representing the average number of packets communicated (i.e. transmitted and received correctly) per transmission. The throughput T_{SR} is obtained as the capacity of an M-ary erasure channel, where M is the number of possible choices for a packet [41]. Hence the selective-repeat strategy represents the optimal form of ARQ when the receiver buffer size is unlimited.

We can consider P_c to be a discrete random variable taking values

$$\begin{aligned} P_c &= P_{cu} \quad , \text{ during underdense bursts} \\ &= P_{co} \quad , \text{ during overdense bursts} \\ &= 0 \quad , \text{ elsewhere.} \end{aligned}$$

Hence, its expected value will be

$$E(P_c) = P_{cu} P(P_c = P_{cu}) + P_{co} P(P_c = P_{co}) .$$

Now, the probability that P_c is equal to P_{cu} is the ratio of the total underdense burst time to total observation time

$$P\{P_c = P_{cu}\} = \frac{\frac{\tau_D}{t_{IU}} \bar{t}_{BU}}{T_D} = \frac{\bar{t}_{BU}}{t_{IU}} . \quad (5.1.1-16)$$

Total burst time is a product of the expected number of bursts and their average duration. The mean time between trails is always greater than the average burst duration, in underdense and in overdense case. Similarly, the probability that P_c is equal to P_{co} is found to be

$$P\{P_c = P_{co}\} = \frac{\bar{t}_{BO}}{t_{IO}} . \quad (5.1.1-17)$$

Using Eqs. (5.1.1-16) and (5.1.1-17), the expression for the average throughput of a selective-repeat system becomes

$$T_{SR} = \frac{\bar{t}_{BU}}{t_{IU}} \bar{P}_{cu} + \frac{\bar{t}_{BO}}{t_{IO}} \bar{P}_{co} . \quad (5.1.1-18)$$

The question remaining to be solved is the evaluation of average values for P_{cu} and P_{co} . The beginning of the packet can fall into time instants separated by a packet length T_p , counting from the beginning of a trail. In that sense, P_{cu} is found as the total probability

$$P_{cu} = \sum_{k=0}^{\lfloor t_{BU}/T_p \rfloor} \frac{1}{\lfloor t_{BU}/T_p \rfloor} P_{cu}(kT_p) . \quad (5.1.1-19)$$

where we assumed that packet positions are uniformly distributed inside the trail. Notation $\lfloor x \rfloor$ signifies the integer less than or equal to x . In that context, the ratio t_{BU}/T_p represents the number of packets that will fit into the burst duration. $P_{cu}(kT_p)$ is the probability that a packet in the k -th time slot will be received correctly. Bar on probabilities P_{cu} and P_{co} indicates averaging over electron line densities and a decay constant. Expression identical to the one in Eq. (5.1.1-18) describes the situation with the overdense trails, if t_{BU} is replaced with t_{BO} .

5.1.2 Waiting Time

Waiting time to deliver a data packet is defined as the time elapsed from the moment a transmitter has a packet ready for sending, to the time instant the receiver starts sending back a positive acknowledgment signal.

Underdense and overdense trail arrivals are independent Poisson processes, with respective parameters

$$\lambda_u = \frac{1}{t_{IU}}, \quad \text{and} \quad \lambda_o = \frac{1}{t_{IO}}. \quad (5.1.2-1)$$

The random process consisting of all trail arrivals is also Poisson with the parameter

$$\lambda = \lambda_u + \lambda_o. \quad (5.1.2-2)$$

what says that the mean time between bursts in this new process is

$$t_1 = \frac{1}{\lambda} = \frac{t_{IU} t_{IO}}{t_{IU} + t_{IO}}. \quad (5.1.2-3)$$

When trail arrivals are modeled as Poisson random points t_i , the waiting time t_w for stop-and-wait strategy is given by

$$t_w = x_{n+1} = t_{n+1} - t_0,$$

where x_{n+1} is the time distance from the fixed beginning of the observation time t_0 (i.e. the instant a transmitter has a packet ready for sending,) to the $(n + 1)$ th random Poisson point to the right of t_0 . Namely, if the number of transmissions required to receive a packet correctly is equal to n , we must wait to the $(n + 1)$ th trail for the receiver confirmation. Random variable x_{n+1} has Erlang probability density function [39]

$$f_{n+1}(x) = \frac{\lambda^{n+1}}{n!} x^n e^{-\lambda x},$$

and averaging over x leads to

$$E_x\{t_v\} = \int_0^\infty x_{n+1} f_{n+1}(x) dx = \frac{n+1}{\lambda}.$$

Averaging further over n , a discrete random variable defined by Eq. (5.1.1-4), the expected waiting time becomes

$$\begin{aligned} \bar{i}_v &= (1+E) t_f = \left(1 + \frac{1}{\bar{P}_c}\right) t_f \\ &= \left(1 + \frac{1}{\bar{P}_{cu} P_u + \bar{P}_{co} P_o}\right) t_f. \end{aligned} \quad (5.2.2-4)$$

The minimum possible waiting time is achieved in the case when every packet is correctly received during its first transmission. Expected number of transmissions E is then equal to 1, and the resulting lower bound on waiting time to receive a correct packet in a stop-and-wait strategy is

$$\bar{i}_{w \min} = 2t_f. \quad (5.1.2-5)$$

a function of meteor burst parameters only.

5.1.3 Duty Cycle

The duty cycle of a meteor burst communication system is defined as the percentage of time that the received signal is above some arbitrary threshold, what is equivalent to the condition that the trail electron line density be above some minimum value q_{\min} . It can be found as the ratio of the total burst time within an observation time T_o , to the observation time T_o itself. On the average, the total burst time is the product of the expected number of trails during the observation time and their mean durations. Taking into account both types of trails

$$\begin{aligned} \text{duty cycle} &= \frac{\frac{T_o}{t_{lu}} \bar{i}_{BU} + \frac{T_o}{t_{lo}} \bar{i}_{BO}}{T_o} \\ &= \frac{\bar{i}_{BU}}{t_{lu}} + \frac{\bar{i}_{BO}}{t_{lo}}, \end{aligned} \quad (5.1.3-1)$$

where mean values for underdense and overdense burst durations, t_{BU} and t_{BO} , contain the information about the receiver threshold (i.e. q_{\min} .) Eq. (5.1.3-1)

assumes that trails do not overlap. If that happens to be the case it is an upper bound.

5.2 Meteor Burst Communication System

Digital data are transmitted over a meteor-burst channel using binary phase-shift keying modulation, at a constant data rate R . The transmitted signal is

$$s(t) = \pm \sqrt{2P_T} \cos \omega_0 t, \quad 0 \leq t \leq T_b,$$

where P_T is the transmitter power and $f_0 = 2\pi/\omega_0$ is the carrier frequency. $T_b = 1/R$ is the bit duration.

Multipath phenomena are encountered in meteor-burst communications only at high data rates; there appear very few underdense trails with electron line density high enough to provide sufficient scattered signal power, and overdense trails become dominant propagation medium. At low data rates underdense trails are much more numerous, they act as small coherent sources and scattered continuous-wave signals exhibit good space and frequency correlation. The phase of the received signal is assumed constant, representing only the gross time delay due to the average distance which the signal must propagate. Such delay amounts only to a shift in time origin.

The signal received from an underdense or overdense trail is of the form

$$\begin{aligned} r(t) &= \pm A \cos \omega_0 t + n(t) \\ &= \pm \sqrt{2P_s} \cos \omega_0 t + n(t), \quad 0 \leq t \leq T_b, \end{aligned}$$

where A is a random amplitude and $n(t)$ is a Gaussian noise with one-sided power spectral density defined by Eq. (2.4-1). BPSK signals have the same energy $E_b = P_s T_b$, and the optimum decision threshold is set at $V_t = 0$ volts. Since the attenuation of the signal is always positive, the optimum decision regions are invariant to radial scaling of received signals. Under these conditions, a correlation or matched-filter receiver structure is still optimum, completely independent of the fact whether amplitude A , or probability density function of amplitudes $p(A)$ is known precisely [42].

The received signal amplitude is

$$A = \sqrt{2P_s}.$$

For underdense trails, the received power P_s is equal to P_{su} from Eq. (2.1.1-2), a function of two random variables, q_1 and b . Transforming their density functions from Eqs. (2.1.2-2) and (2.1.3-3) we obtain the probability density for underdense signal amplitudes A_u

$$f(A_u) = 2.46 Q_1 A_u^{-1.6} \int_{\gamma_1}^{\gamma_2} \exp\left(-\frac{0.2t}{\alpha\gamma} - \gamma^2\right) \gamma d\gamma, \quad (5.2-1)$$

that is valid in the interval

$$\sqrt{2C_u} q_{minu} \leq A_u \leq \sqrt{2C_u} q_{maxu}.$$

The integration limits in Eq. (5.2-1) are

$$\gamma_1 = \frac{t}{2\alpha\sqrt{2\ln \frac{q_{minu}\sqrt{2C_u}}{A_u}}}, \text{ and } \gamma_2 = \frac{t}{2\alpha\sqrt{2\ln \frac{q_{maxu}\sqrt{2C_u}}{A_u}}}.$$

For overdense trails, the received power P_s is equal to P_{so} from Eq. (2.1.5-2), a function of one random variable q_2 . Transforming its distribution from Eq. (2.1.6-2), probability density for overdense signal amplitudes A_o becomes

$$f(A_o) = \frac{Q_2 A_o^3 \sqrt{\alpha}}{C_o^{3/4} (k+t)^{3/2}} \exp\left[-\frac{A_o^4}{8C_o^2 (k+t)}\right]$$

valid in the interval

$$\sqrt{2C_o} \left[k \ln \frac{\alpha q_{mino}}{k} \right]^{1/4} \leq A_o \leq \frac{\alpha}{\rho} \sqrt{2C_o} q_{maxo}.$$

Both probability density functions are too complicated as to gain some useful insight into the detection process.

5.2.1 Uncoded Transmission

5.2.1.1 Transmission over Underdense Trails

The probability of the i -th bit in a packet being in error, expressed in terms of received power P_{su} from Eq. (2.1.1-2), is

$$P_{bu}\left(\frac{i}{R}\right) = \frac{1}{2} \operatorname{erfc} \left[\frac{C_u q_1^2}{N_0 R} \exp\left(-\frac{i}{Rb}\right) \right]^{\frac{1}{2}}, \quad (5.2.1.1-1)$$

when BPSK modulation is used. We took the bandwidth to be equal to the bit rate R (1 bit/sec/Hz). The time within the trail has discrete values $t = i/R$. To simplify the analysis, we assumed that P_{su} remains constant during the bit interval and equal to the power at the end of the interval. This is a 'worst case' approach on a small scale, since the actual S/N ratio for every bit will be better than the one used in calculation. The probability that the packet N -bits long is correct is then

$$P_{cu} = \prod_{i=1}^N \left[1 - P_{bu}\left(\frac{i}{R}\right) \right], \quad (5.2.1.1-2)$$

with the average value

$$\bar{P}_{cu} = \int_{b=0}^{\infty} \int_{q_1=q_{\min}}^{q_{\max}} P_{cu} \cdot f_b(b) \cdot f(q_1) dq_1 db. \quad (5.2.1.1-3)$$

In addition, the variable from Eq. (5.1.1-19) is evaluated as

$$P_{cu}(kT_p) = \prod_{i=1}^N \left[1 - P_{bu}\left(\frac{i}{R} + kT_p\right) \right],$$

and its average is calculated in the same way as in Eq. (5.2.1.1-3).

5.2.1.2 Transmission over Overdense Trails

The bit error probability expressed in terms of received power P_{s0} from Eq. (2.1.5-2) is now

$$P_{bo}\left(\frac{l}{R}\right) = \frac{1}{2} \operatorname{erfc} \left[\frac{C_o}{N_o R} \sqrt{\left(k + \frac{l}{R}\right) \ln\left(\frac{a q_2}{k + \frac{l}{R}}\right)} \right]^{\frac{1}{2}}, \quad (5.2.1.2-1)$$

with all the underlying assumptions stated for Eq. (5.2.1.1-1). Accordingly, the probability of a packet being correct in these conditions becomes

$$P_{co} = \prod_{i=1}^N \left[1 - P_{bo}\left(\frac{l}{R}\right) \right], \quad (5.2.1.2-2)$$

with the corresponding average value

$$\bar{P}_{co} = \int_{q_2=q_{min0}}^{q_{20}} P_{co} \cdot f(q_2) dq_2. \quad (5.2.1.2-3)$$

5.2.2 Coded Transmission

For coded transmission, convolutional codes were chosen because of their superior performance compared to block codes, for the same implementation complexity of the encoder-decoder [43].

We did not consider the class of burst-error correcting codes, since very few statistical data are available on the length of meteor-burst channel memory. Although exponential decay of received power toward the end of the burst in underdense case leads to conclusion that bit errors become more frequent, the noise model from Eq. (2.1.4-1) shows that for narrowband modulation the noise may be considered white, and noise samples in successive bit intervals are consequently independent.

For higher data rates or for spread spectrum systems noise can not be taken as white any more, since its power spectral density will change inside the signaling bandwidth. Noise samples become dependent, and this noise model predicts the appearance of channel memory. If experimental data confirm these conclusions,

use of interleaving will become necessary to "randomize" transmission errors and maintain the performance of convolutional codes, which are not best suited for burst errors.

We considered both rate $1/n$ and rate k/n convolutional codes. Rate $1/n$ codes provide for superior error-correcting performance, at the cost of substantial lengthening of the original packet. For this reason, codes with n greater than 2 are at disadvantage in meteor burst communications, since the coded packet length becomes prohibitively large and will often exceed burst duration, resulting in the loss of many bits as their time slots fall beyond the receiver threshold point. Rate k/n codes are less powerful but more compact, and their error-correcting capability is not easily overwhelmed by the strong limiting factor of relatively short burst durations, particularly when k/n ratio approaches to 1. In our work, code rates of $3/4$, $7/8$, and $15/16$ were considered.

When decoding convolutional codes, the error-correcting capability is difficult to state precisely. With maximum likelihood decoding, a code can correct t errors within 3 to 5 constraint lengths, where t is defined as

$$t = \left\lfloor \frac{d_f - 1}{2} \right\rfloor,$$

in terms of the free distance d_f . The exact length depends on actual error distribution, and for a particular code and error pattern, transfer functions methods are used to obtain bounds [43]. In our case the problem is further aggravated by the fact that signal-to-noise ratio is not constant throughout the packet, but rather changes as the received power varies with time.

One way to overcome these difficulties is to use the notion of cutoff rate R_0 for binary transmission

$$R_0 = 1 - \log_2(1 + D) \quad \text{bits/symbol},$$

in order to decouple the influence of the coding channel characterized by R_0 from the coding technique [44]. For example, in case of rate $1/2$ code with $K = 7$ and hard decision decoding, the decoded bit error rate is bounded by [44]

$$P_{b \text{ coded}} \leq 18D^{10} + 105.5D^{12} + 702D^{14} + 5816.5D^{16} + \dots \quad (5.2.2-1)$$

where

$$D = 2\sqrt{P_b(1-P_b)} , \quad (5.2.2-2)$$

and P_b is the channel bit error rate.

For rate k/n codes, we used the following bound on decoded bit error probability [45]

$$P_{\text{decoded}} \leq \frac{1}{k} \sum_{j=d_f}^{\infty} w_j \frac{1}{2} \operatorname{erfc} \sqrt{\frac{jE_s}{N_0}} , \quad (5.2.2-3)$$

where d_f is the free distance of the code, $E_s = E_b r$ is the symbol energy, r is the code rate, E_b is the bit energy, and N_0 is the noise power spectral density. Code-specific coefficients w_j are summarized in tables for different values of the code constraint length [46].

Infinite-level quantization results in 2.2 dB improvement over two-level quantization. It can be substituted by the 3-bit soft decisions of the channel output, resulting in approximately a 2 dB gain over the hard quantized binary symmetric channel.

Bounds on decoded bit error rate are derived for constant signal-to-noise ratio and arbitrarily large path memory, i.e. the depth of the input bit history stored by the decoder. But, it was shown in [47] that a fixed amount of path history, namely 4 or 5 times the constraint length, is sufficient to limit the degradation from the optimum decoder performance to about 0.1 dB for the BSC and Gaussian channels. In a meteor burst channel signal-to-noise ratio is constantly changing, but most of the time it does not change substantially during the fixed decoding delay, and we took it to be constant for the bits along one path memory length. Furthermore, the decision about a specific bit is brought by analyzing the trellis branches consisting of bits that all have equal or higher signal-to-noise ratios than the bit in question.

5.2.2.1 Transmission over Underdense Trails

Parameter D from Eq. (5.2.2-2) in this case becomes

$$D = 2\sqrt{P_{bu}(1 - P_{bu})} ,$$

when we use the values for P_{bu} from Eq. (5.2.1.1-1). After calculating the values for $P_{bu \text{ coded}}$ according to Eqs. (5.2.2-1) or (5.2.2-3), the probability that encoded packet will be correctly received is found as the product

$$P_{cu \text{ coded}} = \prod_{i=1}^N \left[1 - P_{bu \text{ coded}} \left(\frac{l}{R} \right) \right] .$$

Its average value is then

$$\bar{P}_{cu \text{ coded}} = \int_{b=0}^{\infty} \int_{q_1=q_{minu}}^{q_{uu}} P_{cu \text{ coded}} \cdot f_b(b) \cdot f(q_1) dq_1 db . \quad (5.2.2.1-1)$$

5.2.2.2 Transmission over Overdense Trails

Following the same steps as in Sec. 5.2.2.1. we obtain the parameter D in the form

$$D = 2\sqrt{P_{bo}(1 - P_{bo})} ,$$

the probability that a coded packet is correctly received as

$$P_{co \text{ coded}} = \prod_{i=1}^N \left[1 - P_{bo \text{ coded}} \left(\frac{l}{R} \right) \right] ,$$

and its corresponding average value

$$\bar{P}_{co \text{ coded}} = \int_{q_2=q_{minu}}^{q_{uo}} P_{co \text{ coded}} \cdot f(q_2) dq_2 . \quad (4.2.2-1)$$

6 CONCLUSION AND IDENTIFICATION OF FUTURE WORK

In this work a complex stochastic model for the meteor burst channel was used to serve as the bedrock for the analysis of two different communication systems. The first system assumed we are transmitting with a constant bit rate while the BER is time varying yet constrained to be below some maximum level. The second communications system employs a variable bit rate whose adaptive behavior is controlled so as to maintain constant BER. Both systems operate under the control of a communication feedback protocol that provides knowledge of channel arrival (the instant at which the channel first becomes available) and monitor the strength (power received) of the channel. The research herein focused on throughput and related parameters. The average throughput was shown to depend upon the arrival rate of the bursts and the expected number of bits per burst as averaged over the ensemble of (random) time functions that describe its behavior. In deriving the expressions for the above it was necessary to derive the relationship between the number of bits per given burst and bit rate. This in turn requires understanding of channel duration - the available transmission time - for a given channel (burst).

For constant bit rate system the channel duration decreases with increasing bit rate. Since the number of bits transmitted on the burst is given by the product of burst duration and bit rate a clear tradeoff exists between bit rate and transmission time. This, naturally, implies the existence of an optimal bit rate that would maximize the number of transmitted bits for the burst. Having chosen an optimal bit rate for the burst at hand we must repeat the process for the next burst whose behavior is different. In fact, to optimize the throughput we must change the bit rate from one burst to the next. Having to change the bit rate on a per burst basis, however, requires knowledge of the burst time behavior. The problem with this last requirement is twofold; first, a priori knowledge of the burst is not available and second, estimation of the burst based on assumed ideal behavior is unreliable since the bursts often deviate from such assumed behavior. To counter this limitation we derived the relationship between the constant bit rate and the expected average number of bits per burst since the latter is directly proportional to throughput. We then find the constant bit rate (for the system) which will maximize the throughput. This bit rate is fixed over all bursts and therefore it is a system-optimal bit rate. Having found the maximum average number of bits per burst we multiply by the arrival rate of burst and get the maximum throughput expression in terms of system

parameters and constraints. The significance of such expression is its utility in analyzing/improving existing systems and in designing future constant bit rate meteor burst systems.

In variable bit rate systems we change the bit duration (on a bit by bit basis) so the bit energy remains constant corresponding to our desired fixed BER. The bit energy is given by the time integral of the power received function over the duration of the bit. Finding the individual bit durations is tantamount to dividing the power received curve into equal strips each of area equal to the bit energy. As discussed earlier a priori knowledge of the burst time function is not available and estimation is at best problematic. This precludes exact solution of the bit duration. The best we can do is determine the bit duration based on the bit power at the beginning time of the bit. This may yield an optimistic (too short) bit duration if the power decays during the duration of the bit. The energy per bit for such a case would be below the desired fixed one. If the power is monotonically decreasing there will be a bit whose bit energy relative to the assumed bit energy will be unacceptable. The restriction on maximum bit duration in turn constrains theoretically yet not practically, as has been shown, the total time of transmission for the burst. The number of bits transmitted during a burst can be approximated by the area under the power received for the interval given by transmission time. The throughput is found by multiplying the arrival rate by the average number of bits per burst.

As it turns out the throughput for variable rate system is about six dB higher for a conservative sample system. The interesting point however is the fact that the improvement of throughput for variable over constant bit rate system (using underdense bursts only) was in large part due to the arrival rate. For constant bit rate system the high optimal bit rate precluded many bursts (those with electron line density below the minimum line density threshold) from being useful resulting in a low arrival rate. For variable rate systems since the bit rate can be quite low (though limited) implies a lower level of cutoff for useful bursts and higher arrival rate. The tradeoff lies in the fact that a low threshold rate for the adaptive rate increase system complexity.

The improvement in throughput however must be kept in perspective. Our analysis assumed that the constant BER under variable rate system is same as the worst BER for the constant bit rate system. Consequently, given N transmitted bits the probability of all being error free is lower for the constant bit rate than for the variable bit rate system.

The higher throughput for overdense relative to underdense bursts is a natural outcome of its longer average burst duration. The tradeoff, however, is in the much longer inter-arrival time of the overdense bursts compared with underdense; a ratio of 15:1. We see then that for short urgent messages where waiting time is crucial if we are given a constant bit rate system it is advantageous to operate the system at the optimal rate corresponding to underdense burst utilization.

Two transmission protocols were investigated in automatic-repeat-request strategy: stop-and-wait, when one data packet is transmitted per burst, and selective-repeat, when entire duration of the burst is used for transmission.

Fig. 23 shows the throughput rate for stop-and-wait strategy as a function of packet length, for the uncoded case and rate $1/2$, $3/4$, $7/8$, and $15/16$ convolutional codes. In coded as well as in uncoded transmission there exists an optimum packet length for a given data rate. Improvement in throughput is obtained in the coded case, but only for code rates close to 1. High rate convolutional codes are less powerful than low rate ones, but they do not excessively increase the original packet length and still can correct some of the transmission errors. Low rate codes are at disadvantage because of the strong limiting factor of relatively short burst durations. Fig. 24 shows the waiting times necessary to receive a specific data packet correctly. For a given packet length there always exists an optimum data rate, in coded and in uncoded transmission. High rate codes yield lower waiting times with respect to uncoded case for all data rates, and with respect to high rate codes at low data rates when throughput is at its maximum. Low rate codes show better performance in terms of minimizing the waiting time at higher data rates, but then the throughput becomes prohibitively low.

Throughput performance for selective-repeat strategy is summarized in Fig. 25. Here again high rate codes are superior to low rate ones and to uncoded case. There is no optimum packet length and short packets yield higher throughputs, with the ultimate maximum obtained for packet length of 1 bit. The practical lower limit on the packet length is imposed by necessary overhead bits and user considerations.

In this analysis many parameters considerations and variables interplay. Amongst them complexity of model, empirical values, transmitter power antenna design link geometry and geographic location, frequency, noise behavior modulation bit rate and BER. All of the above have been integrated and the derived closed-form relationships are stated in the most general form incorporating all possible variables to facilitate their usage as design and analysis tools. Furthermore, these expressions define and better delineate the tasks for future analysis.

Some of the issues that need be investigated are coding, packet design, modulation protocol development and networking. Each of these requires extensive research and, clearly, there is no 'ultimate' meteor burst system but rather application dependent design. With faster and cheaper hardware for control and storage and renewed focus on this complex channel it is clear that we are in the exciting phase of using this natural phenomenon for communication.

7 TABLES

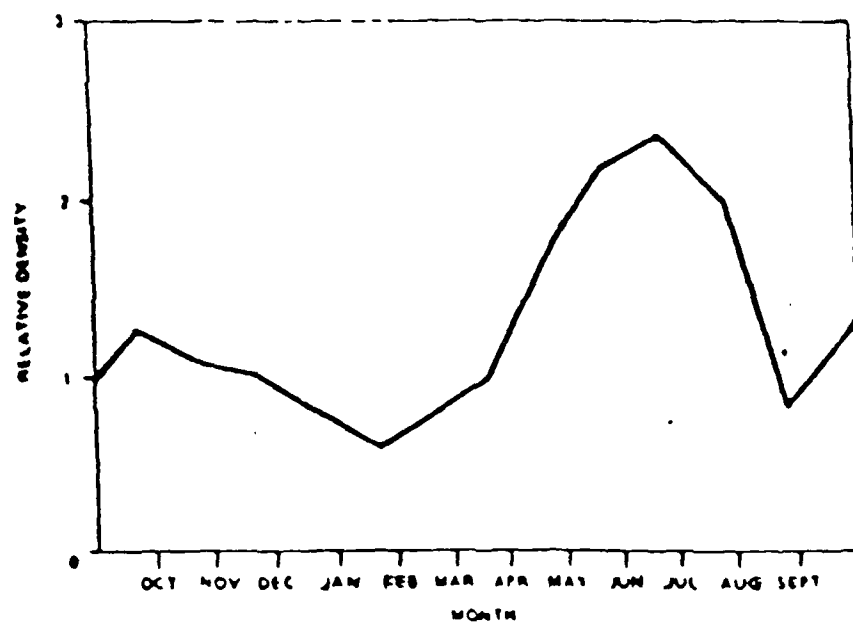
Table 1 — Order-of-Magnitude Estimates of the Properties of Sporadic Meteors [1]

Meteor Particles	Mass (g)	Radius	Number of This Mass or Greater Swept Up by the Earth Each Day	Electron Line Density (electrons per meter of trail length)
Particles pass through the atmosphere and fall to the ground	10^4	8 cm	10	—
Particles totally disintegrated in the upper atmosphere	10^3 10^2 10 1 10^{-1} 10^{-2} 10^{-3} 10^{-4} 10^{-5}	4 cm 2 cm 0.8 cm 0.4 cm 0.2 cm 0.08 cm 0.04 cm 0.02 cm 80 μ m	10^2 10^3 10^4 10^5 10^6 10^7 10^8 10^9 10^{10}	— — 10^{18} 10^{17} 10^{16} 10^{15} 10^{14} 10^{13} 10^{12}
Approximate limit of radar measurements	10^{-6} 10^{-7} 10^{-8}	40 μ m 20 μ m 8 μ m	10^{11} 10^{12} ?	10^{11} 10^{10} ?
Micrometeorities (Particles float down unchanged by atmospheric collisions)	10^{-9} 10^{-10} 10^{-11} 10^{-12}	4 μ m 2 μ m 0.8 μ m 0.4 μ m	Total for this group estimated as high as 10^{20}	Practically none
Particles removed from the solar system by radiation pressure	10^{-13} —	0.2 μ m —	— —	— —

Table 2
AVERAGE INTERVAL BETWEEN BURSTS FOR THE
COMET SYSTEM

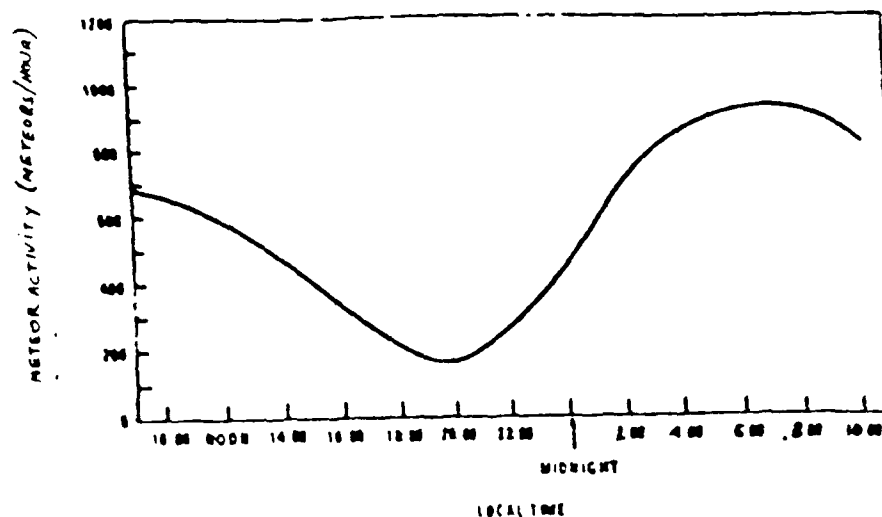
TIME OF DAY	JULY MAX	FEBRUARY min	YEARLY AVERAGE
4 AM MAX ACTIVITY	2.5 s	6.25 s	4 s
6 PM min ACTIVITY	25 s	16.67 s	20 s

8 FIGURES

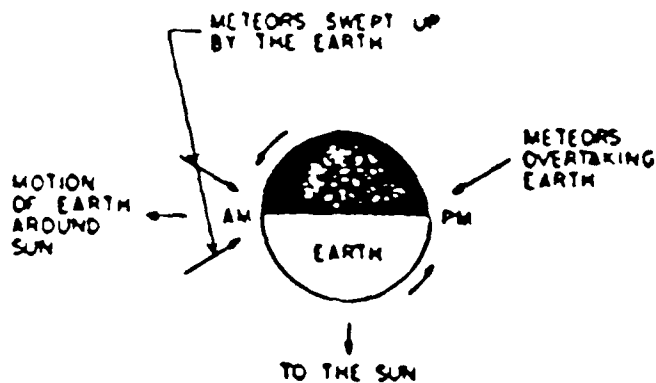


Variation in the space density of meteors along the Earth's orbit (reproduced from *Monthly Notices of the Royal Astronomical Society*, vol 116, by permission of The Royal Astronomical Society and G S Hawkins).

FIGURE 1

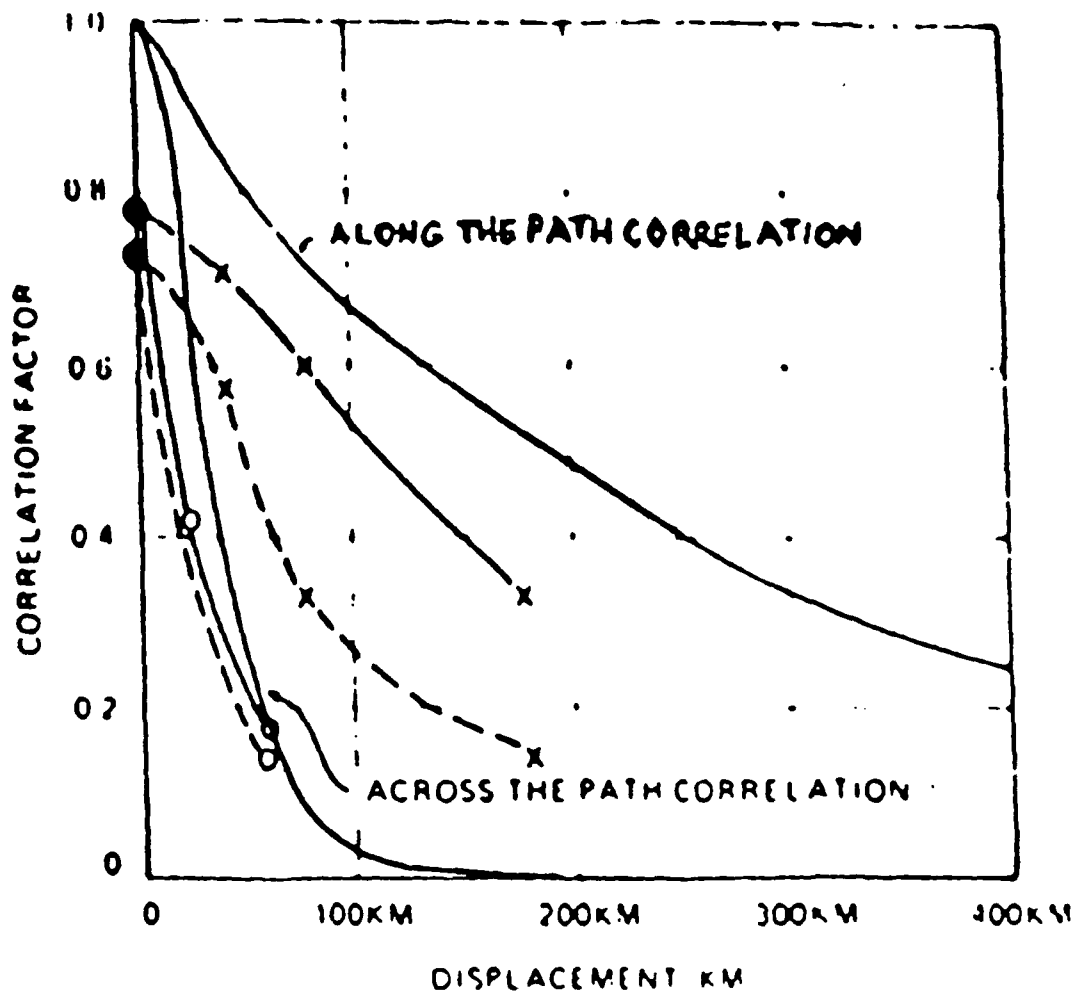


Diurnal variations in meteor activity.



— Diurnal variations of meteor rates. In the evening only meteors overtaking the earth are observed. In the morning meteors with orbital directions opposite to that of the earth and the slower ones with the same orbital direction are observed.

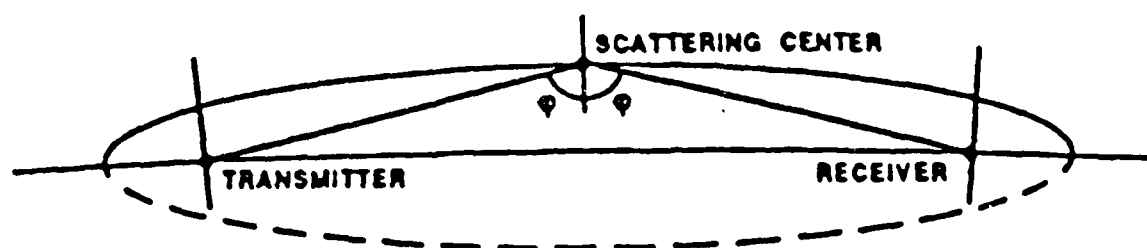
FIGURE 2



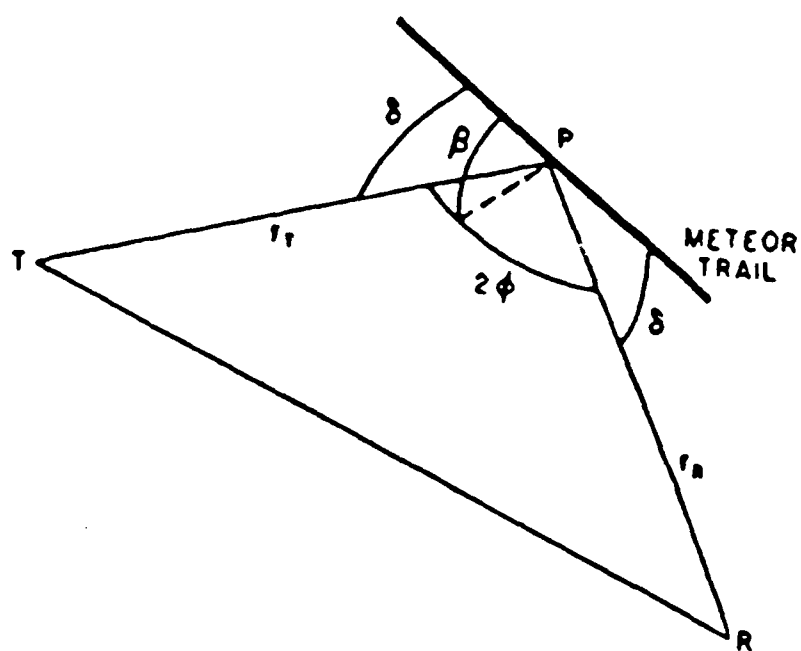
THEORY	—————	
EXPERIMENT (146 MHz)	ALONG THE PATH	· — · — ·
	ACROSS THE PATH	O — O — O
EXPERIMENT (192 MHz)	ALONG THE PATH	· - - - ·
	ACROSS THE PATH	O - - - O

Correlation patterns in the vicinity of a meteor burst receiver

FIGURE 3

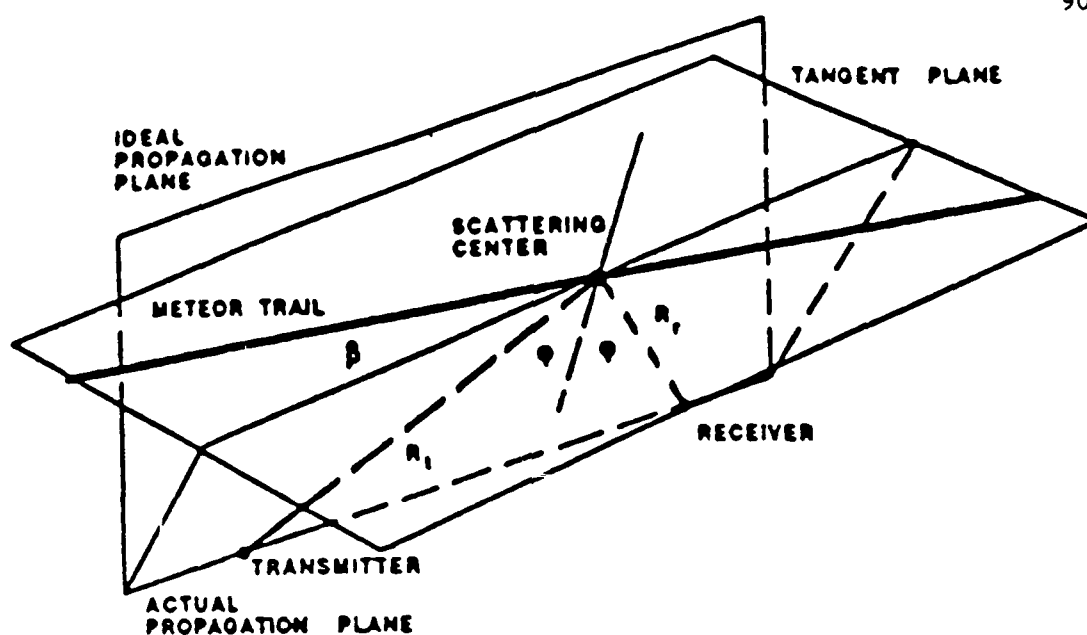


Link Geometry In the Ideal Propagation Plane

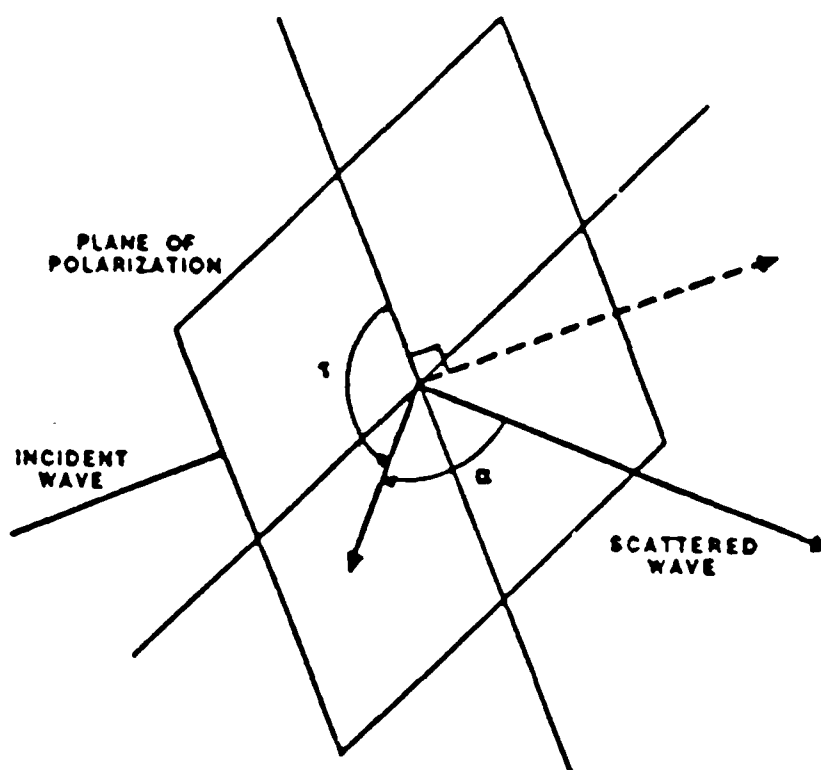


—Geometry of forward scattering from meteor trails.

FIGURE 4

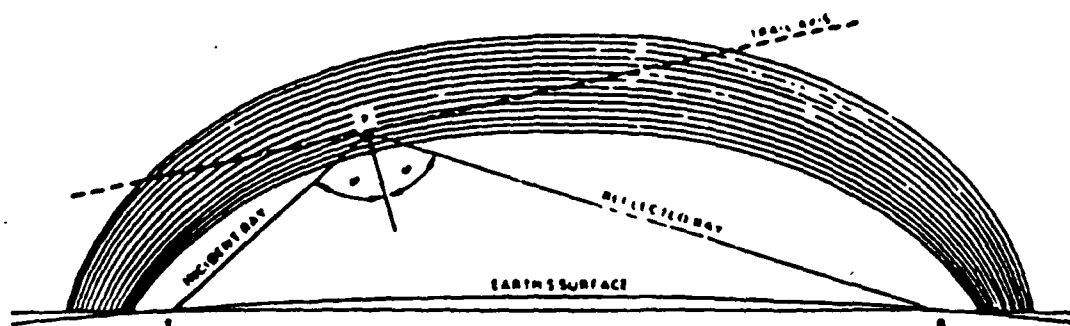


Meteor Scatter Communications Link Geometry



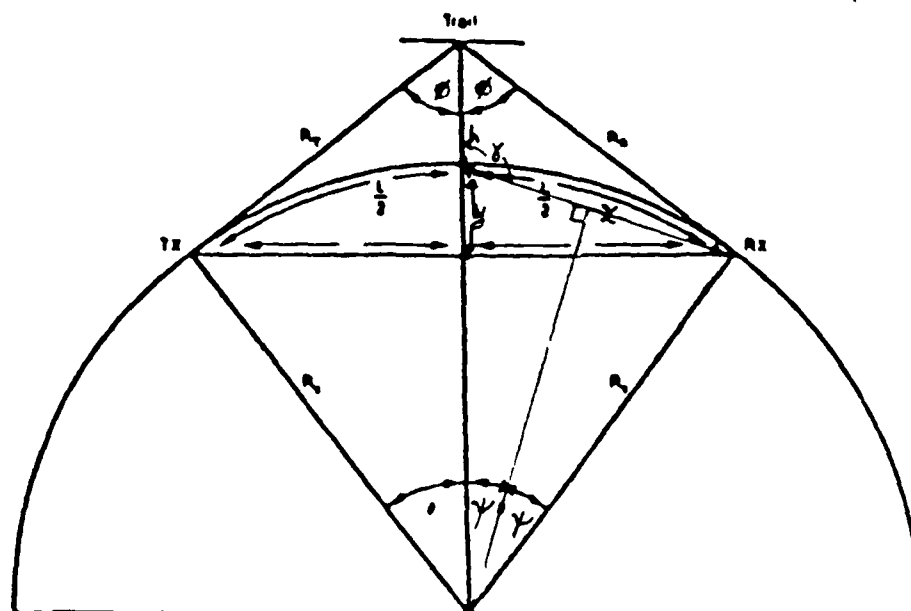
Polarization Geometry At Scattering Center

FIGURE 5



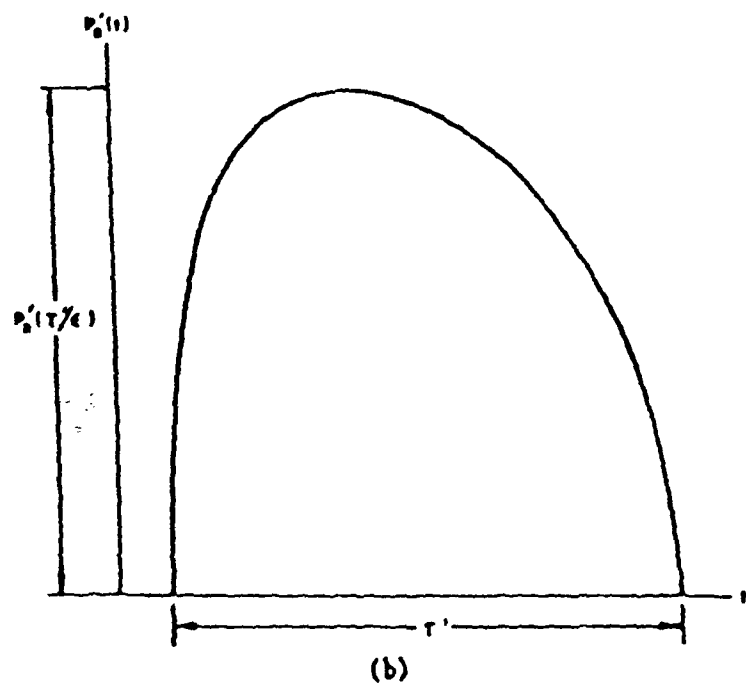
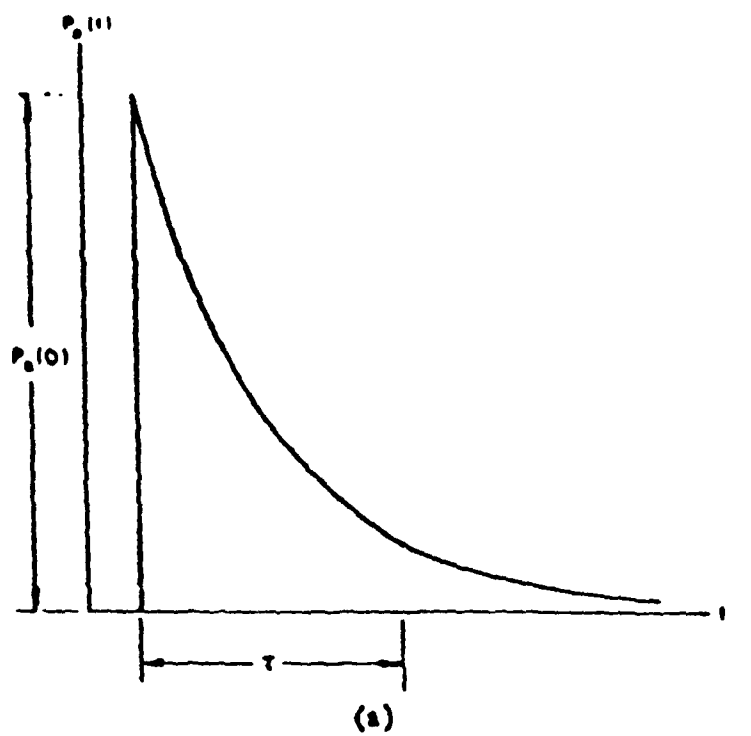
NOTE: NOTATION OF THE ELLIPSES GENERATES A FAMILY OF CONFOCAL PROLATE SPHEROIDS

Geometry of specular scattering from a meteor trail (reproduced from "The fine structure of meteor-burst signals," Tech. Memo. TM-36, Apr. 1962, by permission of the SRIAPL Technical Centre).



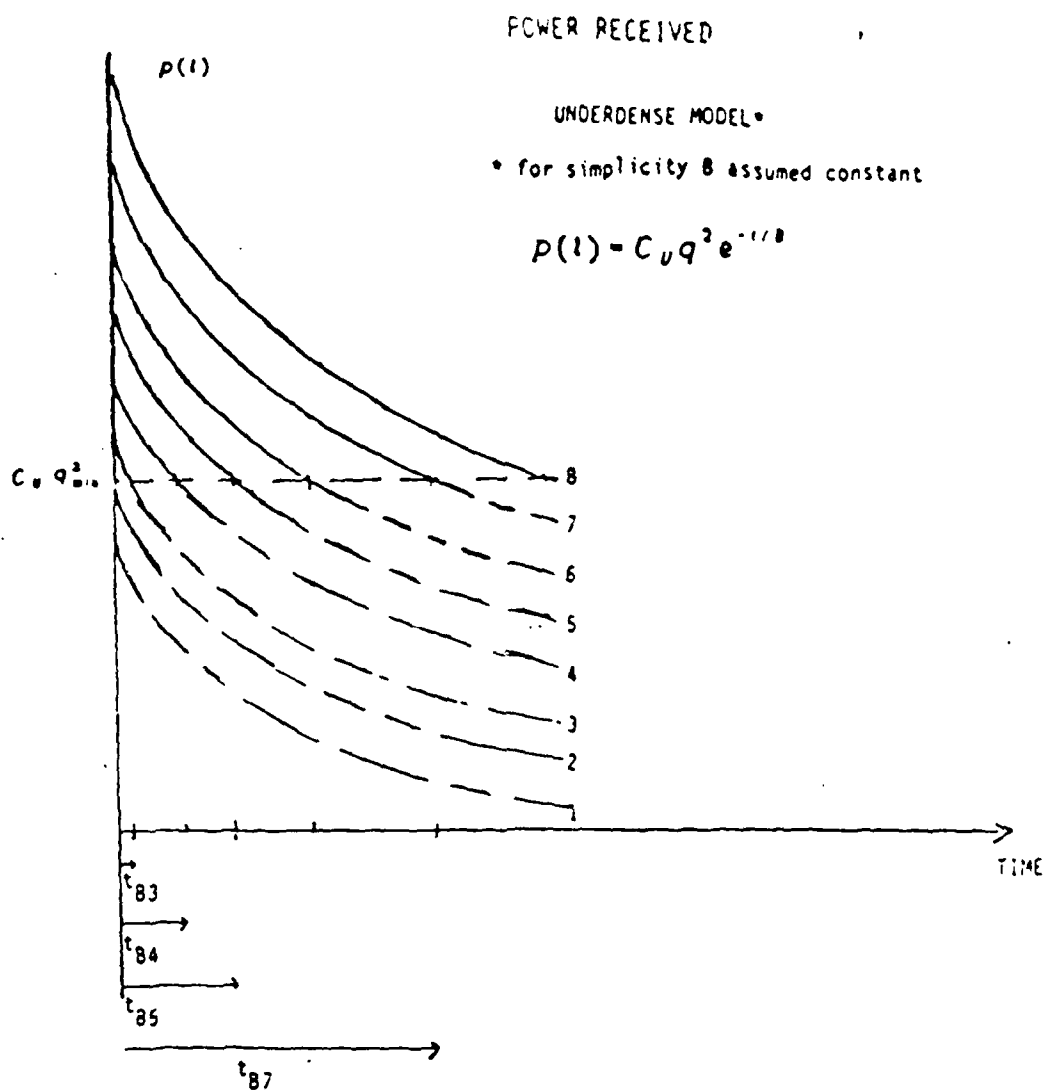
Meteor burst geometry. A signal from TX is reflected to RX by a trail that is h km above the earth. TX and RX are separated by a great circle distance of L km.

FIGURE 6



—Idealized time variations in signals from (a) underdense and (b) overdense meteor trails.

FIGURE 7



C_U : Incorporates effects of transmitter power, antenna gains, link geometry, noise, ...

q : Electron line density (random) $q_L < q < q_U$

B : Decay time constant (random)

t_B : Channel "duration" ($P > P_{min}$ for $t < t_B$)

--- no transmission

P_{min} : Arbitrary, corresponds to max allowed BER, e.g. 10 dB

FIGURE 8

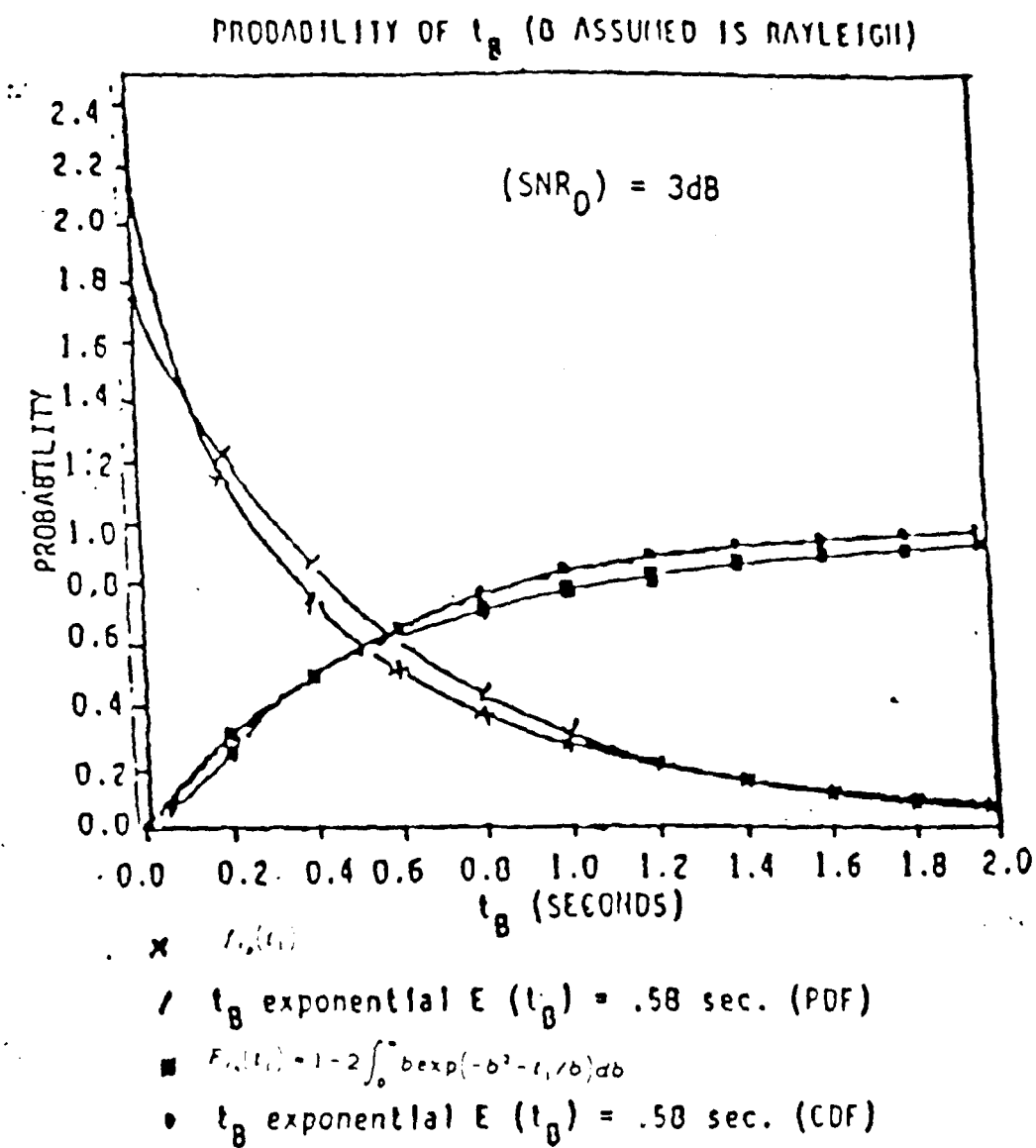
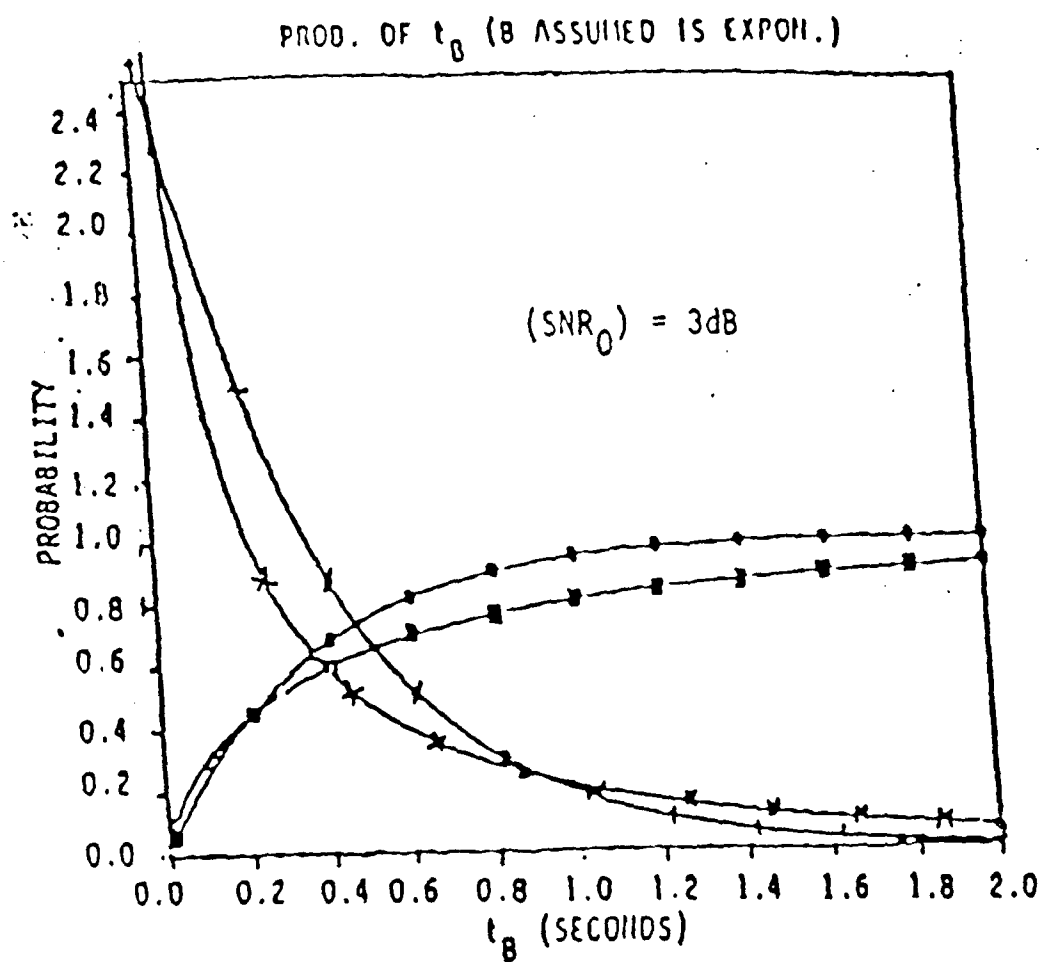
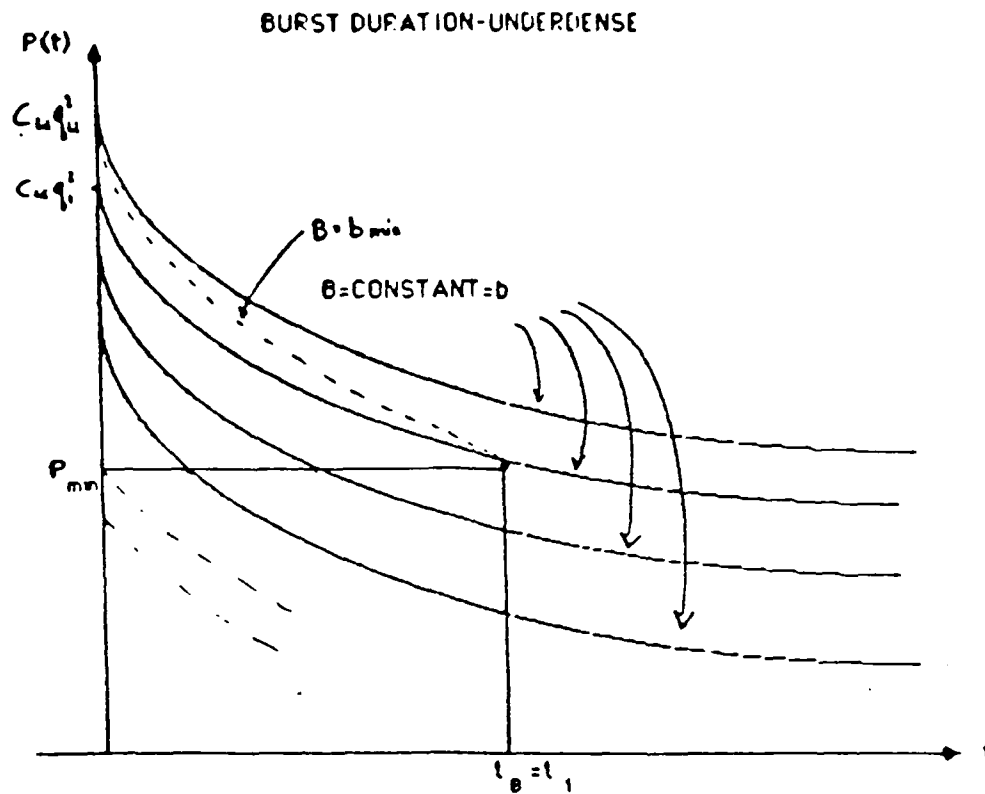


FIGURE 9



- × $f_{t_0}(t_1) = 2 \frac{\rho}{B} K_0(z)$
- + t_B exponential $\mathcal{E}(t_0) = 0.377$ sec. (PDF)
- $F_{t_0}(t_1) = 1 - z K_1(z)$ where $z = \sqrt{4 \frac{\rho}{B} t_1}$
- t_B exponential $\mathcal{E}(t_0) = 0.377$ sec. (CDF)

FIGURE 10



$$P_{min} = R \cdot N_0 \cdot g^{-1}(P_{b,max}) \quad q_l = q_{min} \cdot e^{t_1/2b}$$

$$\text{Prob}\{t_B \leq t_1 \mid B=b\} = \begin{cases} 0 & b \leq b_{min} \\ \text{Prob}\{q \leq q_l\} & b > b_{min} \end{cases}$$

$$t_1 = B \cdot \ln\left(\frac{q}{q_{min}}\right)^2$$

$$q_{min} = \sqrt{\frac{P_{min}}{C_u}}$$

$$P_{min} = N_0 \cdot R \cdot g^{-1}(P_{b,max})$$

FIGURE 11

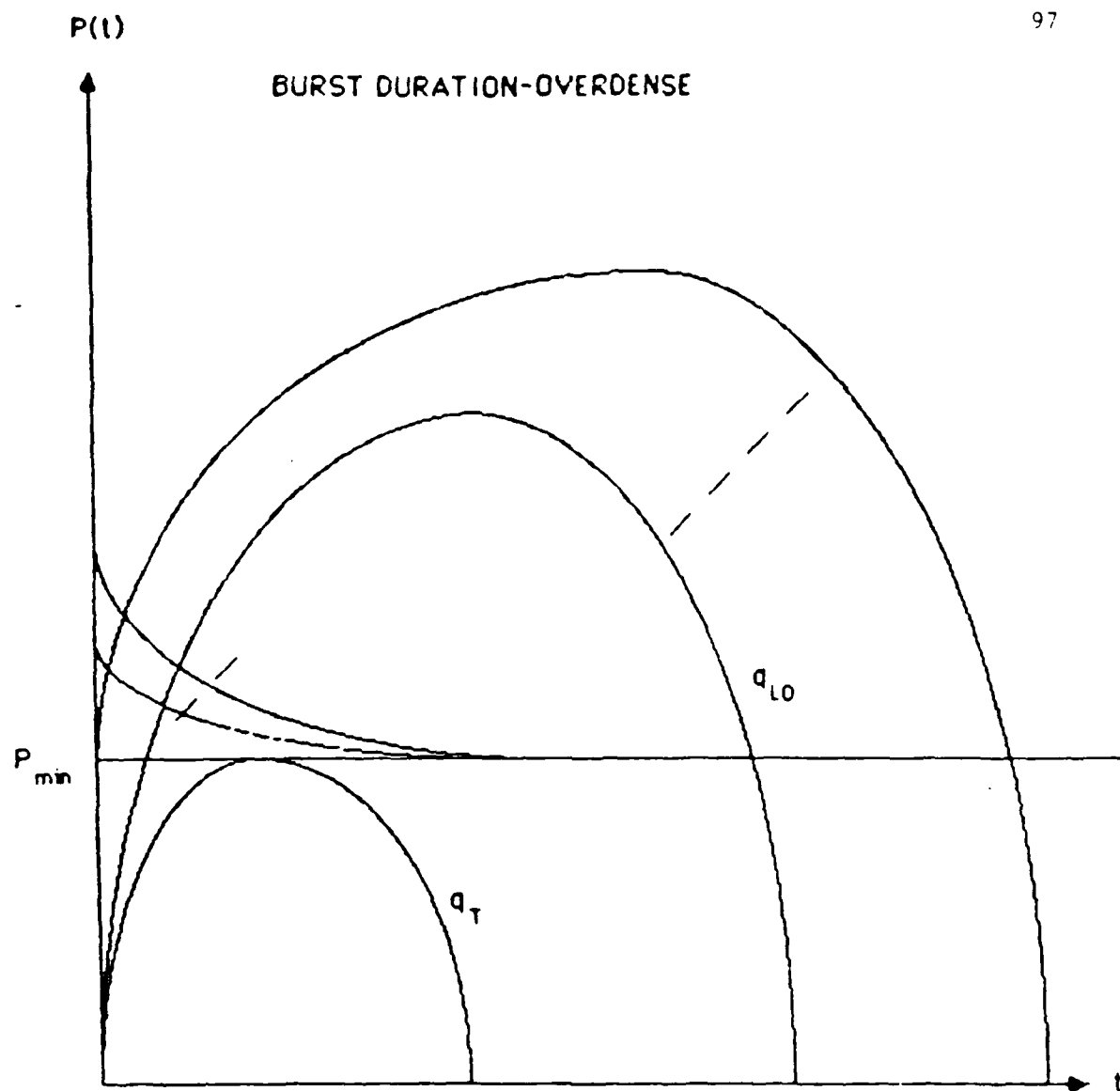


FIGURE 12

BITS PER GIVEN BURST

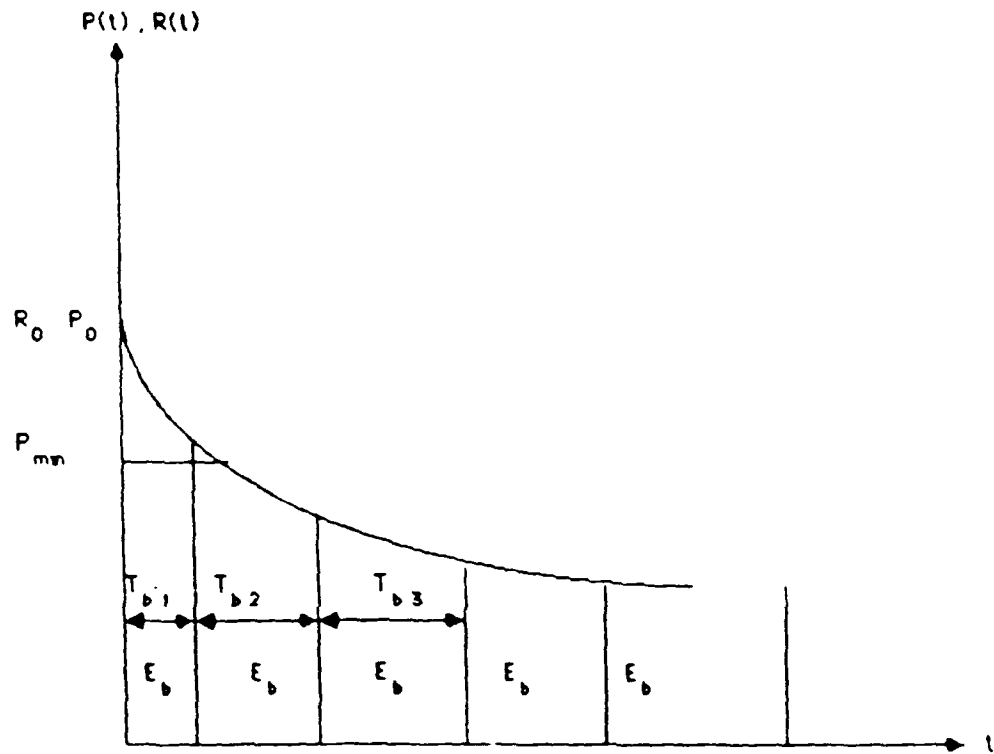


FIGURE 13

AVG. BURST DURATION - UNDERDENSE SAMPLE SYSTEM WITH FREQ=50MHZ

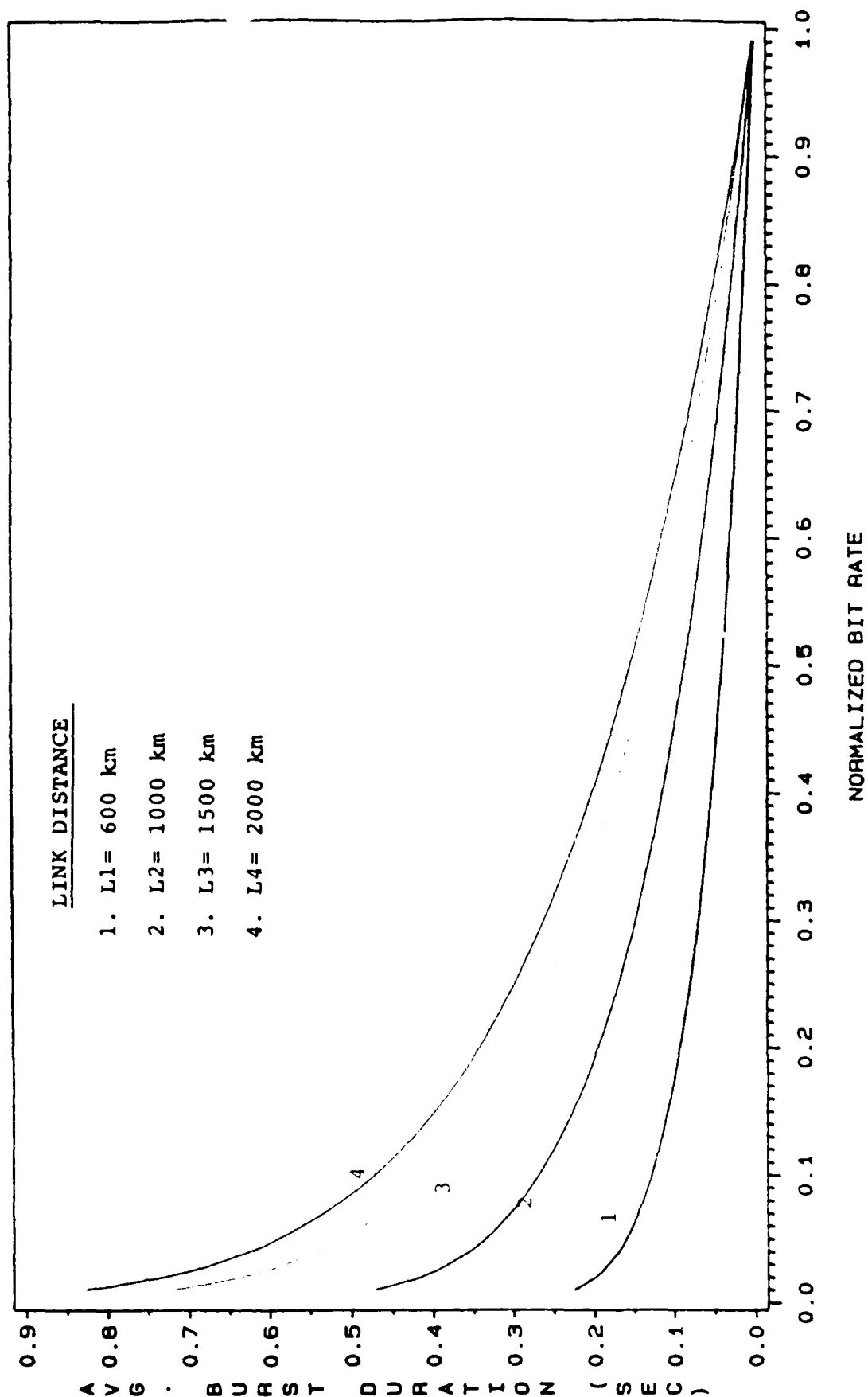


FIGURE 14

PDF FOR UNDERDENSE BURST DURATION SAMPLE SYSTEM WITH FREQ=50MHZ, LD=1000KM

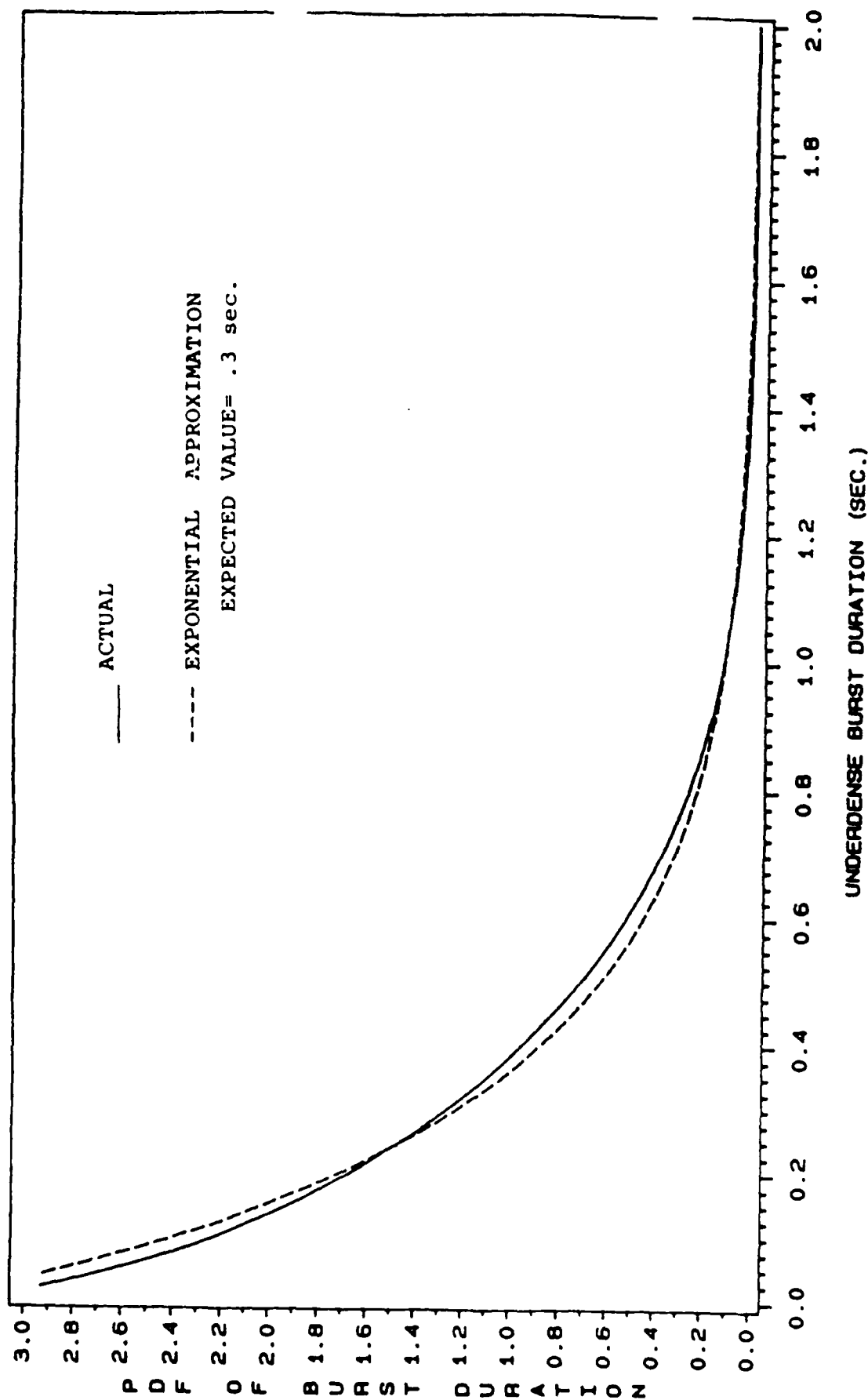


FIGURE 15

NORMALIZED THROUGHPUT – UNDERDENSE ANY SYSTEM

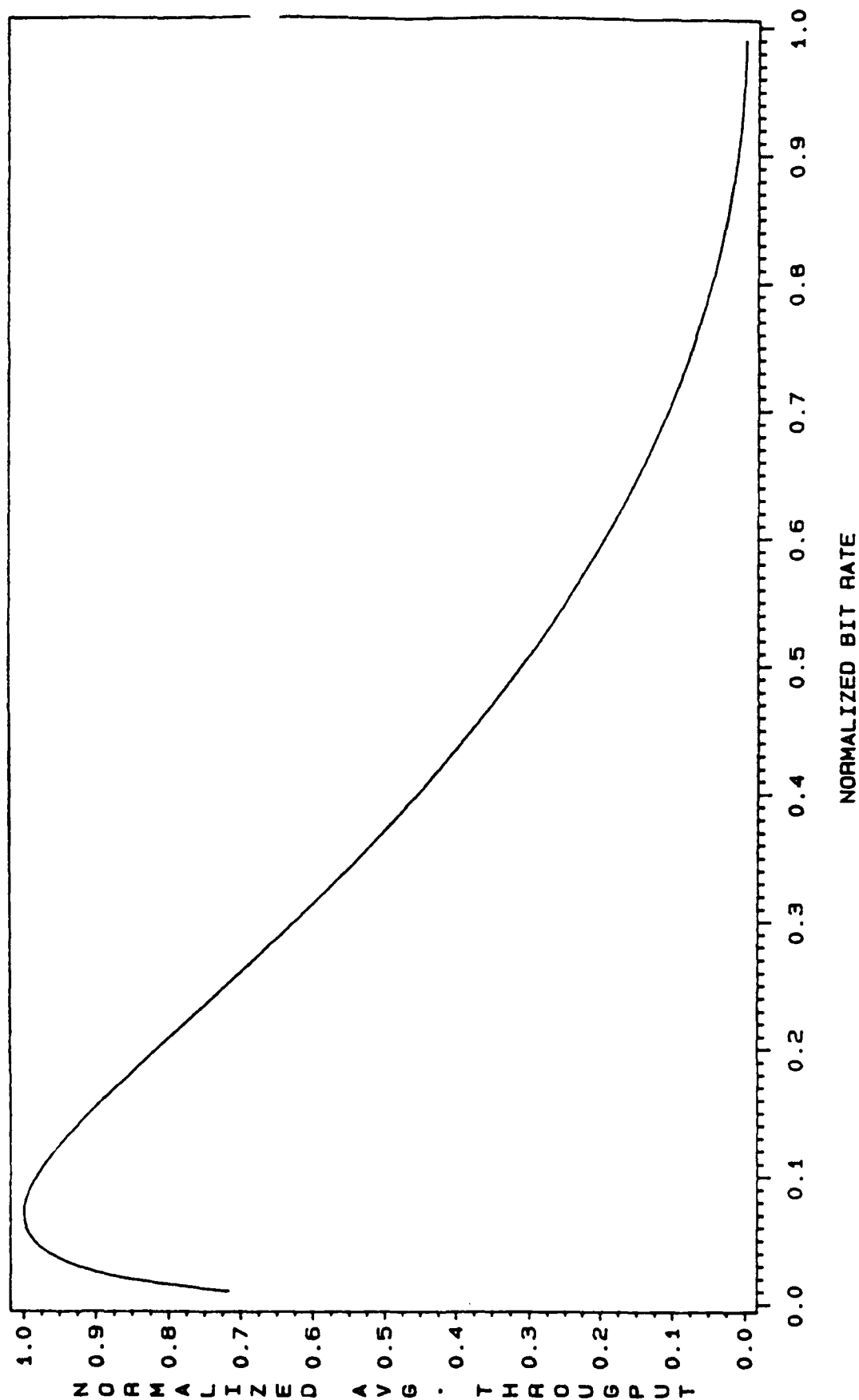


FIGURE 16

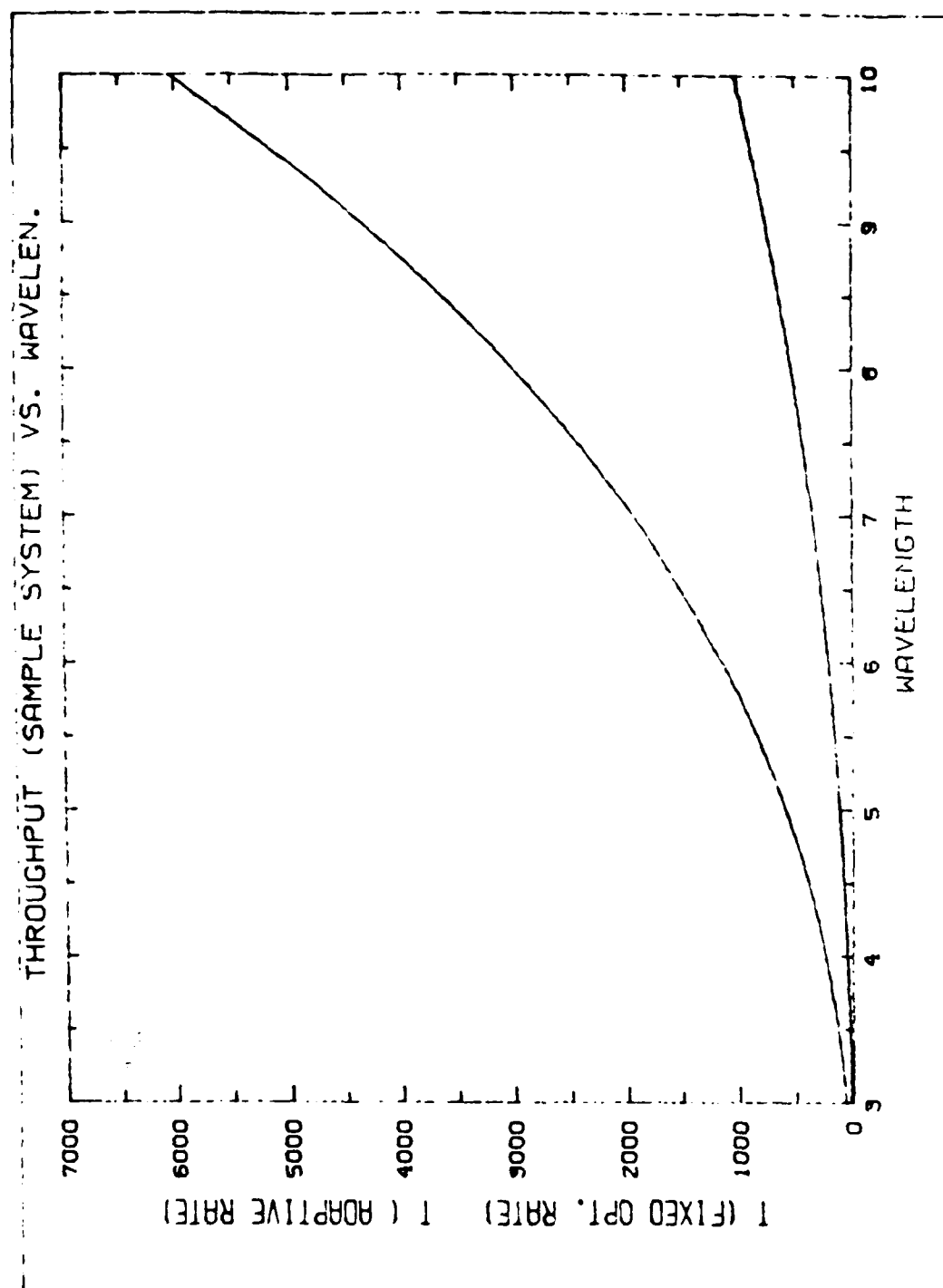


FIGURE 17

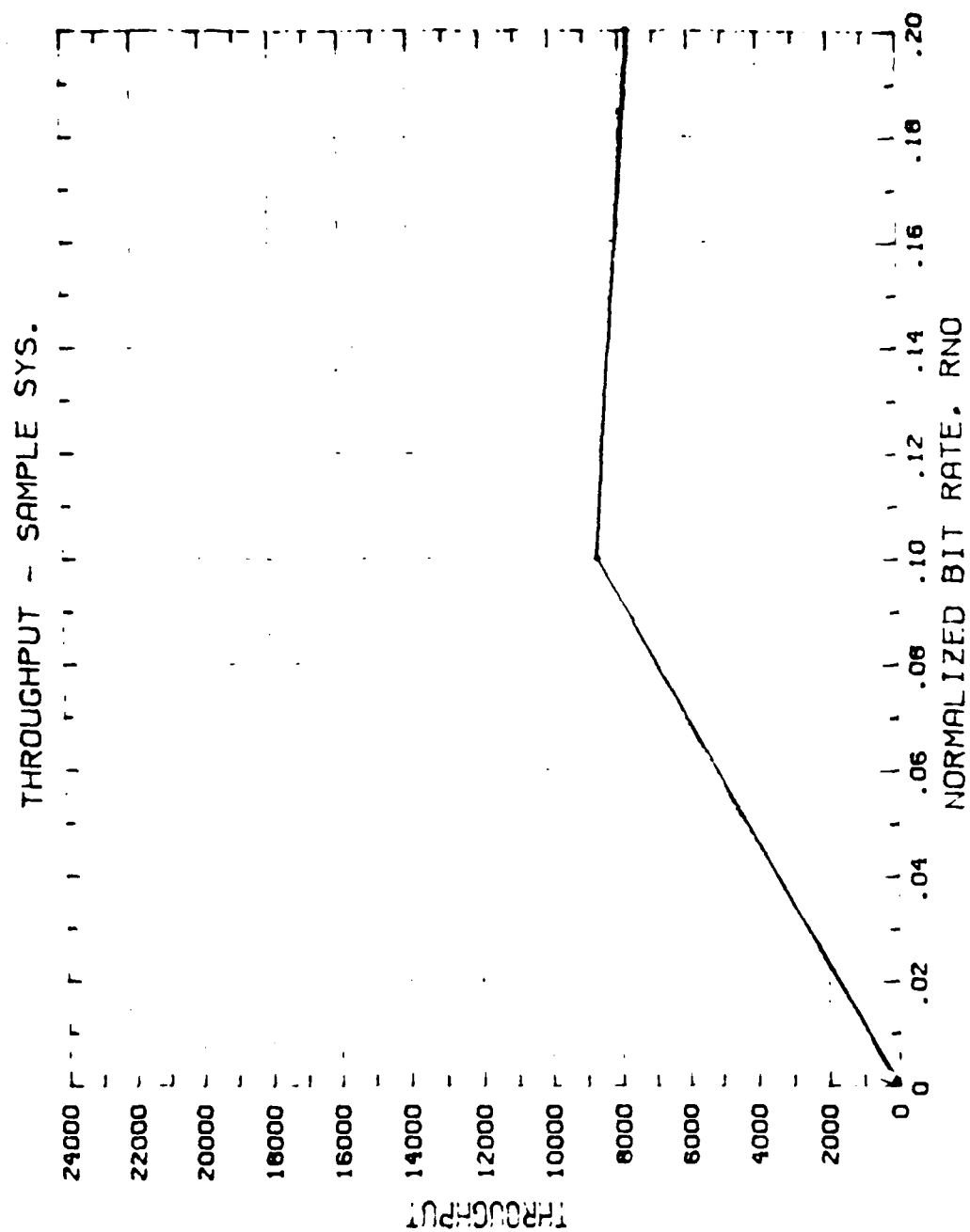


FIGURE 18

OPTIMAL CONSTANT BIT RATE SAMPLE SYSTEM UNDERDENSE

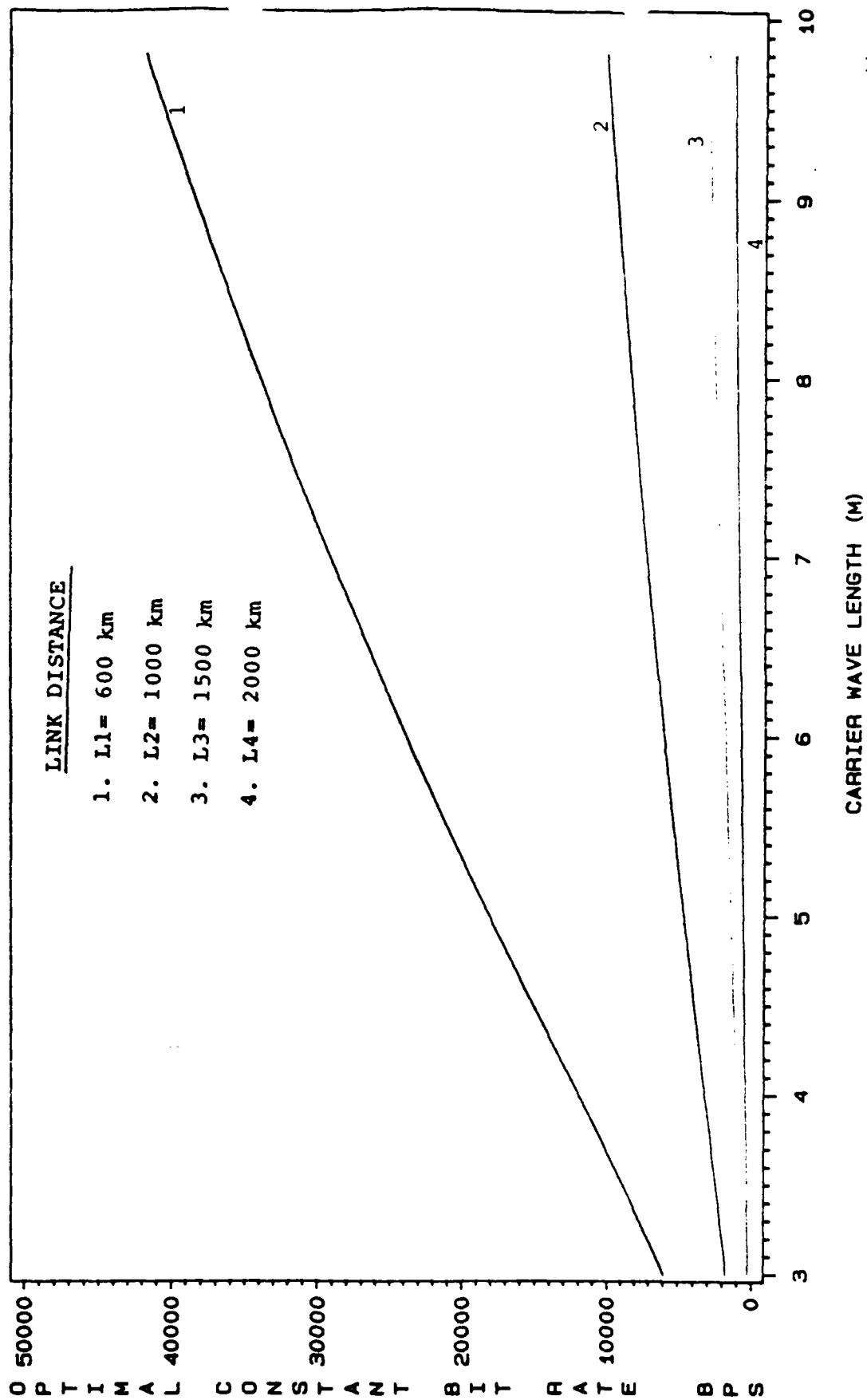


FIGURE 19

OPTIMAL CONSTANT BIT RATE SAMPLE SYSTEM

UNDERDENSE

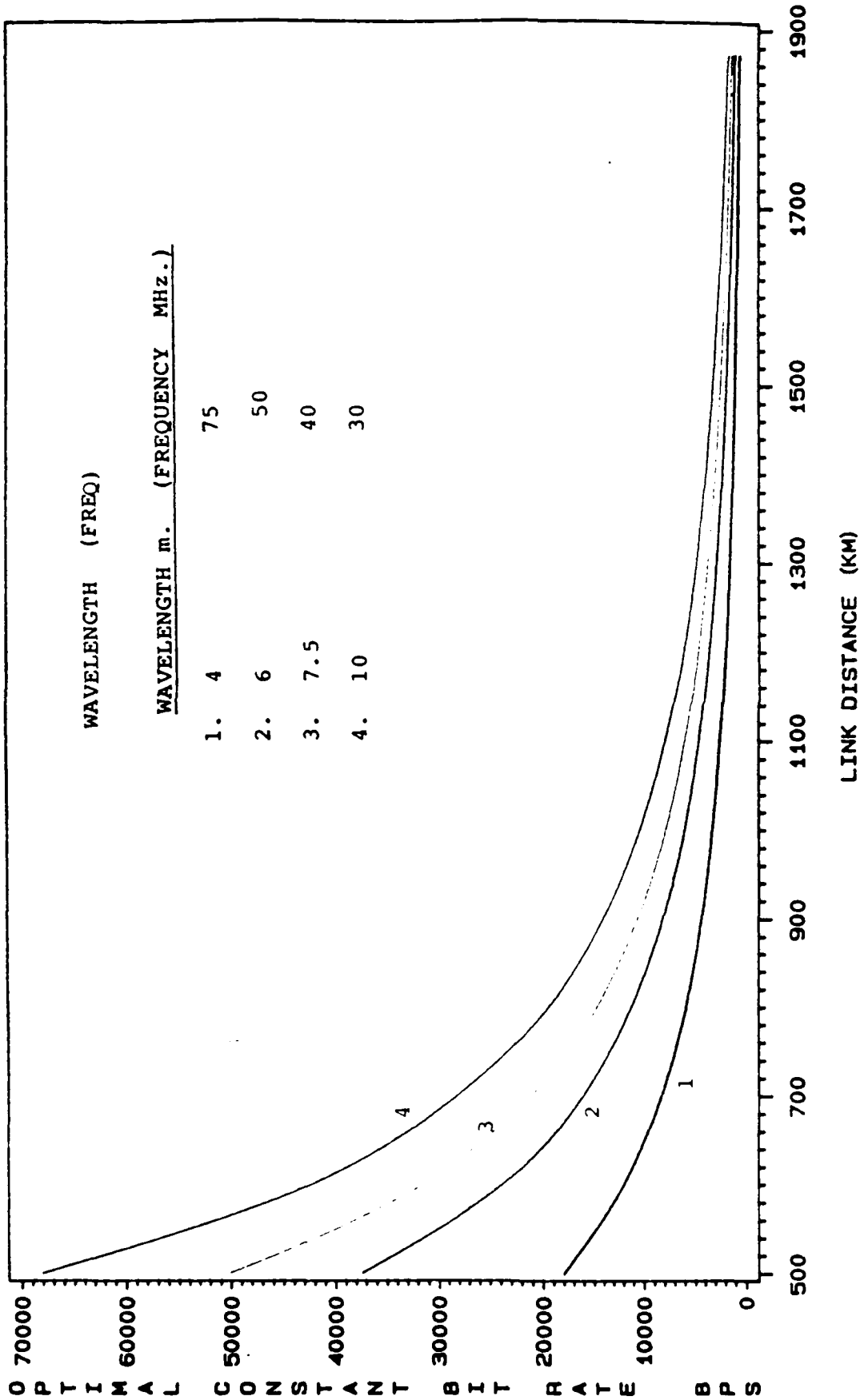


FIGURE 20

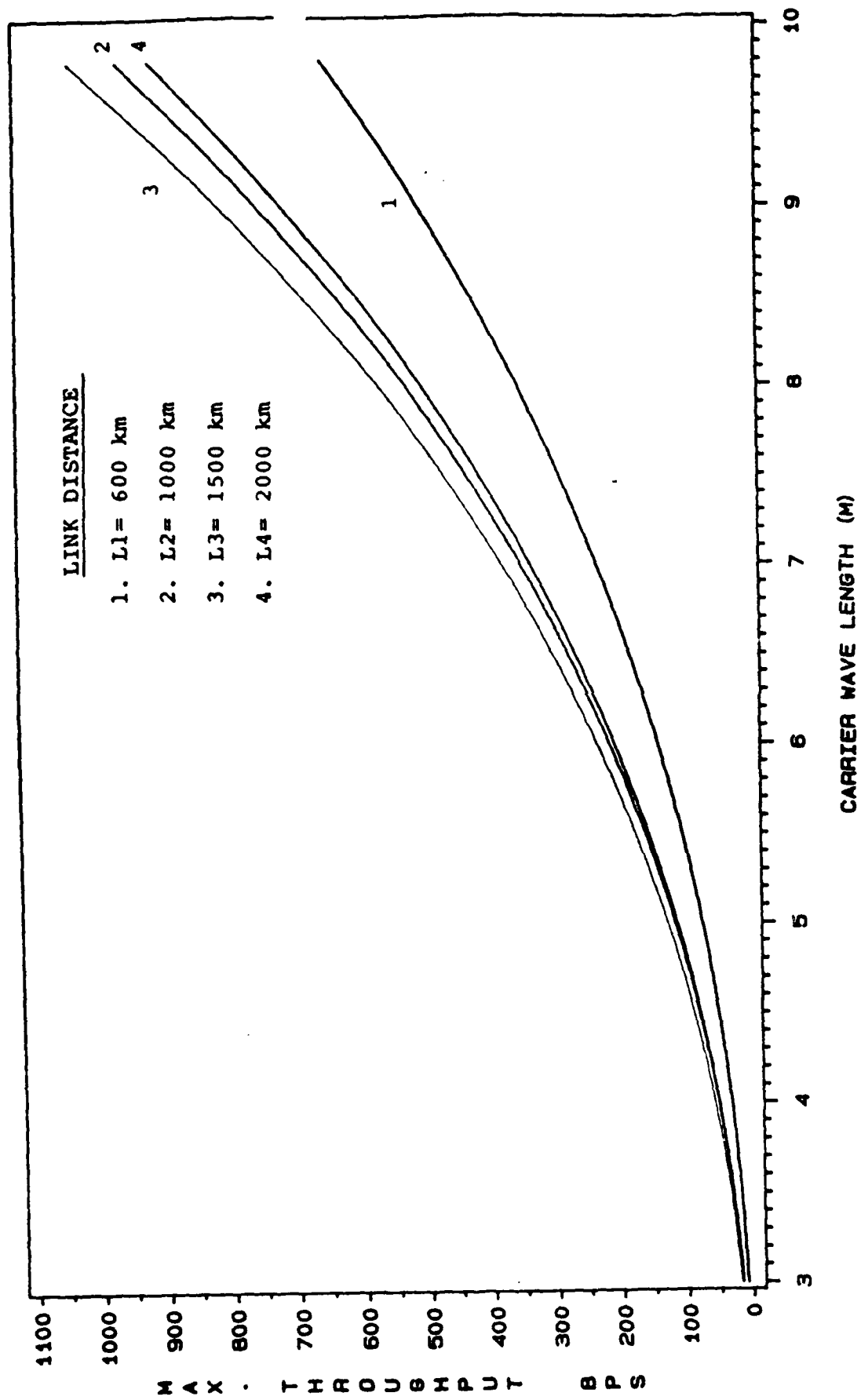


FIGURE 21

MAX. (AVG.) THROUGHPUT — UNDERDENSE SAMPLE SYSTEM

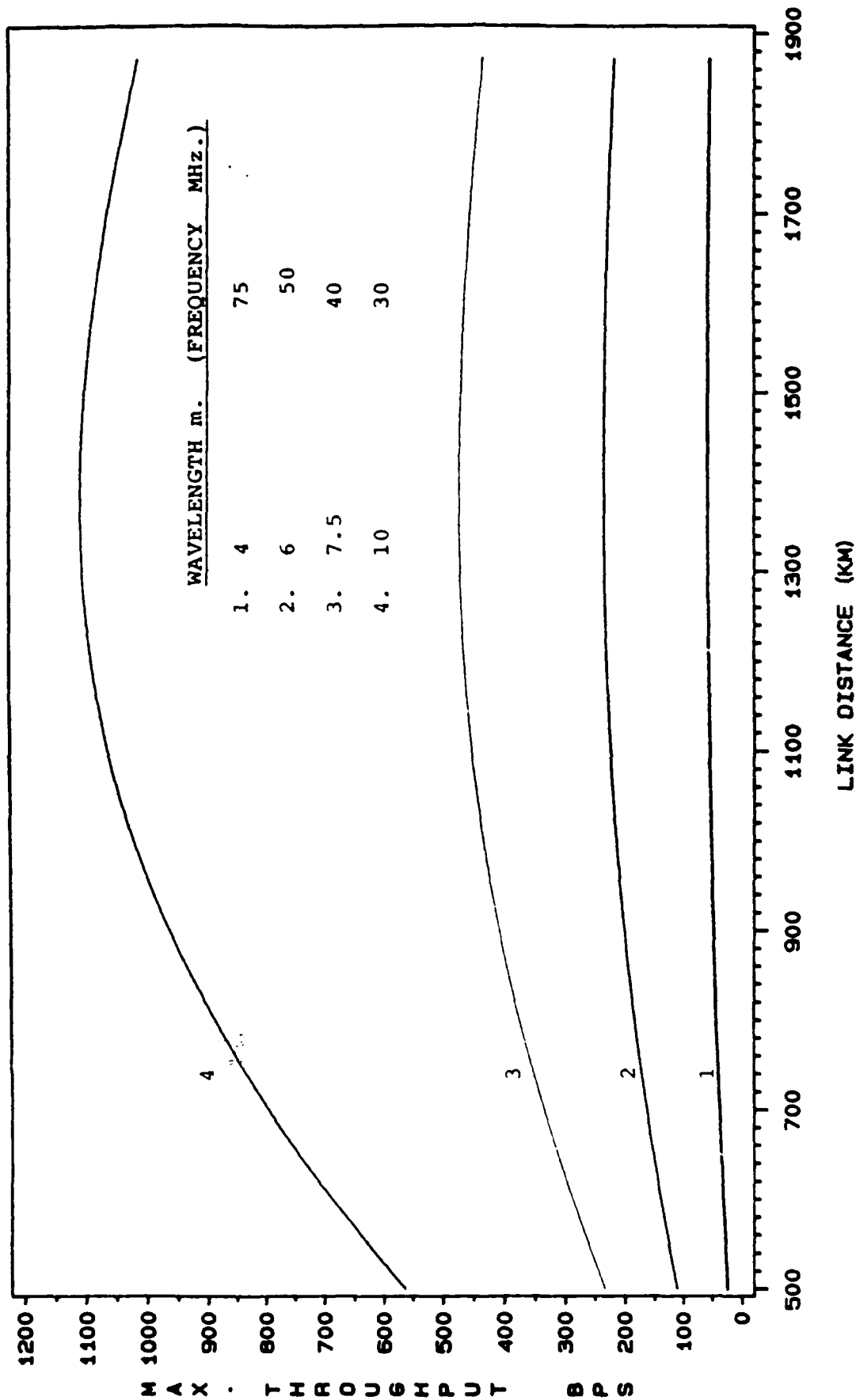


FIGURE 22

THROUGHPUT RATE
STOP-AND-WAIT STRATEGY
(DATA RATE $R = 1$ KBIT/SEC)

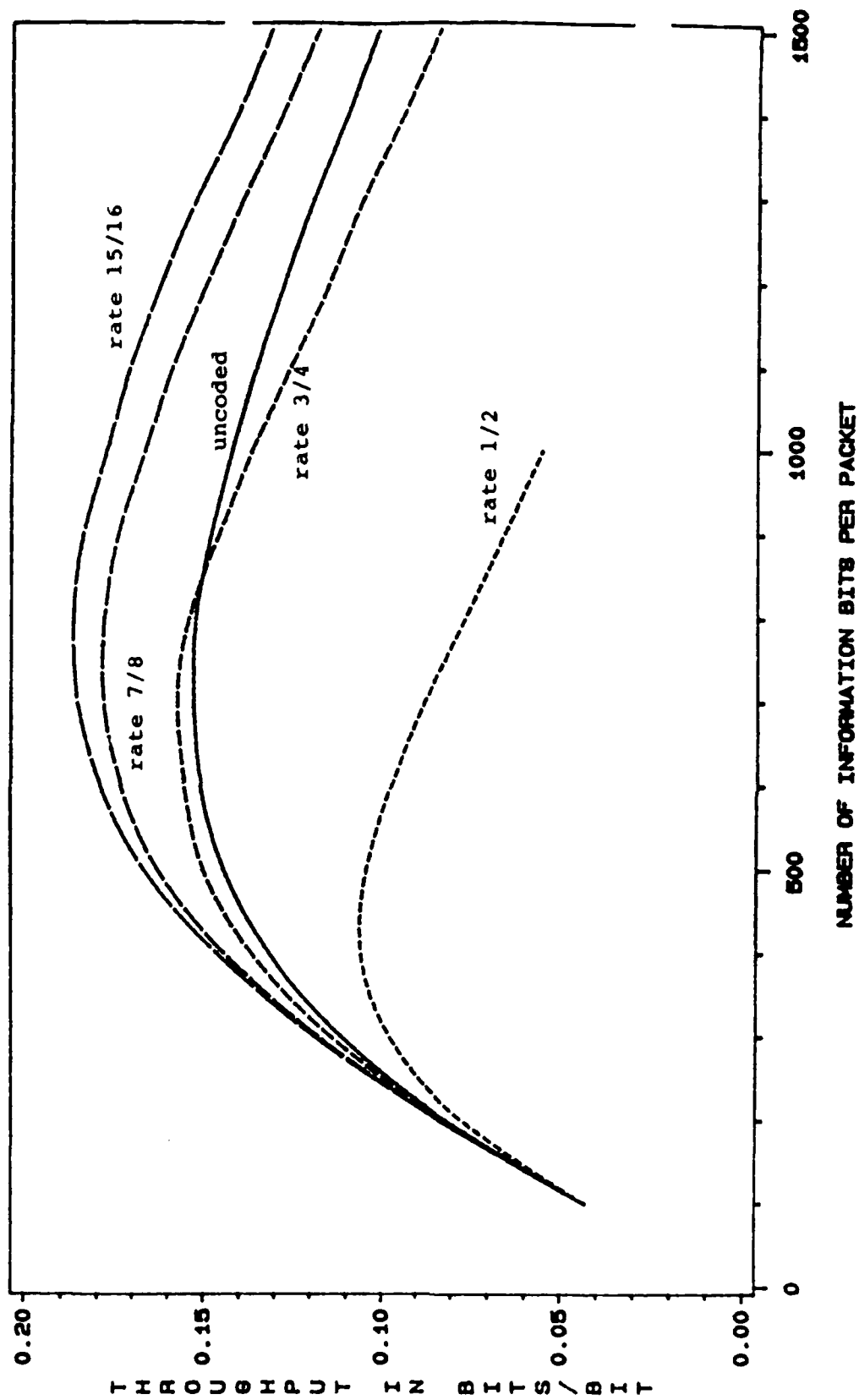


FIGURE 23

WAITING TIME TO RECEIVE A PACKET STOP-AND-WAIT STRATEGY (1000 INFORMATION BITS PER PACKET)

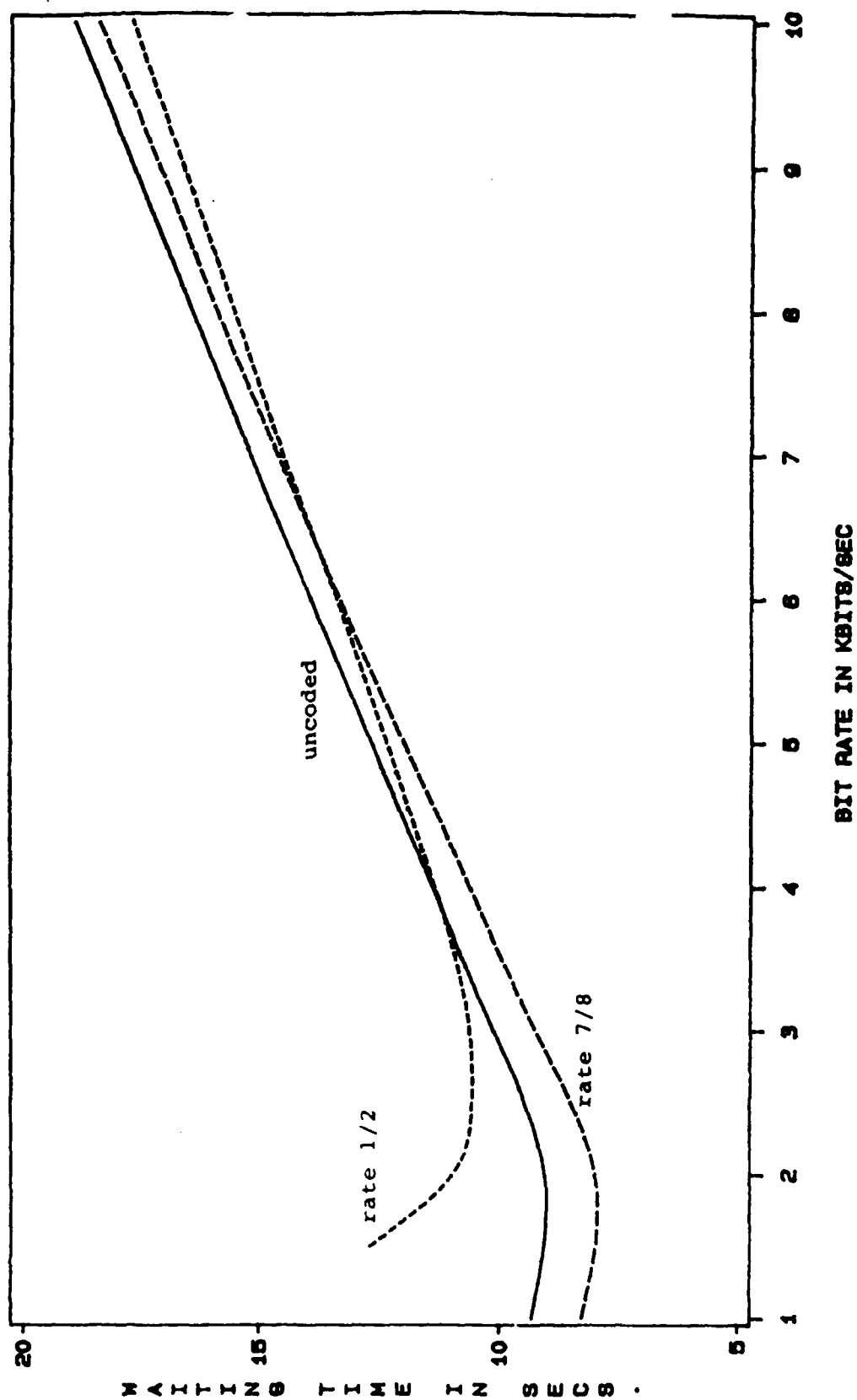


FIGURE 24

THROUGHPUT RATE
SELECTIVE-REPEAT STRATEGY
(BIT RATE 1 KBIT/SEC)

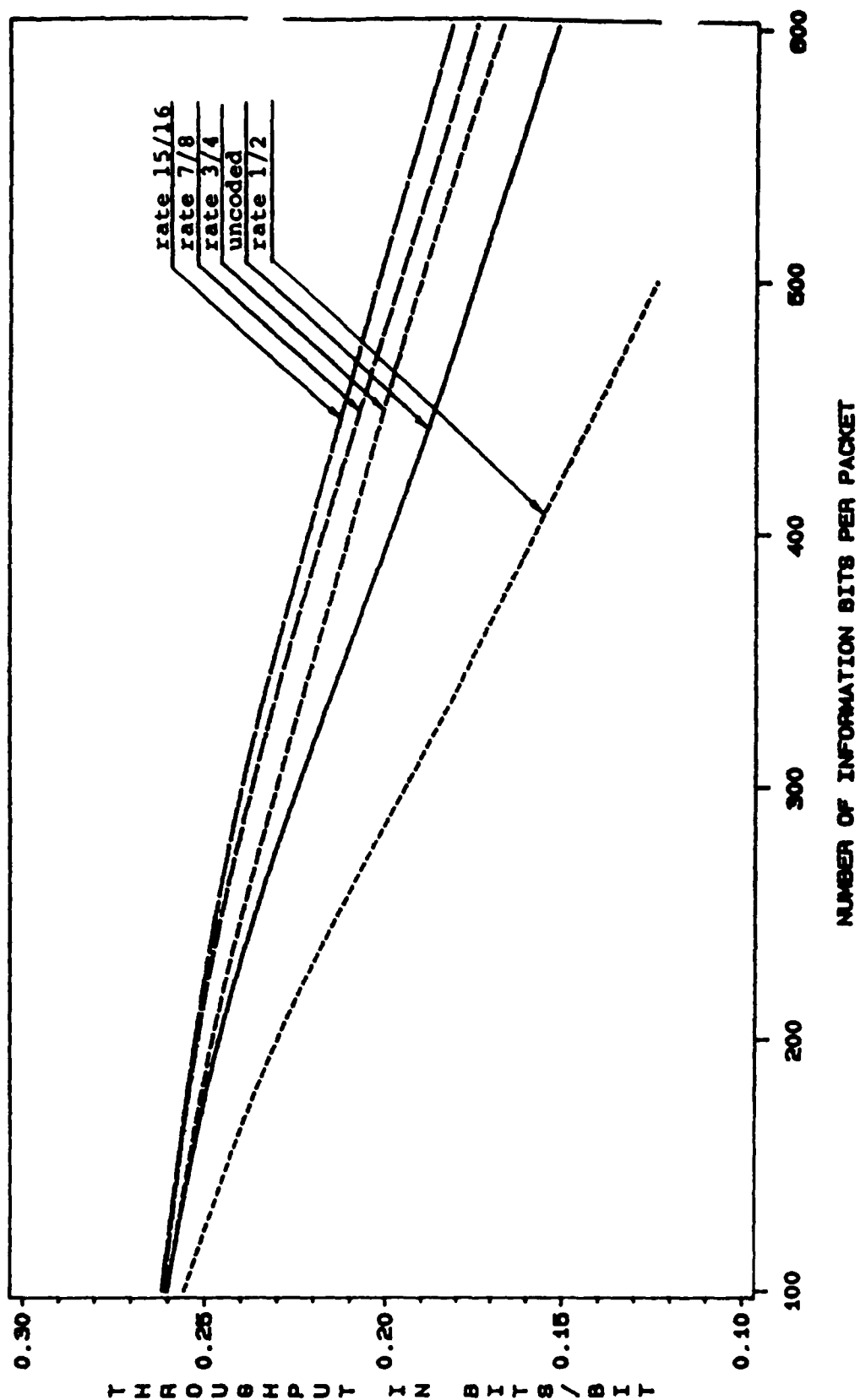


FIGURE 25

9 REFERENCES

- [1] G.R. Sugar, "Radio propagation by reflection from meteor trails," Proc. IEEE, vol. 52, pp 116-136, Feb. 1964.
- [2] V.R. Eshleman and R.F. Mlodnosky, "Directional characteristics of meteor propagation derived from radar measurements," Proc. IRE, Dec. 1957.
- [3] P.J. Bartholome, "Results of propagation and interception experiments on the STC meteor-burst link", "SHAPE Tech. Cen. The Hague, The Netherlands, TM-173, Dec. 1967.
- [4] P.A. Forsyth, E.L. Vogan, D.R. Hansen, and C.O. Hines, "The principles of JANET--A meteor-burst communications system," Proc. IRE, Dec. 1957.
- [5] P.J. Bartholome and I.M. Vogt, "Comet--A meteor-burst system incorporating ARQ and diversity reception," IEEE Trans. Commun. Technol., vol. COM-16, April 1968.
- [6] V.R. Eshleman and L.A. Manning "Radio Communications by Scattering from Meteoric Ionization", Proc IRE, Vol. 42, pp 530-536, March 1954.
- [7] A.E. Spezio, "Meteor burst communication system: Analysis and synthesis." NRL Rep. 8286, Dec. 28, 1978.
- [8] L.B. Milstein, D.L. Schilling, R.L. Pickholtz, J. Sellman, S. Davidovici, A. Pavelchek, A. Schneider, G. Eichmann, "Performance of Meteor Burst Communication Channels", to be published.
- [9] J.D. Oetting, "An analysis of meteor burst communications for military applications," IEEE Trans. Commun., vol. COM-28, pp. 1591-1601, Sept. 1980
- [10] J.A. Weitzen, W.P. Biro kenmeier, and M.D. Grossi, "An estimate of the capacity of the meteor burst channel," IEEE Trans. Commun., vol. COM-32, pp. 972-974, Aug. 1984.
- [11] M.W. Abel, Meteor Burst Communications: Bits per Burst Performance Bounds" IEEE Trans. Commun., vol. COM-34, pp.927-936, Sep. 1986.

- [12] Hibshoosh, E., Schilling, D.L., Time Varying Bit Error Rate for Meteor Burst Channel, MILCOM'86, Monterey, CA, Oct. '86.
- [13] Osterjaard, J.C., Ramusen, J.E., Sousa, M.J., Quinn, M.J. and Kossey, P.A., Characteristics of High Latitude Meteor Scatter Propagation Parameters Over the 45-104 MHz Band, RADC Publications.
- [14] Report 631-2 (MOD F); Frequency Sharing Between the Broadcasting-Satellite Service (sound and television) and Terrestrial Services. Recommendations and Reports of the CCIR, 1982, Vol X/Xi-2.
- [15] Report 540-1; (MOD F); The Use of Frequency Bands Allocating to the Fixed-Satellite Service for Both the Up Link and Down Link of Geostationary-Satellite Systems. Ibid, Vol IV-1.
- [16] C.O. Hines and P.A. Forsyth, "The Forward Scattering of Radio Waves from Overdense Meteor Trails", Canad. J. Physics, Vol. 35, Feb. 1957.
- [17] Withers, D.J., Durkin, J., Frequency Band Sharing and Warc-Orb-85, June 22-25, 1986, Presented at ICC'86, Toronto, Ontario, Canada.
- [18] Bello, P.A., Some Techniques for the Instantaneous Real-Time Measurement of Multipath and Doppler Spread, Sept. 1965, IEEE Trans. on Comm. Tech.
- [19] Bello, P.A., Error Probabilities Due to Atmospheric Noise and Flat Fading in HF Ionospheric Communication Systems, Sept. 1965, IEEE Trans. on Comm. Tech.
- [20] Watterson, C.C., Juroshek, J.R., Bensema, W.D., Experimental Confirmation of an HF Channel Model, Dec. 1970, IEEE Trans. on Comm. Tech.
- [21] J. Hampton, "A Meteor Burst Model With Time Varying Bit Error Rate", Milcom 1985, 32.2.1.
- [22] SEMCOR, Inc., Regency Net Project, Meteor Burst Signalling Architecture study Final Report, Dec. 1985.
- [23] Schanker, J.Z., Meteor Burst Communication Systems, September 5-9, 1983, IREECON International Sydney '83, 19th International Electronics Convention and Exhibition, Digest of Paper, pp 183-5. Sydney, Australia.

- [24] L.A. Manning and V.R. Eshleman, "Meteors in the ionosphere", Proc. IRE, vol 47, pp. 186-199, February 1959.
- [25] O.G. Villard, et al., "The role of meteors in extended range VHF propagation, Proc. IRE, vol 43, pp 1473-1481, October 1955.
- [26] G.S. Hawkins, "A radio survey of sporadic meteor radiants," Monthly Notices Roy., Astron. Soc, vol. 116, pp 92-104, November 1956.
- [27] G.S. Hawkins, "Variation in the occurrence rate of meteors", Astron. J. vol 61, pp 386-391, Nov. 1956.
- [28] Western Union Gov. Syst Div. "Western Union meteor burst communications systems overview", Inform Brochure, Jan 1977.
- [29] V.R. Eshelman, L.A. Manning, A.M. Peterson and O.G. Villard, Jr. "Some Properties of oblique radio reflections from meteor ionization trails", J. Geophys Res., vol 61, pp 233-249, June 1956.
- [30] C.O. Hines and R.E. Pugh, "The spatial distribution of signal sources in meteoric forward scattering", Canad. J. Phys, vol. 34, pp 1005-1015, Oct. 1956.
- [31] O.G. Villard, et al, "Some properties of oblique radio reflections from meteor ionization trails", J. Graphys. Res., vol 61, pp 233-249, June 1956.
- [32] J.A. Weitzen, M.D. Grossi and W.P. Birkemeier, "High resolutions multipath measurements of the meteor scatter channel," Radio Sci. Jan. 1984.
- [33] J.A. Weitzen, Signetron Corp., Private Communications.
- [34] IBM Corp., MBC Model Communication Assessment Program, (rev. 3.0).
- [35] Abramowitz and Stegun, "Handbook of Mathematical Functions", Dover Pub, pp. 1001-1003.
- [36] H. Taub and D.L. Schilling, *Principles of Communication Systems*, 2nd edition, McGraw-Hill Book Company, New York, 1986.
- [37] R.J. Benice and A.H. Frey, Jr., "An Analysis of Retransmission Systems," IEEE Trans. Commun. Technol., vol. COM-12, pp. 135-145, Dec. 1964.

- [38] S. Lin and D.J. Costello, *Error Control Coding - Fundamentals and Applications*, Prentice Hall, Englewood Cliffs, New Jersey, 1983.
- [39] A. Papoulis, *Probability, Random Variables and Stochastic Processes*, McGraw Hill Book Company, New York, 1984.
- [40] E.J. Weldon, "An Improved Selective-Repeat ARQ Strategy," *IEEE Trans. Comm.*, vol. COM-30, pp. 480-486, Mar. 1982.
- [41] C.E. Shannon, "Two-way Communication Channels," *Proc. 4th Berkeley Symp. Prob. and Stat.*, vol. 1, pp. 611-644, Univ. California Press, Berkeley, CA, 1961.
- [42] J.M. Wozencraft and I.M. Jacobs, *Principles of Communication Engineering*, John Wiley & Sons, New York, 1965.
- [43] B. Sklar, *Digital Communications - Fundamentals and Applications*, Prentice Hall, Englewood Cliffs, 1988.
- [44] M.K. Simon, J.K. Omura, R.A. Scholtz, and B.K. Levitt, *Spread Spectrum Communications - Volume I*, Computer Science Press, Rockville, MD, 1985.
- [45] A. Michelson and A. Levesque, *Error Control Techniques for Digital Communications*, John Wiley & Sons, New York, 1985.
- [46] G. Clark and J. Cain, *Error Correction Coding for Digital Communications*, Plenum Press, New York, 1981.

TIME VARYING BIT ERROR RATE FOR METEOR BURST CHANNEL

Eli Hibshoosh, D.L. Schilling*

Department of Electrical Engineering
City College of New York
New York, NY 10031

ABSTRACT

A model is described for the underdense meteor burst phenomenon that takes into account its random decay time-constant and derives the CDF and PDF for the burst duration as well as the joint PDF for burst duration and decay time-constant. In addition the time varying bit error rate BER and its average is calculated for binary FSK and coherent BPSK.

INTRODUCTION

The development and understanding of a model for the behavior of a meteor burst is crucial in the study and use of this phenomenon as a viable communication channel, ref. (1-7, 11). For a communication system engineer it is important to have an accurate understanding of the time varying bit error rate, BER, characteristics.

It is known that the SNR of the underdense trail decays exponentially in time with a random initial amplitude and a random decay time-constant which in turn affect the BER variation in time. To date, however, investigators have used either a constant - (worst case) - SNR based on fixed decay rate in the calculation of the bit error rate, ref. (11, 13) or employed a SNR based on a conditional expected value of decay rate given a fixed burst duration, ref. (10).

This paper takes into account effects of the random decay time-constant in its derivation of BER expression. Using empirically reasonable distributions for initial SNR amplitude and decay constant we derive the cumulative distribution function, CDF, of the burst duration, t_b , as well as the joint PDF of decay time-constant and burst duration. The SNR is then expressed in terms of a minimum SNR level n , decay time-constant, B , and burst duration, t_b . This SNR expression is used in obtaining the appropriate expression for BER and average BER in time for the two cases of binary PSK and coherent BPSK.

THE MODEL FOR METEOR BURST

Meteor bursts are characterized as overdense or underdense. Since the underdense trail phenomenon is the dominant contributor to the overall throughput we shall consider its model, ref. (5).

*Acknowledgement. This work is supported by AFOSR Grant No. 27747 and by SCS Telecom, Inc.

According to ref. (3) we can write the SNR for underdense trail as:

$$SNR = \frac{P_T G_R \lambda^3 \sigma_e \sin^2 \theta \exp(-B \sigma_e^2 r_0^2 / \lambda^2 \sec^2 \phi)}{(4\pi)^3 2R_T^3 (1 - \sin^2 \theta \cos^2 \theta) NF} e^{-t/B}$$

Where,

- P_T is the transmitter power
- G_R is the receiver antenna gain
- G_T is the transmitter antenna gain
- λ is the wavelength of the carrier
- D is the diffusion coefficient of the atmosphere ($7.5 \text{ m}^2/\text{s}$)
- ϕ is the angle of incidence of the transmitted plane wave
- B is the angle between the trail and the great circle path from receiver to transmitter
- R_T is the nominal distance between the trail and the stations
- r_0 is the nominal initial radius of a trail (0.65m)
- σ_e is the effective echoing area of the electron (10^{-28} m^2)
- NF is the background noise floor
- B is the decay time-constant of the burst
- α is the angle between incident E-vector at trail and the direction from the trail to the receiver
- q is the electron line density

Further simplifications are according to ref (10). NF is computed using

$$NF = k T_0 W F_n$$

when k is Boltzman's constant, T_0 is (270°K), W is the receiver bandwidth and F_n is the external noise figure - assumed to be due to galactic noise only.

n and B are assumed to be uniformly distributed over $(-\pi/2, \pi/2)$ and hence $\langle \sin \theta \rangle = \langle \sin \theta \rangle = 2/\pi$.

Also it is assumed for ϕ (the angle of incidence for the transmitted wave) that all trails are located at 100m altitude and halfway between the transmitter and receiver.

For mathematical tractability we rewrite eq (1) as follows:

$$SNR(t) = Aq^2 e^{-t/B}$$

where q the electron line density varies between q_L and q_U the minimum and maximum electron line densities. We denote by η the minimum SNR level that defines the burst end (duration) and corresponds to q_L .

i.e.

$$SNR(t_B) = \eta = Aq_L^2 = Aq^2 e^{-t_B/B} \quad (3)$$

eq. (3) yields an expression for the initial SNR level, $SNR(t=0)$,

$$Aq^2 = \eta e^{t_B/B} \quad (4)$$

which when substituted into eq. (2) provides us with the signal-to-noise ratio in terms of the minimum SNR level, burst duration, t_B , and decay time constant, B .

$$SNR(t) = \eta e^{(t_B - t)/B} \quad (5)$$

CDF AND PDF OF t_B

Throughout this paper we shall use the PDF of q as:

$$f_q(q) = \frac{q}{q_U} \quad q_L < q < q_U \quad (6)$$

Where

$$q = \frac{q_U q_L}{q_U - q_L} \quad \text{and} \quad \frac{q_U}{q_L} \gg 1$$

This yields the CDF of q

$$F_q(q) \approx 1 - \frac{q_L}{q} \quad q_L < q < q_U \quad (7)$$

In addition we shall assume the PDF of B as exponentially distributed

$$f_B(B) = \frac{1}{B_L} e^{-B/B_L} \quad B_L = .35 \text{ sec} \quad B > 0 \quad (8)$$

or Rayleigh

$$f_B(B) = \frac{B}{\sigma^2} e^{-B^2/2\sigma^2} \quad B \geq 0 \quad (9)$$

where

$$\sigma = .89 B_L$$

and $B_L = .35$ sec. B_L is the expected value of B and its value used is from the most recent observations by RADC. (The most extensive program for the study of meteor burst phenomenon is currently conducted by the Air Force (RADC), ref (6)).

Using eq. (2) to represent SNR behavior in time, and eqs. (3) and (7), setting $q_U = q_L$ it can be shown that the joint PDF of t_B and B is given by eq. (10)

$$f_{t_B, B}(t_B, B) = \frac{1}{2B} e^{-t_B/2B} f_B(B) \quad (10)$$

and by integrating over B we get

$$f_{t_B}(t_B) = \int \frac{1}{2B} e^{-t_B/2B} f_B(B) dB \quad (11)$$

We are left now to substitute eq. (8) in eqs. (10) and (11) resulting in the joint PDF of t_B and B (B - exponential)

$$f_{t_B, B}(t_B, B) = \frac{1}{2B_L} \frac{1}{B} e^{-\left(\frac{t_B}{B_L} + \frac{t_B}{2B}\right)} \quad (12)$$

the PDF of t_B (B - exponential)

$$f_{t_B}(t_B) = \frac{1}{B_L} K_1(x) \quad t_B > 0 \quad (13)$$

where

$$x = \sqrt{t_B/(B_L/2)}$$

and $K_1(\cdot)$ is the modified Bessel function of order 1.

and the CDF of t_B

$$F_{t_B}(t_B) = 1 - x K_1(x) \quad t_B > 0 \quad (14)$$

eqs. (13) and (14) are compared graphically to an exponential distribution with $E(t_B) = .377$ sec. and depicted in fig. 1.

Similarly we repeat the process by substituting eq. (9) (B Rayleigh) into eqs. (10a) and (11) to provide us with the joint PDF of t_B and B

$$f_{t_B, B}(t_B, B) = \frac{1}{2\sigma^2} e^{-\frac{1}{2}\left(\frac{t_B^2}{\sigma^2} + \frac{t_B}{B}\right)} \quad (15)$$

PDF for t_B (B Rayleigh)

$$f_{t_B}(t_B) = \frac{1}{2\sigma^2} \int_0^\infty e^{-\frac{1}{2}\left(\frac{t_B^2}{\sigma^2} + \frac{t_B}{B}\right)} dB \quad (16)$$

and CDF for t_B

$$F_{t_B}(t_B) = 1 - \frac{1}{\sigma^2} \int_0^\infty e^{-\frac{1}{2}\left(\frac{t_B^2}{\sigma^2} + \frac{t_B}{B}\right)} dB \quad (17)$$

eqs. (16) and (17) are compared graphically with an exponential behavior where $E(t_B) = .58$ sec. and are depicted in Fig 2.

Eq. (17) for the CDF of t_B assuming B as Rayleigh is well approximated by

$$F_{t_B}(t_B) = 1 - (C_2^3 e^{-t_B^2/C_2} + (C_2^2 - C_2^2) e^{-C_2^2 t_B^2} + C_2^3) \quad (18)$$

where $T = 1 \left(\frac{t_B}{\sigma} \right)^{2/3}$

and

$$C_2 = .2, C_3 = 2.4 \text{ and } C_H = 3.18$$

CALCULATION OF BER (t) AND BER (t)

In general the bit error rate is equal to a function $g(\cdot)$ of the SNR:

$$BER = g(SNR \cdot W/R)$$

where, W is the bandwidth of the receiver and R is the data rate, $W/R = 1.25$ as used in the COMET system. SNR is defined by equation (1).

In our discussion two cases are considered binary FSK and coherent BPSK.

For FSK we have

$$BER(t) = \frac{1}{2} \exp \left(\frac{1.25 SNR(t)}{2} \right) = \frac{1}{2} \exp \left(\frac{-1.25 \eta}{2} e^{-(t_B - t)/\theta} \right) \quad (19)$$

and for BPSK

$$BER(t) = \frac{1}{2} \operatorname{erfc}(\sqrt{1.25 SNR}) = \frac{1}{2} \operatorname{erfc}(\sqrt{1.25 \cdot \eta} \exp((t_B - t)/(2 \cdot \theta))) \quad (20)$$

Multiplying eqs. (19) and (20) by eqs. (12) and (15) and integrating over t_B and B yield the average bit error rate for FSK and BPSK.

For FSK: B assumed is exponential ($B_L = .35$)

$$BER(t) = \frac{1}{2} \frac{1}{2\theta} \int \frac{1}{B} \exp \left[-\left(\frac{1}{2} e^{-\frac{(t_B - t)}{\theta}} + \frac{t_B}{2\theta} + \frac{\theta}{t_B} \right) \right] dt_B dB \quad (21a)$$

B assumed is Rayleigh ($\sigma = .28$)

$$BER(t) = \frac{1}{2} \frac{1}{2\sigma^2} \int \exp \left[-\frac{1}{2} \left(\eta e^{-\frac{(t_B - t)}{\theta}} + \frac{t_B}{\theta} + \frac{\theta}{t_B} \right) \right] dt_B dB \quad (21b)$$

For coherent BPSK: B assumed is exponential

$$BER(t) = \frac{1}{2} \frac{1}{2\theta} \int \frac{1}{B} \operatorname{erfc} \left(\sqrt{1.25 \eta} e^{-(t_B - t)/2\theta} \right) \exp \left(-\left(\frac{t_B}{2\theta} + \frac{\theta}{t_B} \right) \right) dt_B dB \quad (22a)$$

B assumed is Rayleigh ($\sigma = .28$)

$$BER(t) = \frac{1}{2} \frac{1}{2\sigma^2} \int \operatorname{erfc} \left(\sqrt{1.25 \eta} e^{-(t_B - t)/2\theta} \right) \exp \left(-\left(\frac{t_B^2}{2\sigma^2} + \frac{t_B}{\sigma} \right) \right) dt_B dB$$

Eqs. (21a) and (21b) for $\theta = 2$ are depicted in Fig. 3

Eqs. (22a) and (22b) for $\theta = 2$ are depicted in Fig. 4

RESULTS

Eqs. (13) and (16) for the probability densities of t_B under the assumptions that B is exponential and Rayleigh respectively provide us with the quantitative information to evaluate events of burst duration accurately. Perhaps more important their depiction suggests a good agreement with an exponential behaviour for t_B - the currently prevailing dogma - particularly for the case when B is Rayleigh. The case for which B is assumed Rayleigh seems correct for it yields zero probability for small B - fast decays - which agrees with our physical intuition.

The results for bit error rate and average bit error rate are graphed in Figs. 3 and 4 and the expressions in eqs. (21) and (22) can be modified to test the effects of other modulating schemes and effects of different average decay time constants and minimum signal to noise ratios.

It is important to note, however, that assuming the same fixed maximum allowable bit error rate for both modulating schemes, FSK and PSK, implies a higher minimum SNR, η , for FSK than PSK and a shorter burst duration for FSK resulting in a worse throughput performance for FSK.

In addition, the graph for BPSK (the modulating scheme used in the COMET System) shows lower average bit error than FSK as expected. The lower average BER encountered when B assumed Rayleigh as opposed to B assumed exponential can be explained by noting the B^2 in the exponent of eqs. 21b and 22b.

CONCLUSIONS

A model has been described for a meteor burst communication channel that takes into effect the statistical variation in the decay rate of the signal-to-noise ratio of the channel. Both the PDF for t_B , the burst duration, and joint PDF of t_B and B, decay constant, were derived and are consistent with empirical observations made by RADG (6). The bit error rate for two

modulating schemes FSK and LK were calculated by averaging over the effect of decay rate and little difference is found whether the initial assumption for the distribution of the decay time constant was Rayleigh or exponential. The expressions found for average BER can be modified to test for other coding techniques. The high BER suggests the need for further study of the channel and the use of coding for improving the BER.

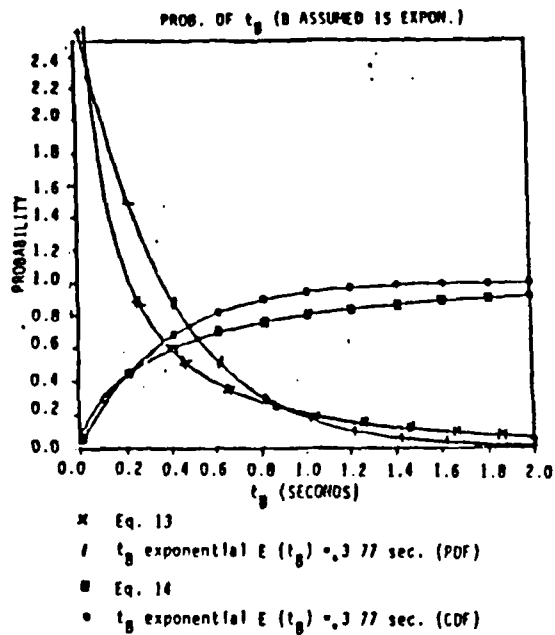


FIGURE - 1

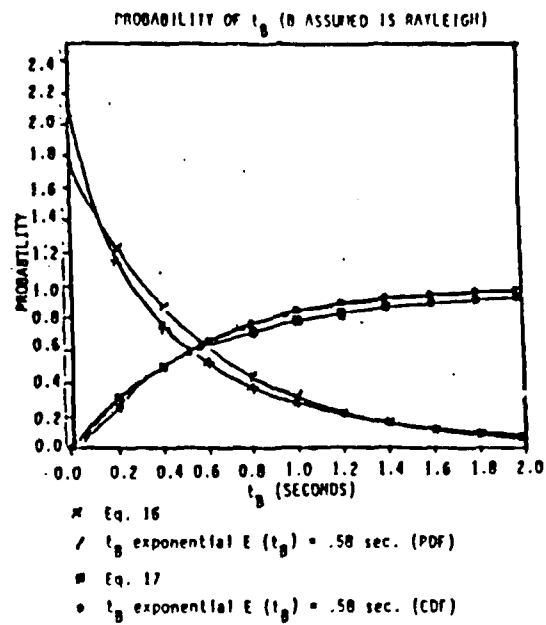


FIGURE - 2

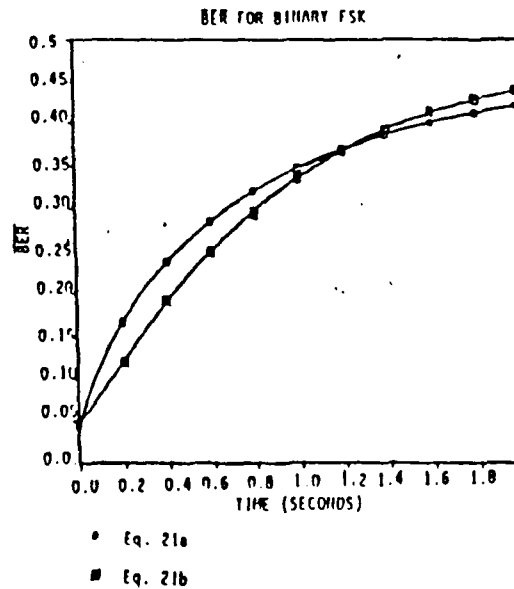


FIGURE - 3

ANALYSIS OF TWO PROTOCOLS FOR METEOR-BURST COMMUNICATIONS

L. B. Milstein
Dept. of E.E.C.S.
Univ. of Calif., San Diego
La Jolla, CA 92093

D. L. Schilling
Dept. of E.E.
City College of N.Y.
New York, NY 10031

R. L. Pickholtz
Dept. of E.E.C.S.
George Washington Univ.
Washington, DC 20052

J. Sellman
USAISMA
Ft. Monmouth, NJ 07703-5501

S. Davidovici
Dept. of E.E.
Rutgers University
Piscataway, NJ 08854

A. Pavelchek
SCS Telecom, Inc.
Sands Point, NY 11050

A. Schneider
Cybercom Corporation
Arlington, VA 22203

G. Eichmann
Dept. of E.E.
City College of N.Y.
New York, NY 10031

ABSTRACT

In this paper we present the results of an analysis of a meteor-burst channel showing the expected throughput and the probability of completing a given message under two different scenarios. In the first scenario, the transmitter is presumed to have knowledge (obtained by appropriate probe signals) of the entire duration of a given meteor-burst (MB). In the second, only the starting time of each MB is known. Numerical results based on the analysis are provided, and it is concluded that, through the use of appropriate signal design and error-correction coding, sufficiently reliable communications over the MB channel is achievable.

I. INTRODUCTION

The possibility of using ionization trails created by meteors entering the earth's atmosphere to provide beyond line-of-sight communications has been known for a long time. Several experimental [1], [2] and practical [3] systems have been built using this mode of propagation. The physics of the phenomena generating these ionization trails and the resultant reflection of radio waves has been described in detail elsewhere in the literature [4], [5].

In this paper, we examine the performance of two protocols. A fixed length packet is assumed. The first protocol attempts to optimally use all available bursts. The terminal to receive data is assumed to be continually broadcasting so as to probe for a channel opening. The terminal sending the message data begins transmitting as soon as it hears the probing signal. As a result, the time delay between the opening of the channel and the start of the data transmission is at most equal to the one-way propagation time. Once the channel closes, the probing signal disappears and data transmission ceases; the search for another channel opening now begins.

The second protocol examined utilizes the trail duration less efficiently. However, it is simpler to implement and it reduces the exposure of terminals to detection by decreasing the transmission requirements. In this protocol, the message sending terminal probes for a channel. Channel openings are detected when the sending terminal receives a response to its probe. This results in a delay almost equal to the two-way propagation time prior to the start of data transmission. However, for typical trail durations (.2 to 1 second), the two-way propagation time, which is usually less than 14 msec, can be considered negligible in most circumstances. Using this protocol, only one packet is transmitted per burst.

We assume packetized data transmissions using binary FSK. Noncoherent matched filter detection is used, and a rate $-1/2$ Reed-Solomon code is employed. A similar analysis of the expected performance of a communication system attempting to utilize meteor bursts for packet communication was presented in [5]. However, most of our models differ from that of [5], and we are able to provide closed-form analytical solutions for three of our four key expressions. These are the throughput expressions for each of two modes of operation of the meteor-burst channel, as well as the probability of successfully completing a packet for one of the two modes. The probability of successful completion for the other mode of operation is presented as an infinite summation, similar to an expression given in [5].

II. ANALYSIS

In this section, expressions for both throughput and probability of correctly transmitting a given message are presented. The supporting analysis leading up to these results can be found in [6]. As indicated above, two different modes of system operation are considered. In the first mode, it is assumed that the receiver continuously transmits a sounder to the transmitter. Any time the transmitter receives the sounder signal, it knows that the meteor burst (MB) channel is present and hence starts to transmit its message. As soon as reception of the sounder

signal ceases, the transmitter stops transmitting. The transmission of a given packet might, however, span many MB's, and it is assumed that a certain amount of overhead is necessary for the transmitter to acquire the MB channel on each and every separate burst. Specifically, it is assumed that t_0 seconds are necessary for each acquisition. In essence then, the first mode of operation corresponds to the transmitter knowing precisely each instant of time when the MB channel is present.

With this scenario, the following mathematical model is used: Let n be the total number of meteor bursts that occur in some time interval T_D seconds, and let N_j be the number of bursts in T_D seconds that allow exactly j packets-per-burst to be transmitted. Then

$$P(N_j) = \sum_{n=1} P(N_j|n)P(n), \quad (1)$$

where n is taken to be a Poisson random variable with probability mass function given by

$$p(n) = \frac{e^{-\frac{T_D}{T_I}} \left(\frac{T_D}{T_I}\right)^n}{n!} \quad (2)$$

In (2), T_I is the average interval between bursts. Clearly, this model is only approximate, since the summation in (1) allows an infinite number of bursts to occur in a finite interval of time. However, if the average interval between bursts is much less than the time duration T_D , the approximation should yield reasonable results.

If we define P_j as the probability that a given burst lasts for a duration equal to that of exactly j packets, then

$$P(N_j|n) = \begin{cases} \binom{n}{N_j} P_j^{N_j} (1 - P_j)^{n-N_j} & N_j \leq n \\ 0 & N_j > n \end{cases} \quad (3)$$

To evaluate $P(N_j)$, the distribution of the duration of a burst must be known. Towards that end, assume the probability density of a burst duration is given by

$$f(d_b) = \frac{1}{T_L} e^{-\frac{d_b}{T_L}} \quad (4)$$

where T_L is the average length of a burst. With this model, it is straightforward to show that N_j is also Poisson. That is,

$$P(N_j) = \frac{\left(\frac{T_D}{T_I}\right)^{N_j} \exp(-\frac{T_D}{T_I})}{N_j!} \quad (5)$$

where

¹ To as great an extent as is possible, we use the formulation and notation of [5].

$$P_j = \left[e^{-j \frac{T_P}{T_L}} - (j+1) \frac{T_P}{T_L} e^{-\frac{t_0}{T_L}} \right] \quad (6)$$

and where T_P is the duration of a packet.

To obtain the expected number of information bits that can be transmitted over the MB channel in T_D seconds, which we refer to as the throughput², let N_{B1} be defined as

$$N_{B1} = \sum_j j I N_j \quad (7)$$

where I is the number of information bits per packet. That is, N_{B1} is the actual number of

transmitted bits in one realization of the process. Then

$$E\{N_{B1}\} = I \sum_j j E(N_j) = \frac{I T_D}{T_I} \frac{\exp[-(T_P + t_0)/T_L]}{1 - \exp(-T_P/T_L)} \quad (8)$$

Consider now the second protocol, whereby the transmitter makes no attempt at monitoring the presence of the channel other than the start of the burst. However, each time a burst is detected, an entire packet is transmitted. Then, with I again equal to the number of information bits per packet, the number of bits transmitted across the channel in a time duration of T_D seconds is given by

$$N_{B2} = I N_P \quad (9)$$

where N_P is defined as the number of bursts whose duration is greater than or equal to $t_0 + T_P$. Notice that the parameter t_0 is larger in this second mode of operation than it was in the first mode.

With this model, the expected number of bits that can be transmitted over the channel can be shown to be given by

$$E\{N_{B2}\} = \frac{I T_D}{T_I} \exp[-(T_P + t_0)/T_L] \quad (10)$$

While the throughput expressions derived above give some perspective regarding the performance of a MB channel, at times a more meaningful performance measure is the probability of successfully completing a message within a specified period of time. Considering first the mode of operation wherein the receiver

² Note that this definition ignores the effect of thermal noise. The throughput expressions given here can be modified as in [5] to include errors due to noise by assuming a specific ARQ model. However, noise effects are included in this paper when the probability of correct transmission is considered.

continuously sounds the channel, suppose a given packet is repeated for as many times as possible over a given duration of time, say T_D seconds. Let L_1 be defined as the greatest integer less than or equal to T_D/T_L , and let P_{CH} be the probability of correctly completing the message³ on at least one of L_1 successive transmissions of the same packet.

If P_p is defined as the probability of making an error in a specific packet, given that it has been received (i.e., given that the channel was present long enough for the packet to be completed), then it can be shown that

$$P_{CH} = \sum_{n=1}^{L_1} \sum_{i=1}^{L_1} (1-P_p)^i \frac{1}{(n-1)!} \left[r(n, \frac{LT_p + nt_0}{T_L}) - r(n, \frac{(i+1)T_p + nt_0}{T_L}) \right] \frac{\exp[-T_D/T_L](T_D/T_L)^n}{n!} \quad (11)$$

Note that in deriving (11), it was assumed that errors in all packets occur with the same probability. This is not true in reality, since the strength of a MB decays approximately exponentially. However, if we use the smallest signal-to-noise (SNR) in any packet for computing the probability of error of all the bits in the packets, then (11) will be a worst-case result.

Finally, for the second protocol, it can be shown that

$$P_{CH} = 1 - e^{-\frac{T_D + t_0}{T_L}(1-P_p)} \quad (12)$$

The results derived up to this point are in terms of the parameter P_p , the probability of making an error in the packet. Hence an explicit expression for P_p is needed in order to evaluate the overall system performance. Towards this end, assume that binary FSK with noncoherent detection is the modulation format and that the overall packet is to be broken up into smaller groups of information digits which are to be encoded with a forward-error correction (FEC) code and then transmitted over the MB channel.

As indicated above, because the SNR of a given MB decays approximately exponentially in time, the probability of error due to thermal noise at the receiver will vary from symbol-to-symbol. Therefore, to keep the analysis tractable, the probability of error results will be computed using the SNR that is present at the end of a MB (i.e., using the smallest SNR of the burst), so that the final results will really be

upper bounds. Also, again because of the exponential decay in SNR, it is reasonable to assume that the channel will be quite bursty in nature. Hence the FEC scheme should be one that performs well in the presence of bursty errors, and for the purposes of this paper, a Reed-Solomon (RS) code will be used.

To be specific, assume the packet consists of I bits of information, and these I bits are broken up into J groups of mK bits per group. An (N, K) RS code is then used to encode each group, where $N = 2^m - 1$. To receive the packet correctly, all J codewords must be correctly received. The probability of this occurring is

$$1 - P_p = (1 - P_w)^J, \quad (13)$$

where

$$P_w = \sum_{i=E+1}^N \binom{N}{i} P_b^i (1 - P_b)^{N-i}, \quad (14)$$

E is the error-correction capability of the RS code and P_b is the error probability of a RS symbol. It is given by

$$P_b = 1 - (1 - P_d)^M, \quad (15)$$

where

$$P_d = \frac{1}{2} e^{-\frac{1}{2} \text{SNR}} \quad (16)$$

is the bit error rate for noncoherent binary FSK.

III. NUMERICAL RESULTS

Figures 1 and 2 contain curves showing the probability of completing a message for the first and second protocols, respectively (i.e., equation (11) is plotted in Figure 1 and equation (12) is plotted in Figure 2). The abscissa in both cases is T_D , the total observation time during which the message is to be completed. The curves in each figure are parameterized by the signal-to-noise ratio, which in turn implies a value for T_L , the average time between bursts. For the results presented in Figures 1 and 2, the following pairs of SNR and T_L were used:

SNR(dB)	T_L (seconds)
7	28
7.5	29
8	31
10	39
12	50

The message duration (packet size) was taken as 2400 information bits, and those 2400 bits were divided into 32 codewords. Each codeword corresponded to a $(31, 15)$ RS code. Finally, T_L and T_p were each taken to be 0.2 seconds, and t_0 was taken to be .03 seconds for the first protocol and .06 seconds for the second protocol.

Because the value of T_L increases as the required SNR increases, at some point requiring a larger SNR becomes self-defeating, since the

³ For the purposes of this section, a message will be taken to be a single packet.

number of meteor-bursts in a given T_0 second interval becomes too small to maintain a specified degree of reliability. This is clearly indicated in each of the two figures, where it is seen that, for the parameter values chosen, an SNR of 8 dB provides the best results.

If, then, an 8 dB SNR threshold is used, and if, for example, it is desired to have a probability of message completion of 0.9, from Figure 1 it is seen that the observation time must be about three minutes when the first protocol is used. Similarly, if the second protocol is chosen, Figure 2 indicates that the observation time should be increased to about four and one-half minutes in order to achieve the same performance.

IV. CONCLUSIONS

An analysis of two different protocols for use over an MB channel has been presented. It was found that with sufficient repetition of the message and with a sufficient amount of error-correction coding, reliable communications could be achieved. This indicates that, at least in a back-up mode, the MB channel is quite appropriate for the transmission of relatively short messages. In fact, it should be emphasized that the results presented here are pessimistic results, in the sense that they were

derived under the assumptions that the instantaneous SNR on the channel was at all times equal to the lowest SNR that was deemed acceptable.

REFERENCES

- [1] P. A. Forsyth, E. L. Vogan, D. R. Hansen and C. O. Hines, The Principles of JANET - A Meteor-Burst Communication System. Proceedings of the IEEE, December 1957.
- [2] P. J. Bartholome, The STC Meteor-Burst System. SHAPE Technical Center Tech. Memo. TM-156, July 1967.
- [3] R. E. Leader, Meteor Burst Communications, Advanced Concepts and Techniques in Snow and Ice Resources. National Academy of Sciences, 1974.
- [4] George R. Sugar, Radio Propagation by Reflection from Meteor Trails. Proceedings of the IEEE, February 1964, pp. 116-136.
- [5] John D. Otting, An Analysis of Meteor Burst Communications for Military Applications. IEEE Comm. Trans., Vol. COM-28, No. 9, September 1980, pp. 1591-1601.
- [6] L. B. Milstein, D. L. Schilling, R. L. Pickholtz, J. Sellman, S. Davidovici, A. Pavelcheck, A. Schneider and G. Eichmann, Performance of Meteor-Burst Communication Channels. Submitted to the IEEE Journal on Selected Areas in Communications.

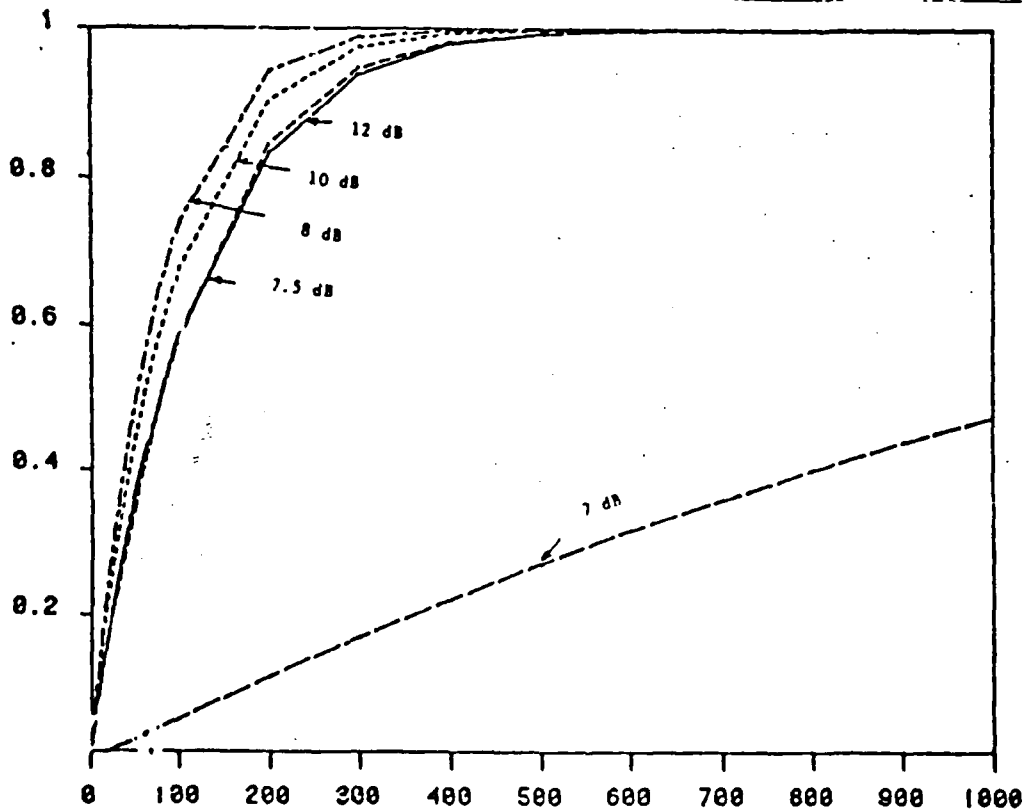
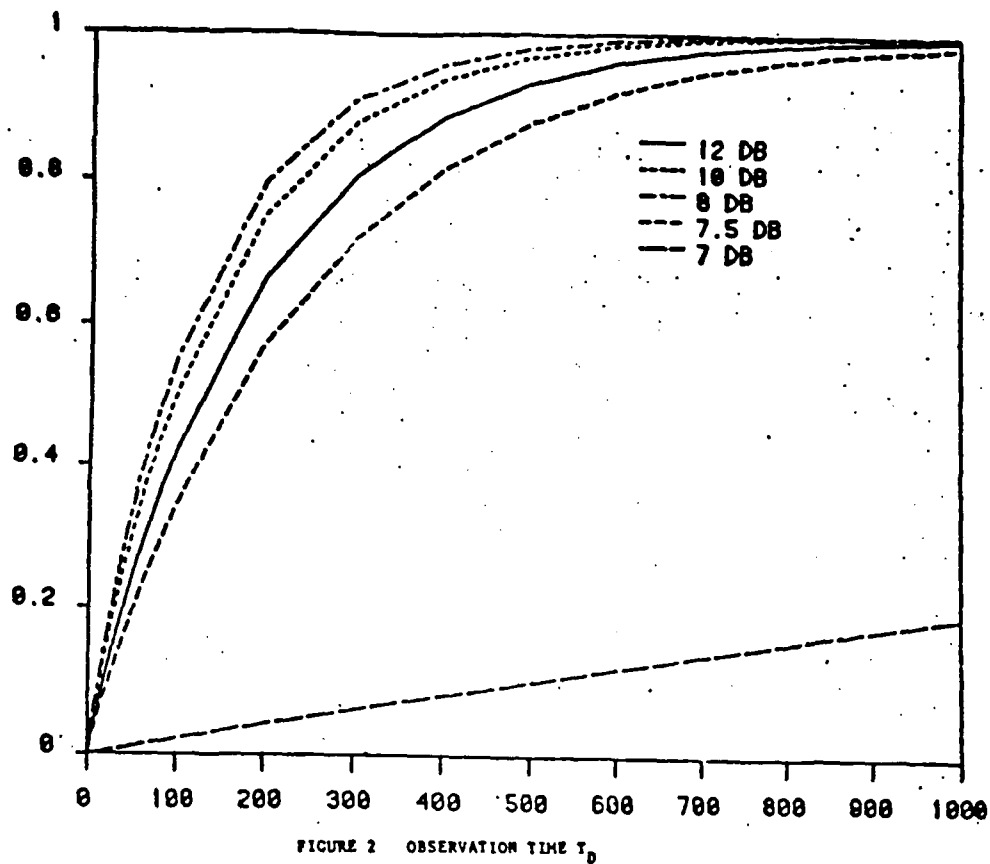


FIGURE 1 OBSERVATION TIME T_0



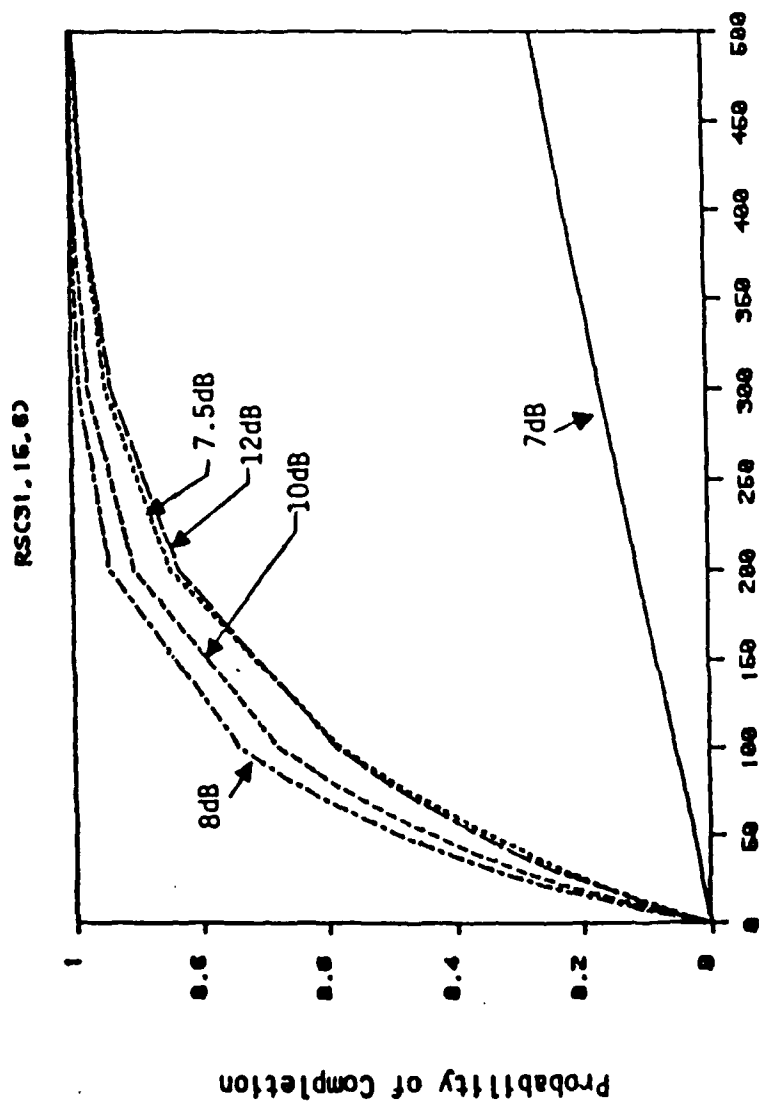


Figure 1 - Observation time T_D , seconds

RS (31,15,8)

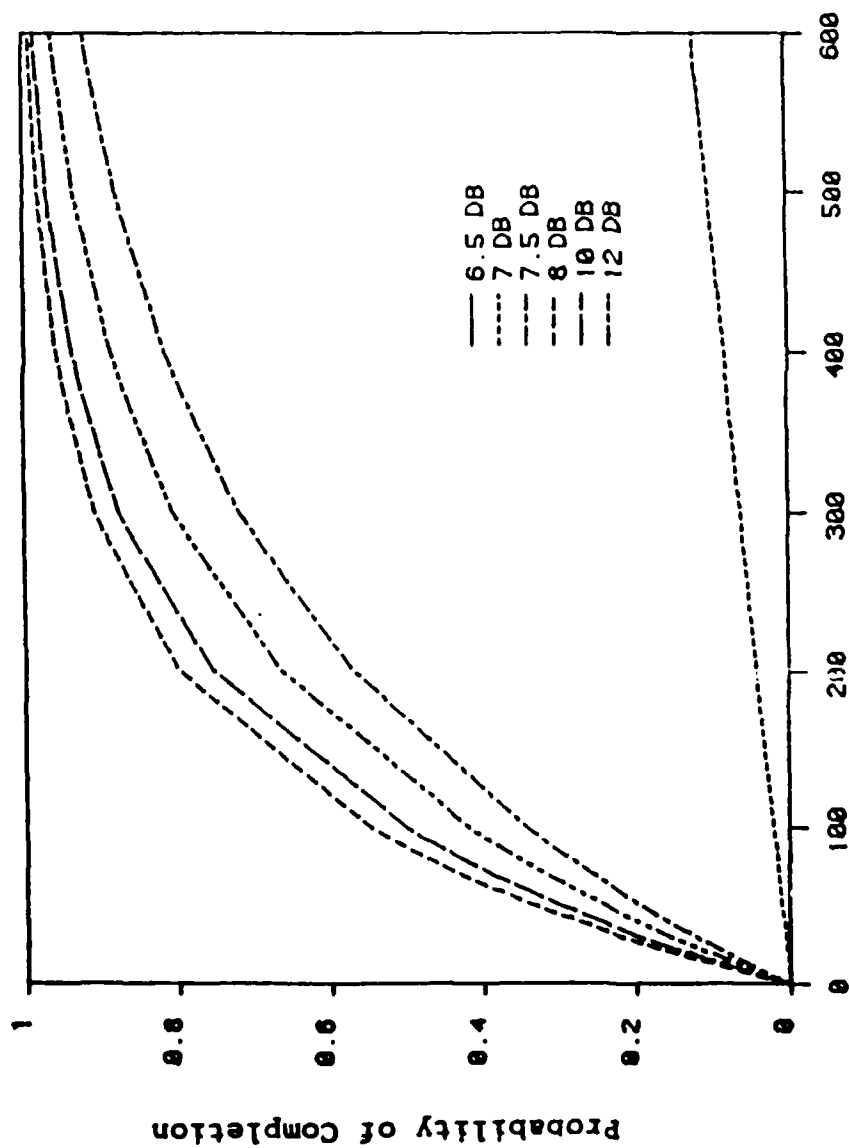


Figure 2- Observation time T_D , seconds

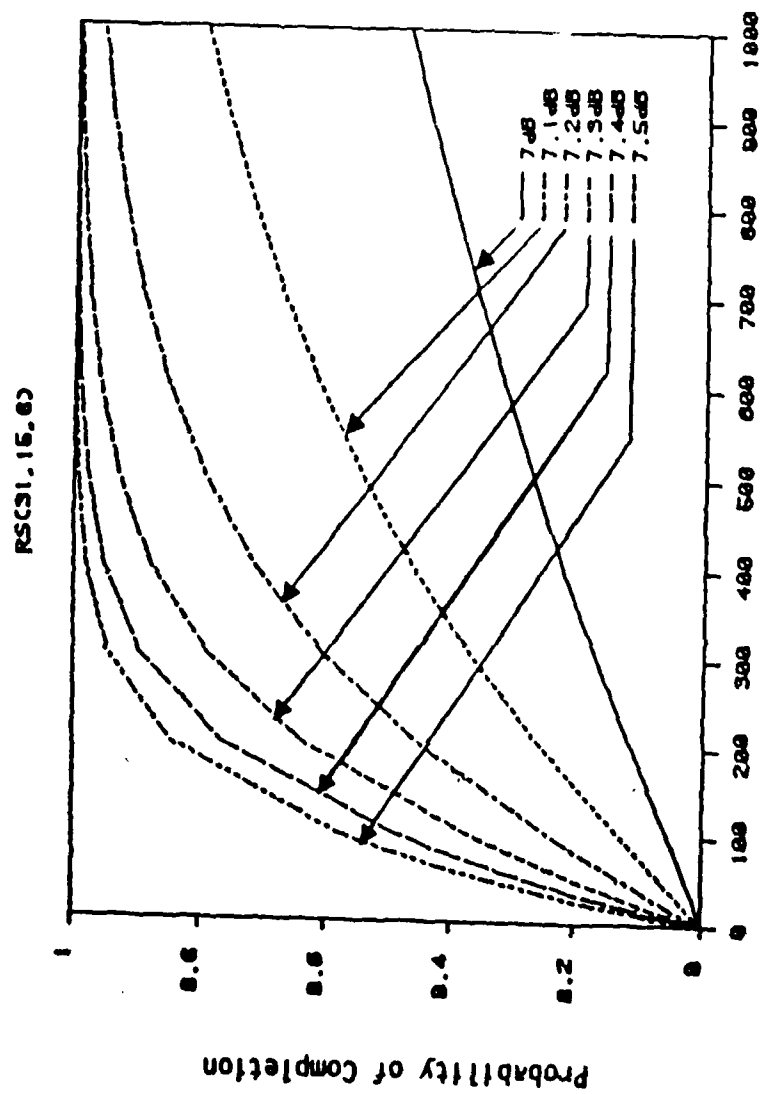


Figure 3 - Observation time T_D , seconds

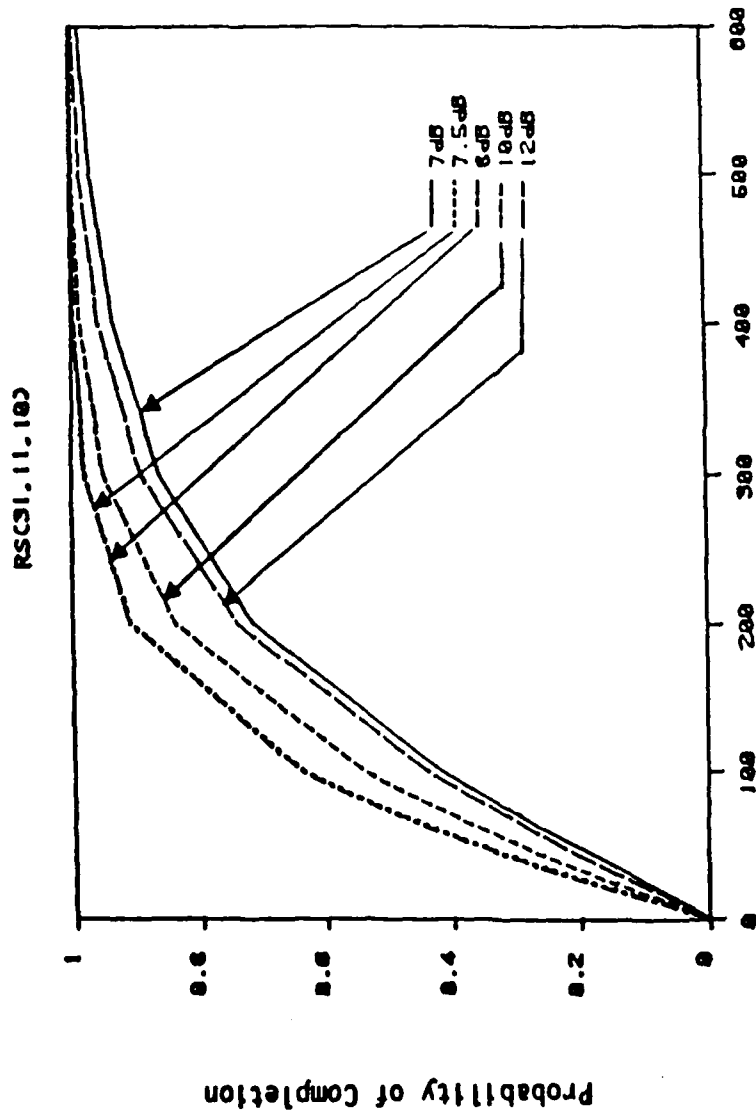


Figure 4 - Observation time T_0 , seconds

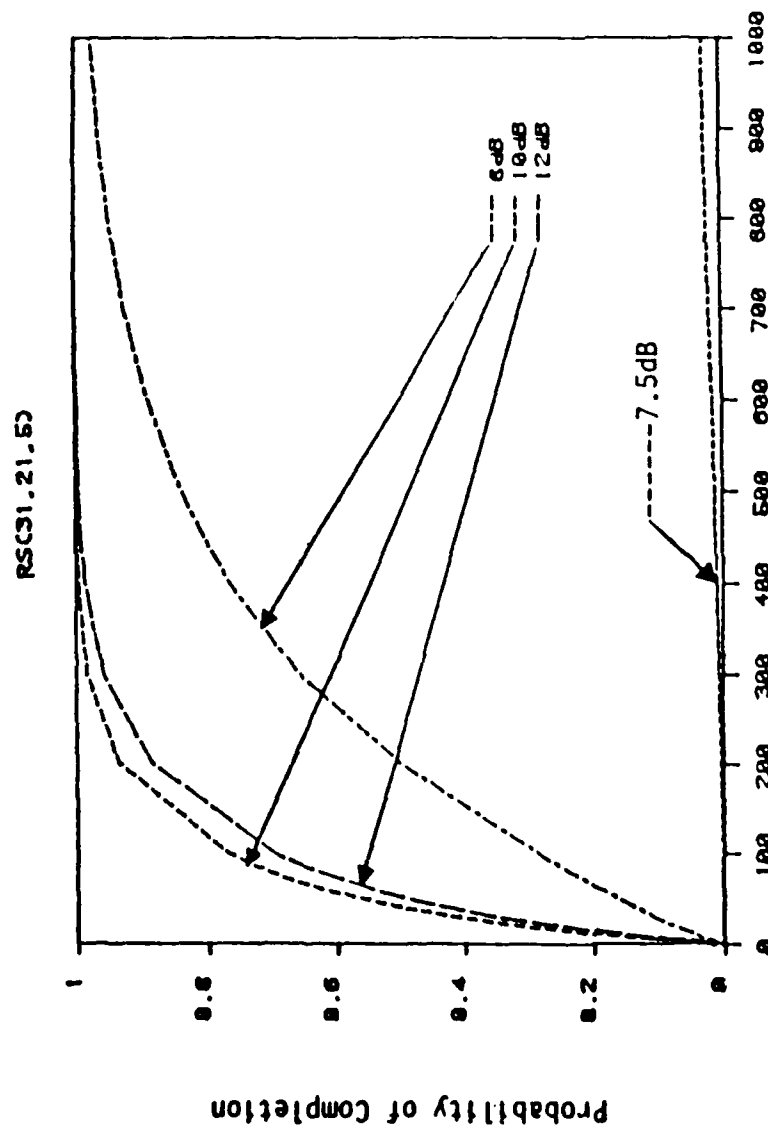


Figure 5 - Observation time T_D , seconds

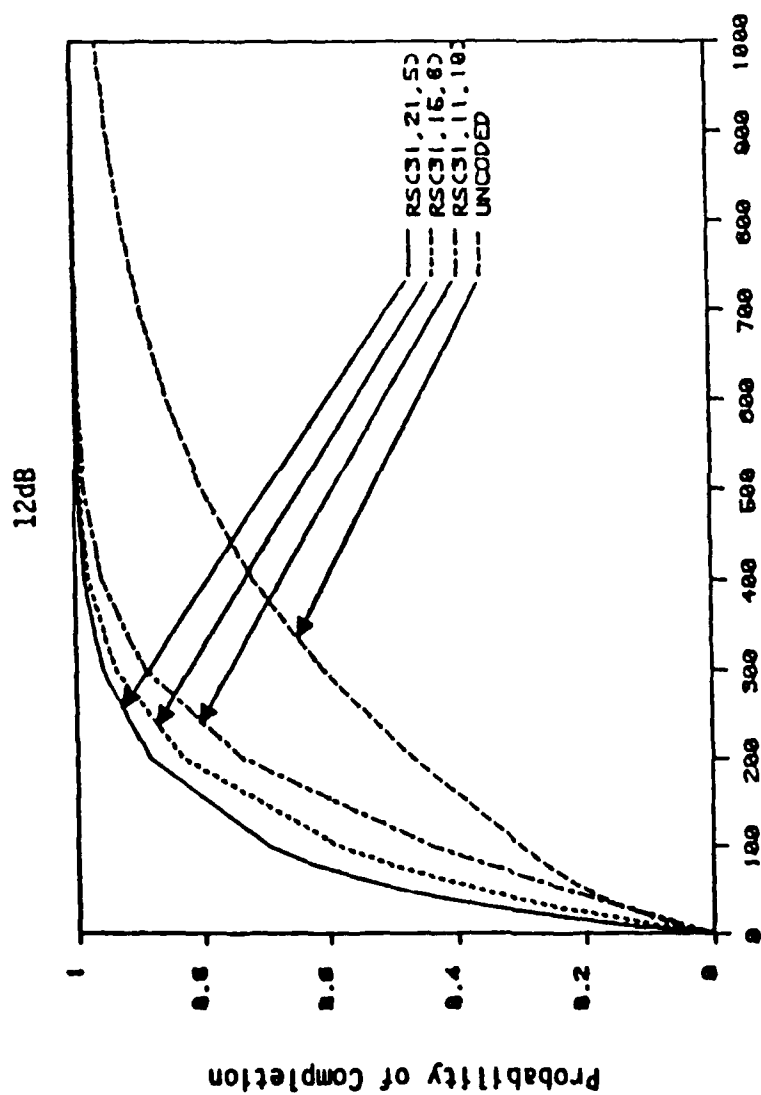


Figure 6 - Observation time T_D , seconds

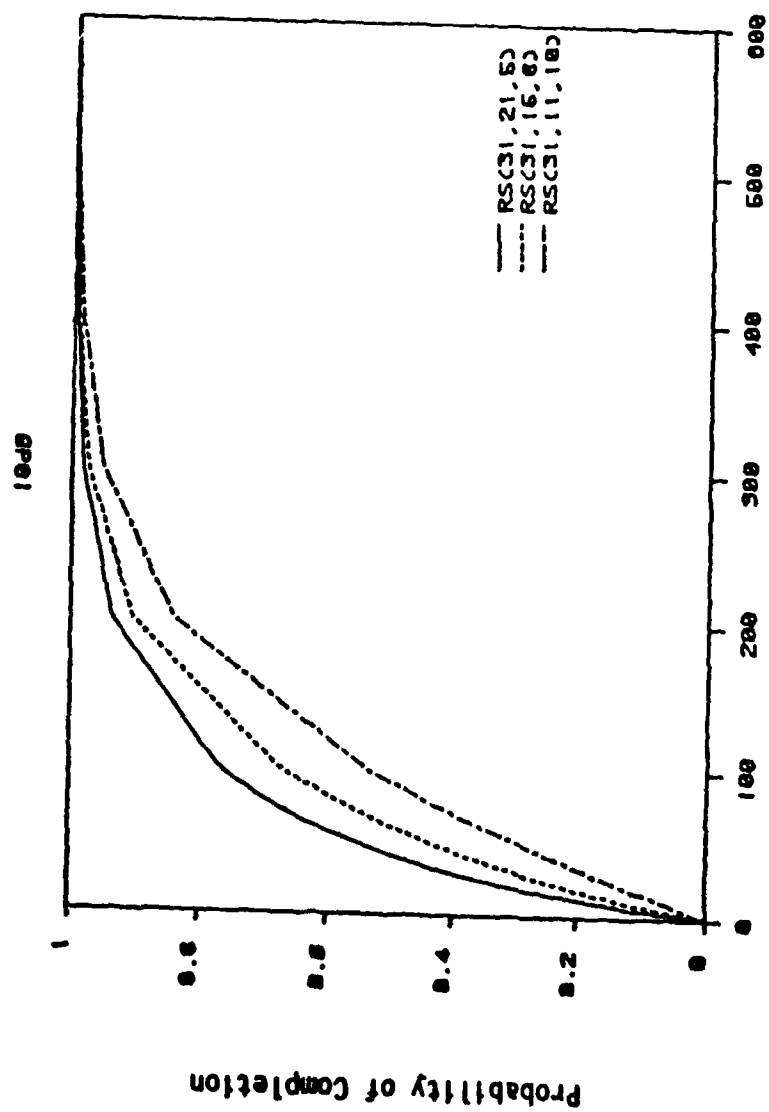


Figure 7 - Observation time T_D , seconds

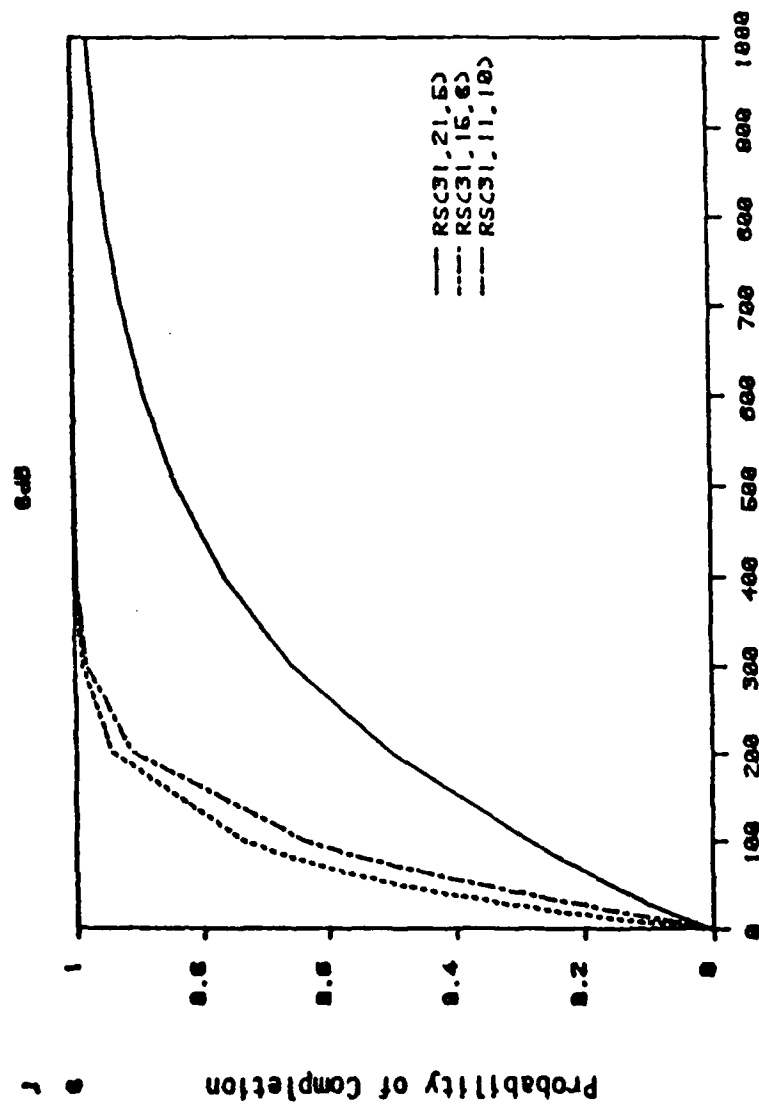


Figure 8 - Observation time T_D , seconds

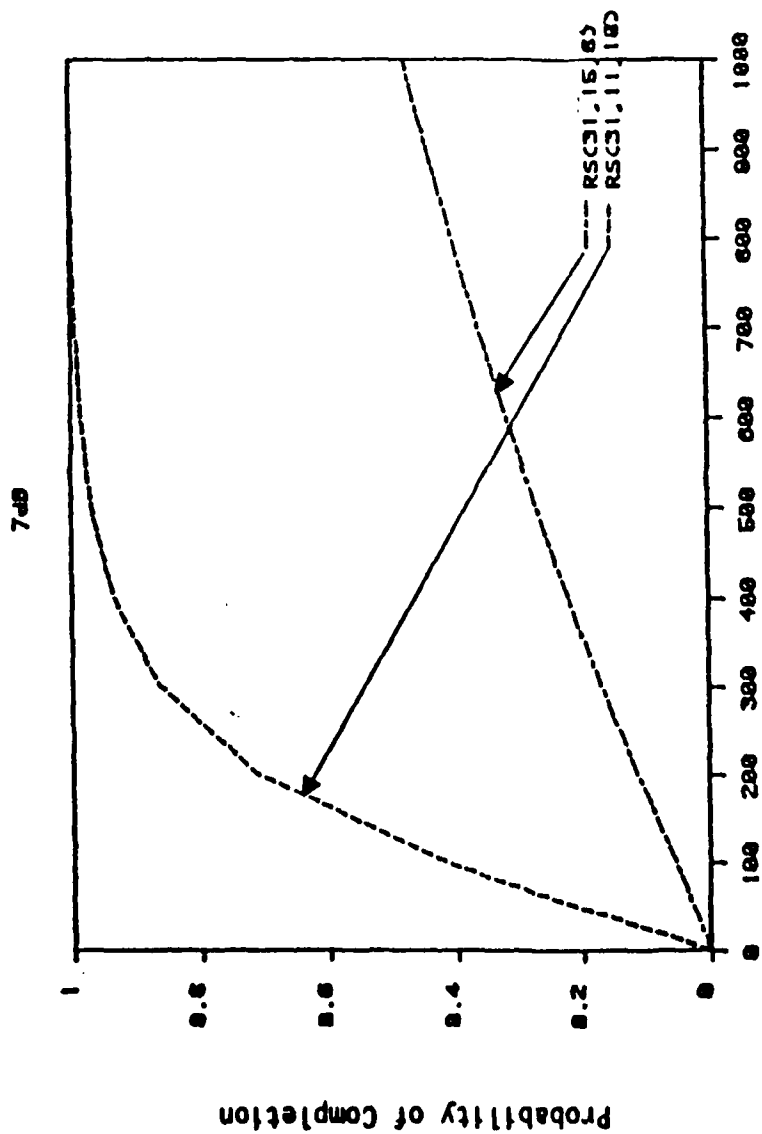


Figure 9 - Observation time T_D , seconds

Optimal Constant System Bit Rate for Maximum Throughput in Meteor Burst Systems

E. Hibshoosh¹, D. L. Schilling^{2*}, J. Weitzen²

Department of Electrical Engineering of:

1. City College of New York 2. University of Lowell, Lowell Ma

ABSTRACT

In this paper we analyze an accurate channel model based on the classical underdense equations and recent empirical data. The analysis results in analytical expressions for channel duration and throughput to be used as design and analysis tools in constant transmission rate communication systems. In addition, we derive the optimum constant transmission rate for a given communication system where all bits are constrained not to exceed a given maximum bit error rate. This optimum bit rate yields the maximum average throughput.

1 INTRODUCTION

For a communications system engineer the statistical behavior of meteor burst channel duration is crucial in understanding throughput performance. We start by employing a complex stochastic model for the channel where both the underdense electron line density and the decay time-constant are random. Clearly, for a given set of communication system parameters, noise and maximum allowed bit error rate (BER), choice of bit rate is equivalent to specifying received signal power threshold above which we operate. The expressions for channel duration and its statistics as defined by the maximum allowed BER are derived in terms of the system (fixed) transmission rate. We then derive the expression for throughput in terms of bit rate and average it over the ensemble of underdense trails. The optimal bit rate that maximizes throughput is then found; demonstrating the improvement over existing sub-optimal systems.

*Acknowledgement. This work is supported by AFOSR Grant No. 85-0234.

2 MATHEMATICAL MODEL AND CONCEPTUAL FRAMEWORK

In this section the basic equations that model the MB channel are presented. In addition, assumptions, constraints and empirical factors are stated.

2.1 Power Received and Related Parameters

The power received from the trail model use here is from the classic papers by Eshelma and Manning [2] and Sugar [1].

2.1.1 Power Received from an Underdense Trail

Meteor trails with fewer than 10^{14} electron per meter of length are referred to as underdense and the equation governing the power received from the trails is given by:

$$P(t) = \frac{P_t G_T G_R r^2 \sin^2(\alpha) \lambda^4 \exp\left(-\frac{4\pi^2 R^2}{\lambda^2 \sin^2 \theta}\right)}{16\pi^2 R_T R_R (R_T + R_R) (1 - \cos^2 \beta \sin^2 \theta)} \exp\left(-\frac{32\pi^2 D}{\lambda^2 \sec^2 \theta} t\right) \quad (2.1.1-1)$$

where,

- P_t Transmitter power.
- G_T, G_R Transmitter and receiver antenna gains.
- r_e Classical radius of an electron.
- α Angle between the electron field vector E and R_T .
- q Electron line density of the trail.
- λ Carrier wavelength.
- R_0 Initial radius of the trail (.65 m.).
- θ Angle of incidence/reflection of the transmitted plane wave.
- R_T Distance from transmitter to trail.
- R_R Distance from receiver to trail.
- D Diffusion coefficient of the atmosphere.
- β Angle between the trail and the propagation plane formed by R_T and R_R .

A minimal set of assumptions is applied in the literature [3,4,5] for analysis:

- 1.) The trail occurs at midpoint between receiver and transmitter i.e. $R_T = R_R$
- 2.) The burst occurs at an altitude of 100 km.
- 3.) The trail is travelling at a plane perpendicular to the plane formed by R_T and R_R i.e. $\theta = \pi/2$. In addition, we set $\alpha = \pi/2$.

Under these assumptions and after substituting for the physical constants we rearrange the above equation to arrive at the power received equation for the underdense case.

$$P(t) = C_U q^2 e^{-t/B} \quad (2.1.1-2)$$

where,

$$C_U = 2.5179581 \cdot 10^{-32} \cdot \frac{P_T G_T G_R \lambda^3 \exp\left(-\frac{33.359}{1^2 \sec^2 \theta}\right)}{R_T^2}$$

$$B = 3.166 \cdot 10^{-3} \cdot \frac{\lambda^2 \sec^2 \theta}{D}$$

It should be emphasized that:

- 1.) $P(0)$, the maximum power from the underdense trail is proportional to q^2 ; for a specific trail q is fixed.
- 2.) C_U , the constant of proportionality, incorporates the effects of link geometry, transmitter power, antenna gains and carrier wavelength. For a given communication system C_U is constant.
- 3.) The decay time constant B given above is found to be randomly varying from trail to trail. The expression in the classic model corresponding to a decay time constant is taken as the average decay time constant in accordance with observations. To date, however, researchers have assumed all underdense trails to share the same decay time constant to facilitate their analysis. It is in this added complexity to the model that our treatment deviates from published analysis and enhances its accuracy.
- 4.) The decay time constant B and the electron line density q are and statistically independent [1] [3].
- 5.) For a given communication system (i.e. C_U fixed) knowledge of the electron line density q , and decay time constant B , completely specify the underdense trail behavior in time.

2.1.2 Electron Line Density Statistics

Based on recent empirical data [6] the pdf for q is:

$$f_q(q) = Q q^{-p}; \quad q_{\min} \leq q \leq q_{\max} = 10^{14} \quad (2.1.2-1)$$

where,

$$Q = (p-1) q_{\min}^{p-1} \cdot \frac{1}{1 - \left(\frac{q_{\max}}{q_{\min}}\right)^{p-1}} \quad p = 1.6$$

q_{\min} is the minimum electron line density q trail must possess to be 'seen' by the communication system i.e. $C_U q_{\min}^2$ is the minimum power level P_{\min} detected by the communication system. In the context constant transmission rate systems (discussed later) P_{\min} is the power level that corresponds to the maximum allowed bit error rate (for a given bit rate and noise)

2.1.3 Decay Time Constant Statistics

We start by stating that the expected value of the decay time constant B is well approximated by:

$$E(B) = \bar{B} = 3.166 \cdot 10^{-3} \cdot \frac{\lambda^2 \sec^2 \theta}{D} \quad (2.1.3-1)$$

The random decay time constant B is assumed to be Rayleigh or exponential which has been shown to be consistent with recent experimental observation [6].

Rayleigh:

$$f_B(b) = \frac{b}{\alpha^2} e^{-b^2/\alpha^2}; \quad \alpha = \sqrt{\frac{2}{\pi}} \bar{B} \quad (2.1.3-2)$$

2.1.4 Joint PDF of q and B

Since the electron line density and the decay time constant are statistically independent the joint pdf is given by their product.

2.2 Link Geometry

In this section we present the relationships between link distance, L , and station trail distance, R_T ($=R_R$) and angle incidence/reflection ϕ

$$R_T = R_R = \sqrt{(h + L^2/8R_s)^2 + L^2/4} \quad (2.2-1)$$

$$\sec^2(\phi) = 1 + \frac{L^2}{\left(2h + \frac{L^2}{4R_s}\right)^2} \quad (2.2-2)$$

where,

- h trail altitude (100 km).
- L great circle distance between stations.
- R_t distance from transmitter to trail.
- R_R distance from receiver to trail.
- R_e radius of the earth, 6400 km.

2.3 Trail Arrival

We let $A'(q)$ be the number of trails/s with an electron line density between q and $q+dq$ e/m. Using Weitzen [7] we write

$$A'(q) = \frac{19.1667 \cdot \phi \sin \phi \cdot (R_R \zeta)^2}{q^2} \quad (2.3-1)$$

where $q_{min} < q < q_{max} = 10^{17}$ e/m and ζ is the idealized beamwidth of the antenna and all other parameters have been previously defined. The number of trails/s with q in a given range $[q_1, q_2]$, A , is found by integrating the above density over q yielding the following

$$A = \frac{19.1667 \cdot \phi \sin \phi (R_R \zeta)^2}{q_1} \left[1 - \frac{q_1}{q_2} \right] \quad (2.3-2)$$

2.4 Power Spectral Density of Received Noise

For signal frequencies appropriate to the MBC the received noise power spectral density, N_0 , is a function of the galactic noise picked up by the receiver antenna and the receiver thermal noise. Using Abel [4] we have:

$$N_0 = kT_0 \left[\frac{104}{L_A} \left(\frac{\lambda}{15} \right)^{2.3} + F \right] \quad (2.4-1)$$

where, k = Boltzmann constant, $1.3805 \cdot 10^{-23}$ J/K

T_0 = 290°K F = receiver noise figure

L_A = power loss between the antenna and receiver

λ = wavelength in meters

In our analysis we shall use L_A and F as 1.3 and 2.5, respectively.

2.5 Modulation and Bit Error Rate

The BER, denoted here as P_b , is related to the bit power $P(t)$, transmission rate R and power spectral density of the received noise N_0 as

$$P_b(t) = g \left(\frac{P(t)}{N_0 \cdot R} \right) \quad (2.5-1)$$

where $g(\)$ is determined by the modulation

technique.

or alternatively, we can solve for the power

$$P(t) = N_0 \cdot R \cdot g^{-1}(P_b(t)) \quad (2.5-2)$$

where g^{-1} is the inverse of g .

3 ANALYSIS AND RESULTS

3.1 Introduction and Approach

Our goal is to estimate the optimal average throughput for a given communication system a system with a constant transmission rate and a time varying bit error rate which is constrained not to exceed some maximum allowable value. For a constant bit rate system, since the power is monotonically decreasing in time, the probability of bit error increases with time in a fashion dictated by the relevant modulation function. We see the need then to impose a ceiling on the BER. We thus specify a maximum allowable BER, P_{bmax} , such that all transmitted bits shall have a BER less than or equal to P_{bmax} . This constraint on the probability of bit error for constant transmission rate system implies the existence of a minimum power level P_{min} such that all transmitted bits have a received power greater than or equal to P_{min} . In short, $P_b(t) = P_{bmax}$ when $P(t) = P_{min}$. The time for which the power received from the meteor burst exceeds a prescribe threshold (P_{min}) is defined as the channel (burst) duration t_b . This random burst duration is crucial in determining the number of bits transmitted during a given burst and ultimately in estimating throughput. If we choose to transmit at a higher rate the corresponding P_{min} has to be increased resulting in shortening the effective duration of transmission. This clear trade off between transmission rate and duration of transmission, t_b , suggests an optimal choice for transmission rate (or equivalently a optimal t_b) so as to maximize the throughput. The link between the number of bits transmitted per burst and throughput is done through the average arrival rate statistic and trail shape statistics (variation in and/or B). The judicious choice of transmission rate for the given system provides us therefore, with the optimal throughput.

3.1.1 Protocol

Both stations have receiving and transmitting capabilities. The station which acts as transmitter of data listens continuously for a continuous tone (or a frequently transmitted probe) which is being sent from the receiver. Upon detection of this tone both the presence and the strength of the channel is known to the transmitter which immediately commences transmission. The situation is completely symmetrical with respect to the receiver.

3.2 Improvements

The advantages of the analysis herein stem basically from considering a complex stochastic MBC model where both the initial power and decay time constant are considered random. The expressions derived will enable a system designer to estimate the best throughput by employing the optimal transmission rate.

3.3 Sample System

For quantitative appreciation of the results we assume some practical values for a communication system.

L Varies. Sets R_p and σ (Sec. 2.2)
 $P_t = 1000$ W, $G_t = G_r = 10$ dB, $D = 8$ m²/s
 $\sigma = 45.04$; λ varies; N_0 from Sec. 2.4
 $P_{max} = 10^{-3}$ Using BPSK we get $g^{-1}(P_{max}) = 9$

3.4 Constant Bit Rate: Constrained BER System

3.4.1 Channel Duration

Channel duration or burst duration, t_b is the time for which the power received from the burst exceeds a given minimum value P_{min} .

3.4.1.1 Burst Duration Statistics

Assuming a constant transmission rate, R , some given maximum BER, and power spectral density, N_0 we get from Eq. (2.1.1-1).

$$t_b = B \cdot \ln \left(\frac{q}{q_{min}} \right)^2 \quad (3.4.1.1-1)$$

where

$$q_{min} = \sqrt{\frac{P_{min}}{C_u}}; P_{min} = N_0 \cdot R \cdot g^{-1}(P_{max})$$

and

$$C_u = 2.517958110^{-32} \cdot \frac{P_t G_t G_r \lambda^3 \exp \left(-\frac{32.789}{\lambda^2 \sec^2 \theta} \right)}{R^2}$$

or equivalently as a function of R

$$t_b = B \cdot \ln \left(\frac{C_u}{N_0 \cdot R \cdot g^{-1}(P_{max})} \cdot q^2 \right) \quad (3.4.1.1-2)$$

We now average over the ensemble of underdense bursts (averaging over q and b) to yield the average burst duration:

The Average Burst Duration-- Underdense:

$$\bar{t}_b = \frac{2B}{p-1} \cdot \frac{1}{1-x} \cdot [1-x(1-\ln x)] \quad (3.4.1.1-3)$$

where

$$x = \left(\frac{q_{min}}{q_u} \right)^{p-1} = \left[\frac{N_0 \cdot R \cdot g^{-1}(P_{max})}{C_u \sigma_u^2} \right]^{\frac{p-1}{2}}$$

$$\bar{B} = 3.16610^{-3} \cdot \frac{\lambda^2 \sec^2 \theta}{D} \quad q_u = 10^{14} \quad p = 1.$$

$$R_n = \frac{R}{R_{max}} = \left(\frac{q_{min}}{q_u} \right)^2; R_{max} = \frac{C_u q_u^2}{N_0 g^{-1}(P_{max})}$$

For a given communication system C_u , R , N_0 , P_{max} , B and $\sigma(\cdot)$ are specified. R_n is the normalized (with respect to the highest possible rate for an underdense burst) bit rate.

Fig. 1. plots the above for our sample system as a function of R_n .

The n^{th} moment of t_b is given by:

$$\bar{t}_b^n = \frac{2^n B^n}{(p-1)^n} \cdot \frac{n!}{1-x} \cdot \left\{ 1-x \sum_{i=0}^n (-1)^i \frac{\ln^i(x)}{i!} \right\} \quad (3.4.1.1-4)$$

The PDF and CDF of t_b are:

$$f_{t_b}(t_1) = p' Q' \int_{bmin}^{\infty} \frac{1}{b} \exp \left(-\frac{p' t_1}{b} \right) f_b(b) db$$

(3.4.1.1-5)

$$F_{t_b}(t_1) = Q' \left\{ 1 - x F_b(bmin) - \int_{bmin}^{\infty} \exp \left(-\frac{p' t_1}{b} \right) f_b(b) dt \right\}$$

where x and p are from above. $p' = (p-1)/2$

$b_{min} = t_1 / [(1/p') \ln(1/x)]$; $Q' = 1/(1-x)$

Fig. 2 depicts the pdf for B assume Rayleigh, note the close agreement with the exponentially distributed t_b (dashed curve the current dogma [8]).

3.4.2 Throughput for Constant Bit Rate

Let N_i be the number of bits transmitted in the i^{th} burst and N , as the number of bursts occurring in the period of τ seconds. Since the bursts are independent of each other, assuming no overlap of bursts, we have:

$$T = \lim_{\tau \rightarrow \infty} \frac{1}{\tau} \sum_{i=1}^{N_i} N_i = A \cdot \bar{N}_b \quad (3.4.2-1)$$

where A is the average number of bursts/s and \bar{N}_b is the expected number of bits per burst as averaged over the ensemble of all burst profiles i.e. over q and B .

3.4.2.1 Optimal Average Throughput

The maximum throughput is found by first deriving the dependence of the average throughput (Eq. 3.4.2-1) on the bit rate R and solving for the optimal bit rate R^* that would yield the desired maximum throughput T^* . The solution is done with respect to the normalized bit rate, R_n , which yields result independent of a particular choice of system values.

For a given system P_{max} , N_0 , R and C_u are specified. The average number of bits per underdense burst $\bar{N}_b = R \cdot \bar{t}_b$ can be expressed in terms of the normalized bit rate using Eq.

(3.4.1.1-3) as:

$$N_{\infty} = \frac{2B}{p-1} R_{\max} \frac{1}{1-R_N'} [R_N - R_N'^{p-1} + R_N'^{p-1} \cdot \ln(R_N')] \quad (3.4.2.1-1)$$

where all parameters have been previously defined. Note that in the above expression the bursts considered were those with $q_{\min} < q < q_0$. The arrival rate for such condition is given by Eq. (2.3-2) where q_1 is set to q_{\min} and q_2 is q_0 . Together with the definition of R_N , Eq. (3.4.1.1-3), we have for the arrival rate of underdense bursts:

$$A_U = A \cdot \left[\frac{1}{\sqrt{R_N}} - 1 \right] \quad (3.4.2.1-2)$$

$$A = \frac{19.1667 \cdot \phi \sin \phi (R_N \zeta)^2}{q_0}; q_0 = 10^{14}$$

The expression for throughput using underdense bursts is given by the product of the last two Eqs. as specified by Eq. (3.4.2-1). The result is a function of the normalized bit rate. In the product we substitute for R_{\max} from Eq. (3.4.1.1-3) and for C_0 and B from Eq. (2.1.1-2). For a given set of system parameters we thus have the throughput for any choice of (normalized) bit rate as:

$$T_U = 3.056 \cdot 10^{-10} \cdot \frac{P_T C_T G_A \zeta^2 \phi \sin \phi \sec^2 \phi \exp\left(-\frac{20 \log}{10} \frac{1}{\zeta^2}\right) \lambda^2}{(p-1) N_0 \cdot g^{-1}(P_{\max}) \cdot D \cdot R_T}$$

$$\frac{\sqrt{R_N - R_N'}}{1 - R_N'} [1 - R_N' + p \cdot R_N' \cdot \ln(R_N')] \quad (3.4.2.1-3)$$

where the parameters are defined above. Note that the equation is written in two parts; the first incorporates all the parameters of the particular system and the second part reflects the variation in throughput with choice of bit rate. (Fig. 3) We would like to find from the above equation the optimal normalized bit rate R_N' which yields the maximum throughput T_U . This optimal normalized bit rate for any given system is found numerically to be (Fig. 3) $R_N' = .07$ or equivalently the optimal bit rate. $R^* = .07 R_{\max}$ (3.4.2.1-4) See Figs. 4, 5. resulting in

$$T_U^* = 3.433 \cdot 10^{-10} \cdot \frac{P_T C_T G_A \zeta^2 \phi \sin(\phi) \sec^2(\phi) \exp\left(-\frac{20 \log}{10} \frac{1}{\zeta^2}\right) \lambda^2}{R_T N_0 g^{-1}(P_{\max}) D} \quad (3.4.2.1-5)$$

All the parameters are previously defined. The above expression for the maximum throughput T_U^* allows us to quantify the effects of various system parameters and constraints on the best throughput using a constant bit rate. As an example we plotted the variation of T_U^* as a function of wavelength and link distance for our sample system. See Figs. 6 and 7.

4 CONCLUSION

We note from the result for burst duration statistics that if the curve for the pdf, F 2, is approximated by an exponential, the expected value needed for good approximation is close to the expected decay time constant. This can also be seen from Fig. 1. ($R_N = .0$ curve 2) which is somewhat more conservative than previously believed [8], [9]. The quantitative results for channel duration a throughput lets us choose our bit rate to evaluate the tradeoffs with respect to other communication system parameters such as P , P_{\max} etc.

Fig. 1 AVG. BURST DURATION - UNDERDENSE SAMPLE SYSTEM WITH FREQ-SCHEME

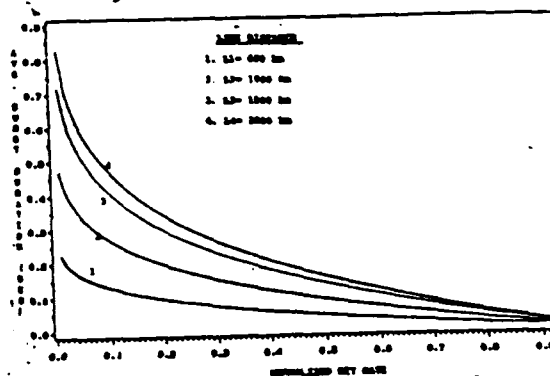


Fig. 2 PDF FOR UNDERDENSE BURST DURATION SAMPLE SYSTEM WITH FREQ-SCHEME, 10-100000 km

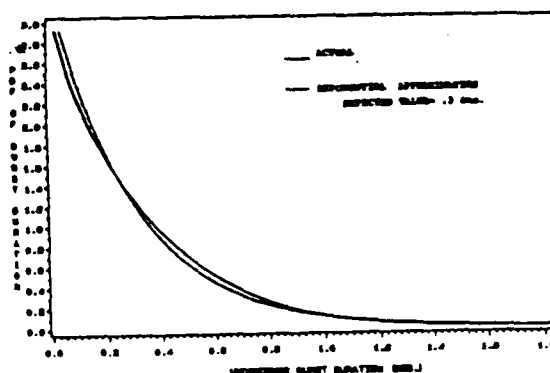


Fig. 3 NORMALIZED THROUGHPUT - UNDERDENSE ANY SYSTEM

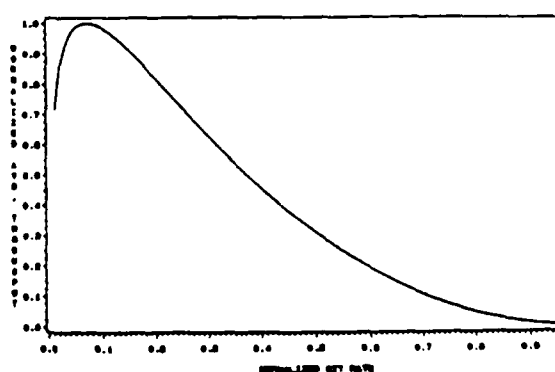


Fig. 4 OPTIMAL CONSTANT BIT RATE
SAMPLE SYSTEM

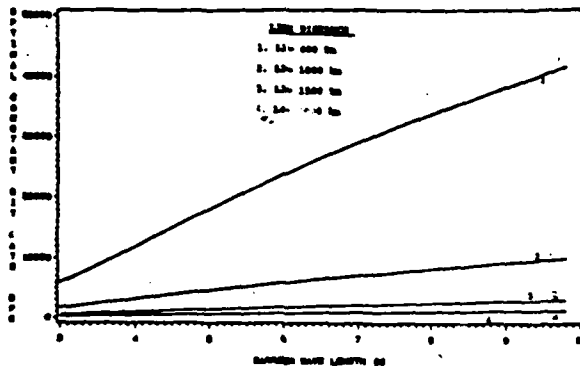


Fig. 5 OPTIMAL CONSTANT BIT RATE
SAMPLE SYSTEM

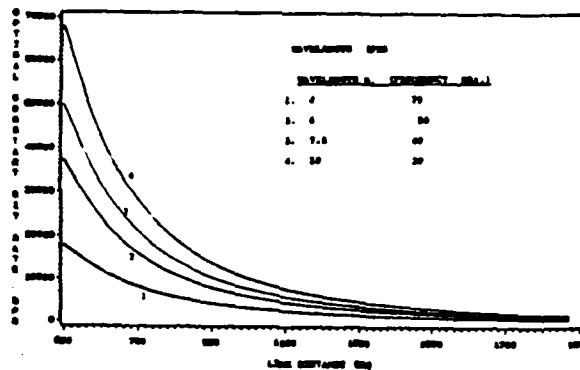


Fig. 6 MAX. (AVG.) THROUGHPUT - UNDERDENSE
SAMPLE SYSTEM

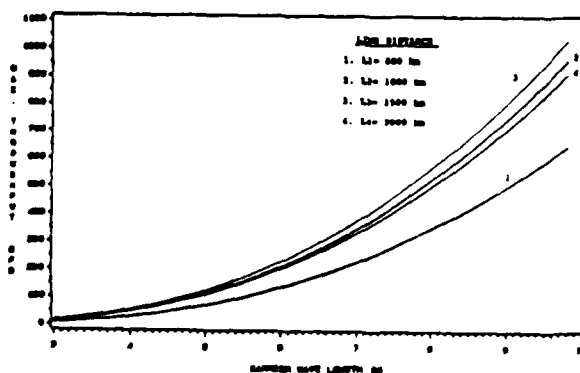
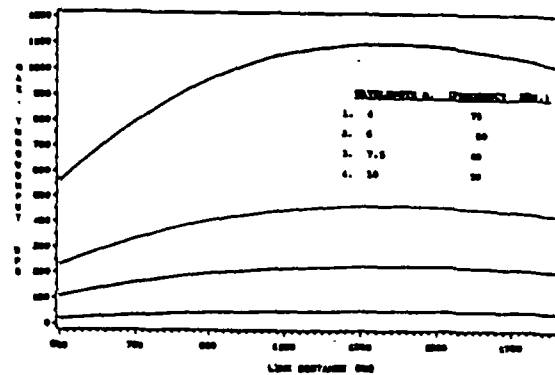


Fig. 7 MAX. (AVG.) THROUGHPUT - UNDERDENSE
SAMPLE SYSTEM



5 REFERENCES

- [1] G.R. Sugar, "Radio propagation & reflection from meteor trails," Proc. IEEE vol. 52, pp 116-136, Feb. 1964.
- [2] V.R. Eshleman and L.A. Manning "Radi Communications by Scattering from Meteor Ionization", Proc IRE, Vol. 42, pp 530-536 March 1954.
- [3] A.E. Spezio, "Meteor burst communicat system: Analysis and synthesis." NRL Rep 8286, Dec. 28, 1978.
- [4] M.W. Abel, "Meteor Burst Communications Bits per Burst Performance Bounds" IEE Trans. Commun., vol. COM-34, pp.927-936, Sep 1986.
- [5] J.Hampton, "A Meteor Burst Model Wit Time Varying Bit Error Rate", Milcom 1985 32.2.1.
- [6] J. Weitzen, Signet-on Corp., privat communications.
- [7] J.A. Weitzen, W.P. Biro kenmeier, ar M.D. Grossi, "An estimate of the capacity c the meteor burst channel," IEEE Trans Commun., Aug. 1984.
- [8] L.B. Milstein, D.L. Schilling, R.I. Pickholtz, J. Sellman, S. Davidovici, A Pavelchek, A. Schneider, G. Eichmannr "Performance of Meteor Burst Communicat Channels".
- [9] J.D. Oetting, "An analysis of metec burst communications for military applicati ons," IEEE Trans. Commun., vol. COM-28, pp 1591-1601, Sept. 1980
- [10] Hibshoosh, E., Schilling, D.L., Tin Varying Bit Error Rate for Meteor Burs Channel, MILCOM'86, Monterey, CA, Oct. '86.